eLife

Reviewed Preprint
v2 • January 14, 2025
Revised by authors

Reviewed Preprint
v1 • May 29, 2024

Neuroscience

Behavioural pharmacology predicts disrupted signalling pathways and candidate therapeutics from zebrafish mutants of Alzheimer's disease risk genes

François Kroll, Joshua Donnelly, Güliz Gürel Özcan, Eirinn Mackay, Jason Rihel

Department of Cell and Developmental Biology, University College London, London, United Kingdom • Institut de la Vision, Sorbonne Université, Paris, France

eLife Assessment

This **important** manuscript sets out to identify sleep/arousal phenotypes in larval zebrafish carrying mutations in Alzheimer's disease (AD)-associated genes. The authors provide detailed phenotypic data for F0 knockouts of each of 7 AD-associated genes and then compare the resulting behavioral fingerprints to those obtained from a large-scale chemical screen to generate new hypotheses about underlying molecular mechanisms. The data presented are **solid**, although extensive interpretation of pharmacological screen data does not necessarily reflect the limited mechanistic data. Nonetheless, the authors address most reviewer concerns in their revised version, providing invaluable new analyses. Phenotypic characterization presented is comprehensive, and the authors develop a well-designed behavioral analysis pipeline that will provide considerable value for zebrafish neuroscientists.

https://doi.org/10.7554/eLife.96839.2.sa3

Abstract

By exposing genes associated with disease, genomic studies provide hundreds of starting points that should lead to druggable processes. However, our ability to systematically translate these genomic findings into biological pathways remains limited. Here, we combine rapid loss-of-function mutagenesis of Alzheimer's risk genes and behavioural pharmacology in zebrafish to predict disrupted processes and candidate therapeutics. FramebyFrame, our expanded package for the analysis of larval behaviours, revealed that decreased night-time sleep was common to F0 knockouts of all four late-onset Alzheimer's risk genes tested. We developed an online tool, ZOLTAR, which compares any behavioural fingerprint to a library of fingerprints from larvae treated with 3,677 compounds. ZOLTAR successfully predicted that *sorl1* mutants have disrupted serotonin signalling and identified betamethasone as a drug which normalises the excessive day-time sleep of *presenilin-2* knockout larvae with

minimal side effects. Predictive behavioural pharmacology offers a general framework to rapidly link disease-associated genes to druggable pathways.

Introduction

To prevent or slow down disease, therapies must target the biological processes that cause the disease. Genomic approaches like family studies or genome-wide association studies (GWAS) can help in this quest for causal processes by exposing genes that are mutated before disease onset. For finding causal processes, studying the genome is advantageous because the chronology from genomic variant to disease is unambiguous, providing a stronger argument for causality than when studying the transcriptome or epigenome. In theory, all we need to do after a genomic study is follow the thread from each gene to the biological process in which it is involved. We know from the genomic study that this process increased or reduced risk when it was altered by mutations in the gene, so modulating more forcefully the process with a drug may unlock a larger therapeutic benefit. In practice, the path from genomic variant to druggable process is far from straightforward.

Research on Alzheimer's disease (AD) exemplifies well both the challenge and benefit of translating genomic studies into druggable biological processes. Family studies of early-onset AD in the 1990's[1] identified causal mutations in amyloid precursor protein (*APP*)[2,3], presenilin 1 (*PSEN1*)[4], and presenilin 2 (*PSEN2*)[5]. Subsequent work demonstrated that amyloid beta (Aβ), a small peptide which forms aggregates in the brains of AD patients[6], was generated by cleavage of APP by γ-secretase[7,8], of which the catalytic subunit is PSEN1 or PSEN2[9,10]. Consequently, the field naturally converged on the amyloid hypothesis of AD, which posits that the disease is caused by toxic aggregates of Aβ[11]. Today, antibodies against Aβ such as lecanemab show promise in slowing down disease progression[12]. This story shows that, although a great challenge, genomic studies (family studies of early-onset AD) can be successfully translated into a causal process (Aβ aggregation) that is now targeted by disease-modifying drugs (lecanemab).

However, the beneficial effects from targeting Aβ aggregation currently remain modest despite substantial reductions in brain amyloid burden[12]. To completely stop disease progression, anti-amyloid therapy will likely need to be combined with drugs modulating other processes that contribute to the disease[13]. GWAS have identified tens of genomic loci where sequence variation is associated with late-onset AD, offering an opportunity to discover new causal processes of AD that potentially go beyond the amyloid hypothesis. For example, analysis of cell types enriched for open chromatin at AD-associated loci pointed to a possible critical role of monocytes, macrophages, and microglia in AD progression[14,15]. Although GWAS are designed to generate new hypotheses, AD-associated loci have rarely been exploited to find new causal processes in an unbiased, systematic manner. Given the challenges inherent to linking genomic variants to causal biological events, new genomic associations are often first more narrowly interpreted in the context of the amyloid hypothesis. While this interpretation may be correct, it tends to create a self-fulfilling prophecy which leaves little room for the discovery of new causal processes[16,17].

As AD is primarily a disease of old age, research often focuses on patients or animal models after disease onset. However, this approach hinders the discovery of new *causal* processes from genomic studies because it largely annuls the advantage of unambiguous chronology—since genomic variants were unambiguously present before disease onset, they must have modulated a process which contributed causally to disease initiation. In patients or animals after disease onset, many biological processes are disrupted, but only a small proportion may be genuinely causal for future disease progression and therefore make suitable targets for disease-modifying therapies. For example, one may find that dopamine is lacking in the basal ganglia of patients and animal models of Parkinson's disease. Treatment with levodopa, a dopamine precursor, temporarily relieves motor symptoms, but does not slow down disease progression, so dopamine deficiency is

not in fact a causal process[18]. Therefore, perhaps counterintuitively, studying the consequences of AD-associated mutations *early* in life seems more likely to identify processes that are genuinely causal to disease, as any disrupted process is less likely to be a secondary disease consequence.

In practice, how can we quickly follow the thread from a disease-associated gene to a (druggable) biological process in which it is involved? In this work, we describe a behavioural pharmacology approach using zebrafish larvae. Our strategy compares the behavioural profile of knockout zebrafish to a behavioural dataset of wild-type animals exposed to thousands of small molecules to predict causal processes and potential compounds that rescue the phenotype[19]. In previous work[20], we introduced the use of zebrafish F0 knockouts to study complex traits such as behaviour. In this study, we demonstrate how the F0 knockout method renders this behavioural pharmacology approach fast and scalable to the parallel study of tens of disease-associated genes, rather than one at a time[21,22]. As genomic studies of AD can likely be further exploited to find causal processes, we used Alzheimer's risk genes as a case study for our strategy. The strategy is not specific to any one disease or set of genes. In theory, any measurable change in behaviour could be used to predict the underlying causal pathways and small molecules that normalise this change.

Results

Most Alzheimer's risk genes are present in zebrafish and expressed early in development

GWAS point to small portions of the genome where variation in sequence is associated with variation in disease risk but do not readily specify the genes whose altered function are responsible for this association. Therefore, as a starting point, we used a meta-analysis of GWAS on AD that found 37 significant loci and annotated each with the most likely causal gene using mainly statistical colocalisation[23,24]. To add confidence to these calls, we cross-referenced these causal gene predictions with a transcription-wide association study and risk gene transcripts that undergo differential splicing in AD brains[25]. Finally, we included the three genes that can cause early-onset AD when mutated: *PSEN1*[4], *PSEN2*[5], and *APP*[2,3], yielding a list of 40 genes associated with AD risk (Supplementary file 1).

Of these 40 Alzheimer's risk genes, 30 (75%) had at least one annotated orthologue in the zebrafish genome (source: Ensembl). Of those, 17 had one orthologue (e.g. the only zebrafish orthologue of human *SORL1* was *sorl1*); 11 had two orthologues (e.g. the zebrafish orthologues of human *APP* were *appa* and *appb*); and 2 had more than two orthologues (e.g. the zebrafish orthologues of human *MS4A6E* included *ms4a17a*, *ms4a17c.2*, *tmem176l*, and more) (**Fig. 1a**). A human gene often has two or more zebrafish orthologues because of a teleost-specific whole-genome duplication event around 340 million years ago[26]. There were no annotated orthologues for 10 Alzheimer's risk genes, including *TREM2*.

Next, we used a published single-cell RNA sequencing (scRNA-seq) dataset of the developing zebrafish brain[27] to ask whether the orthologues of the Alzheimer's risk genes were expressed in zebrafish embryos and larvae. Most of the genes (33/42) were detectable as early as 12 hours post-fertilisation (hpf) and remained expressed throughout development (**Fig. 1b**). At 5 days post-fertilisation (dpf), 38 of the 42 orthologues (90%) were expressed.

From these observations, we selected seven high-confidence Alzheimer's risk genes for further study in zebrafish; the orthologues of the three early-onset Alzheimer's genes: *psen1*, *psen2*, *appa*/*appb*; and four genes associated with late-onset AD: *apoea*/*apoeb*, *cd2ap*, *clu*, *sorl1*. We chose *APOE* as it is the most well-known genetic risk factor for late-onset AD[28]. *CD2AP*, *CLU*, and *SORL1* were chosen because non-coding variants within or near those genes are repeatedly found

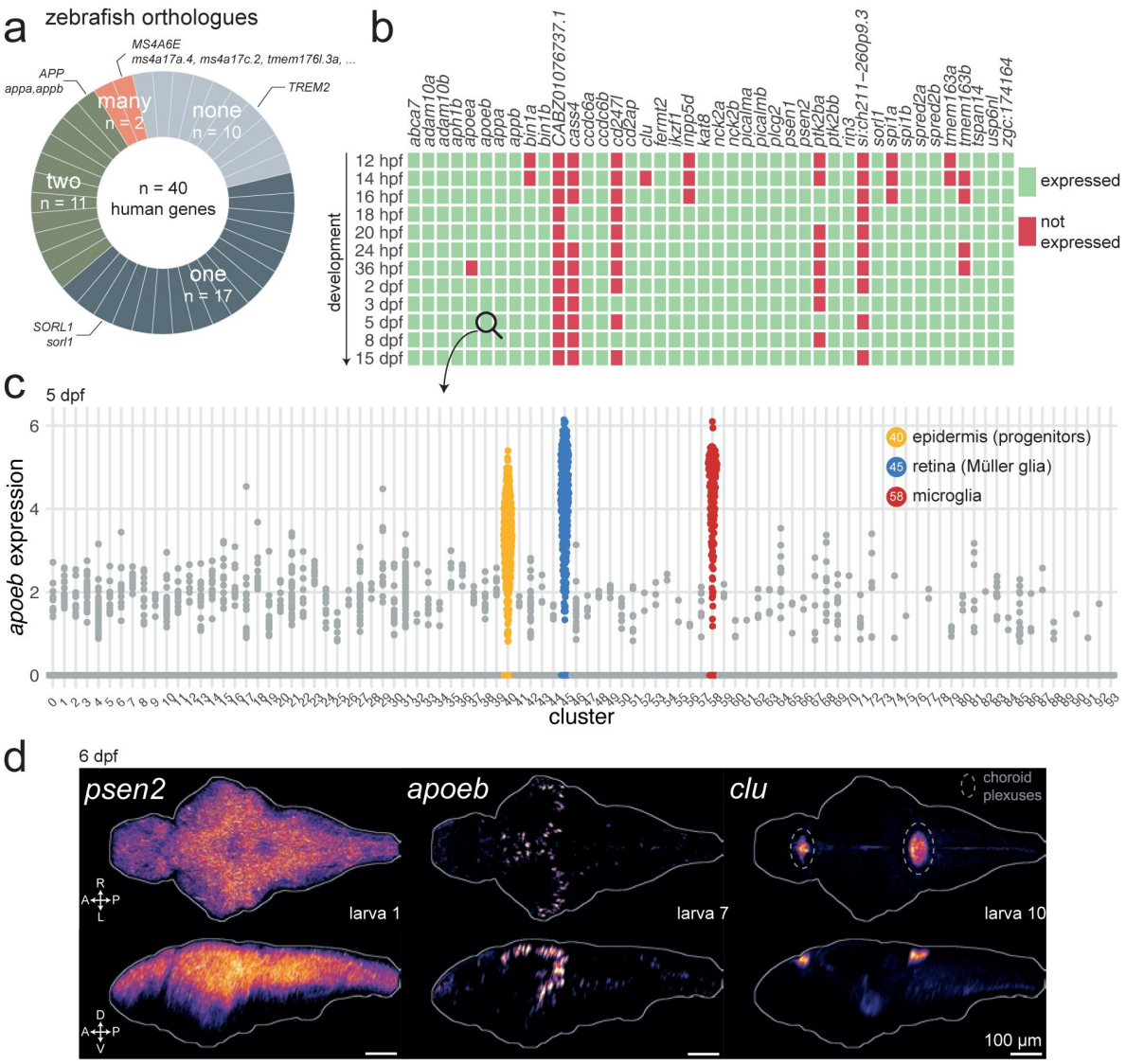

Fig. 1

Most Alzheimer's risk genes are found in zebrafish and expressed early in development.

a, Of 40 Alzheimer's risk genes, 17 had one orthologue in zebrafish; 11 had two orthologues; 2 had more than two orthologues; and 10 did not have any annotated orthologue. More details about orthologues of Alzheimer's risk genes are provided in Supplementary file 1 (source: Ensembl).

b, Expression of Alzheimer's risk genes during early development in zebrafish. Genes were marked as "expressed" (green) if at least three cells had detectable transcripts in the single-cell RNA-seq dataset from Raj et al., 2020. *CABZ01076737.1* is the orthologue of *TSPOAP1*; *cd247l* is the orthologue of *FCER1G*; *si:ch211-260p9.3* is an orthologue of *PLCG2*; *zgc:174164* is an orthologue of *ADAM10*. Other genes have the same name as their human orthologue. The orthologues of *MS4A6E* were not included. hpf, hours post-fertilisation; dpf, days post-fertilisation.

c, Expression of *apoeb* in cells of the nervous system at 5 dpf. Each dot represents one cell. Cells are grouped by cluster identity, which are provided in Supplementary file 1. Single-cell RNA-seq data and clustering from Raj et al., 2020.

d, *In situ* hybridization chain reactions labelling *psen2*, *apoeb*, or *clu* mRNA in the brains of 6-dpf larvae. The images are maximum Z-projections of dorsal (top) and sagittal (bottom) views of three larvae. A, anterior; P, posterior; R, rightwards; L, leftwards; D, dorsal; V, ventral. Larva # labels individual animals across this figure and **Fig. 1–supplement 3** and **4**. See also Fig. 1–supplemental videos 1–9.

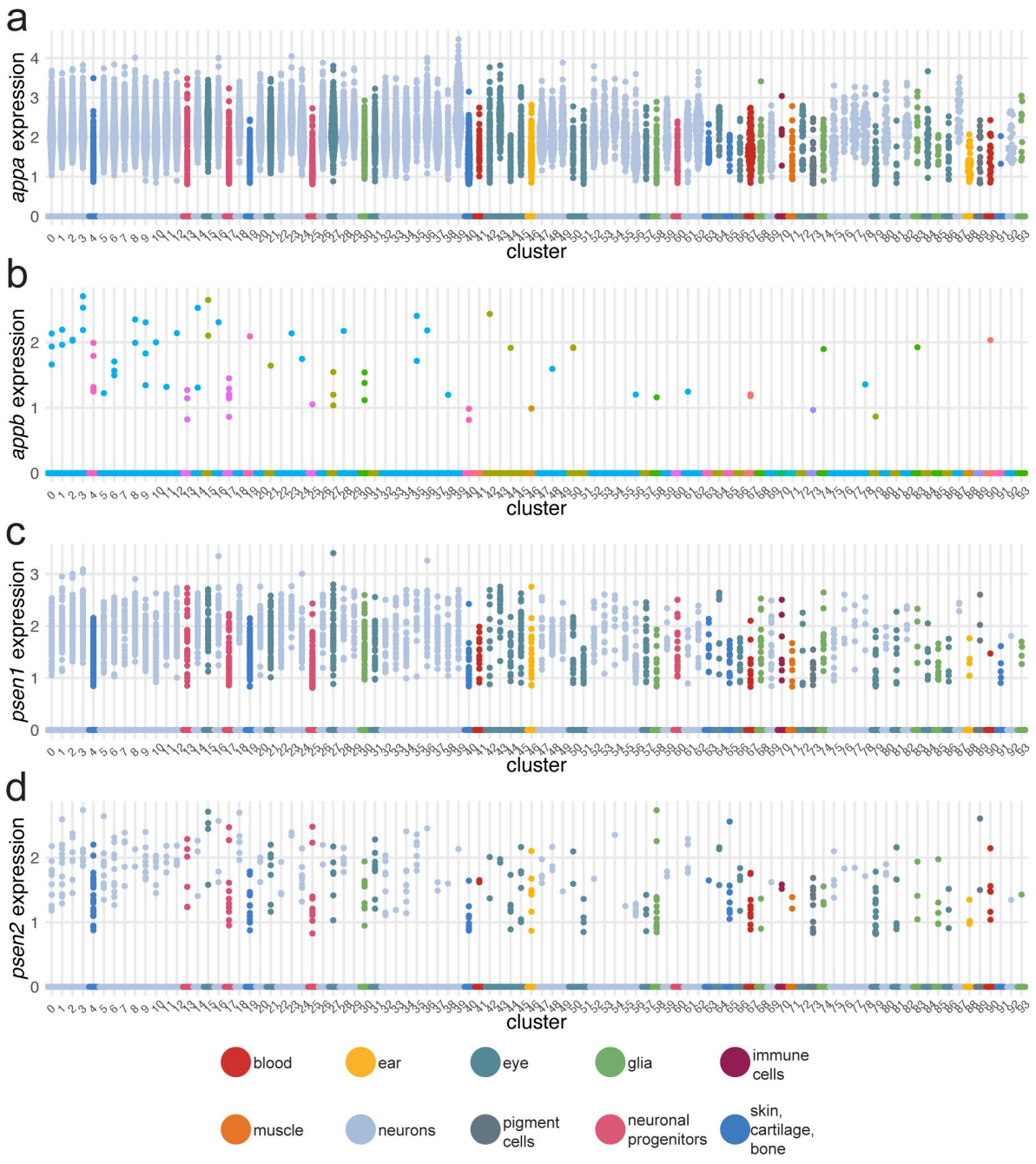

Fig. 1–suppl. 1

Expression of zebrafish orthologues of early-onset Alzheimer's risk genes from single-cell RNA-seq data.

Expression of *appa* (**a**); *appb* (**b**); *psen1* (**c**); *psen2* (**d**) in brain cells of the larval zebrafish at 5 dpf. Each dot represents one cell. Cells are grouped by clusters, which are coloured by broad categories. Cluster identities are provided in Supplementary file 1. Single-cell RNA-seq data and clustering from Raj et al., 2020.

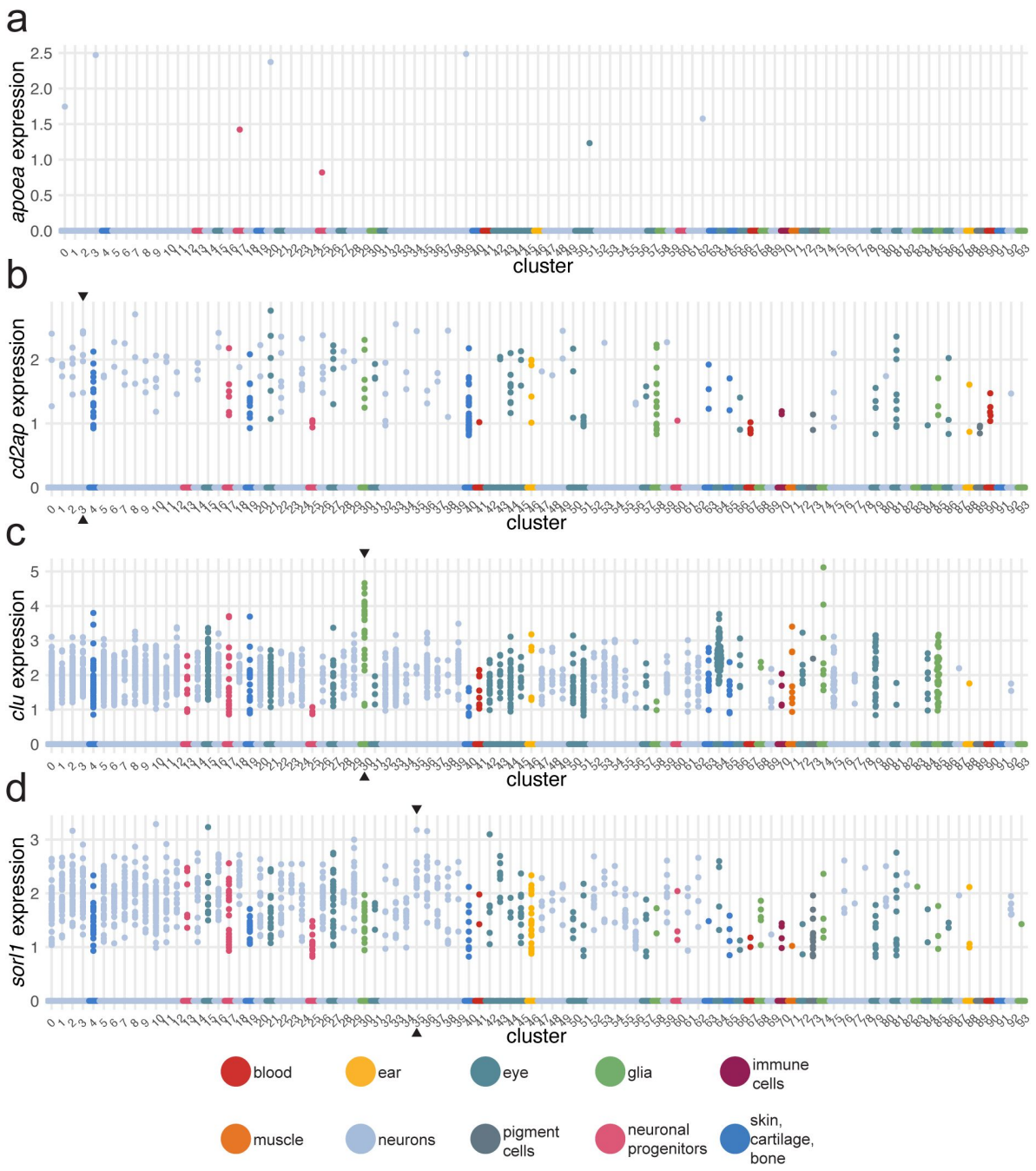

Fig. 1–suppl. 2

Expression of zebrafish orthologues of four late-onset Alzheimer's risk genes from single-cell RNA-seq data.

Expression of *apoea* (**a**); *cd2ap* (**b**); *clu* (**c**); *sorl1* (**d**) in brain cells of the larval zebrafish at 5 dpf. Each dot represents one cell. Cells are grouped by clusters, which are coloured by broad categories. In b), c), and d), black arrowheads mark the cluster with highest average expression, after excluding cells with no expression and clusters with fewer than three cells with positive expression. Cluster identities are provided in Supplementary file 1. Single-cell RNA-seq data and clustering from Raj et al., 2020.

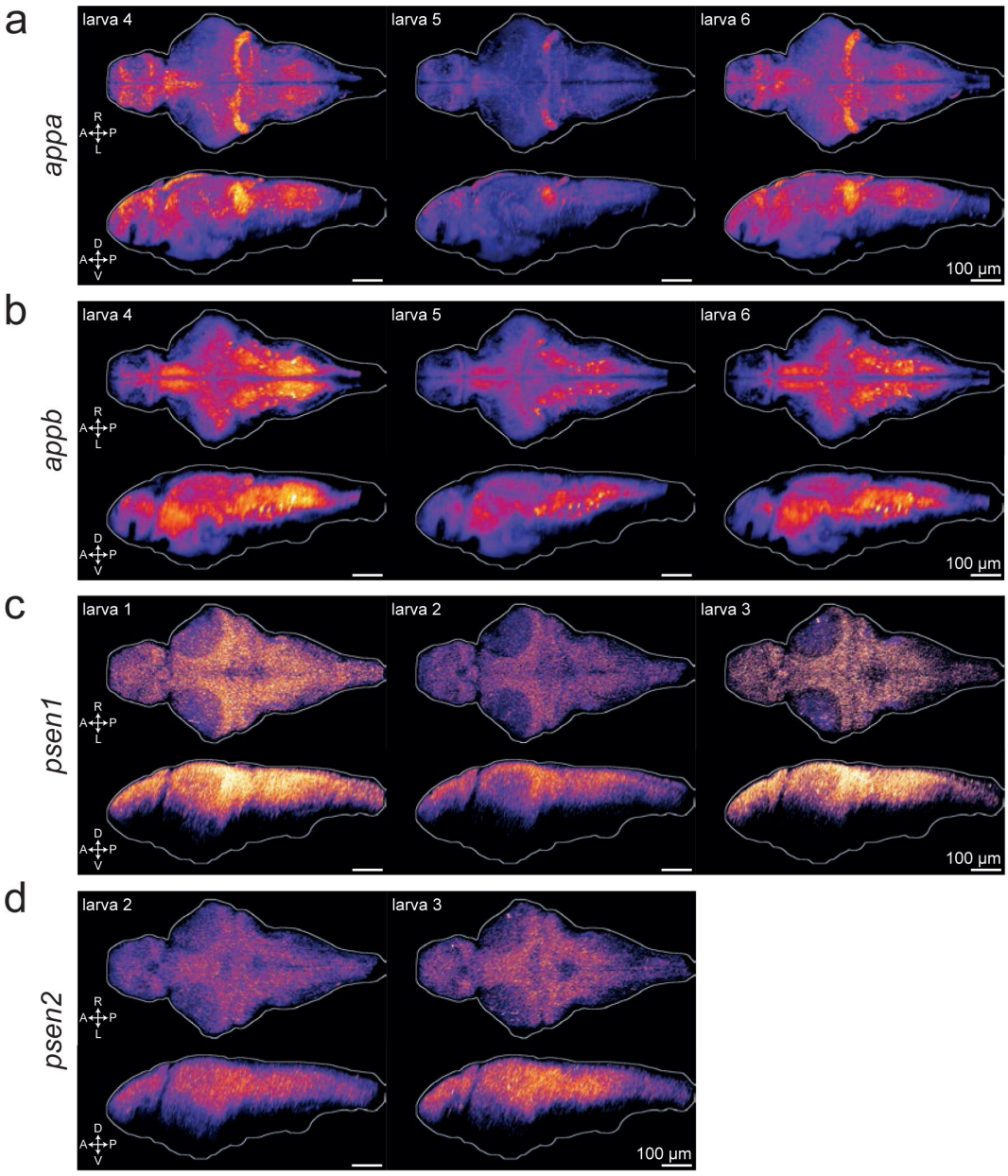

Fig. 1–suppl. 3

Expression of zebrafish orthologues of early-onset Alzheimer's risk genes in the zebrafish brain.

In situ hybridization chain reaction labelling *appa* (**a**); *appb* (**b**); *psen1* (**c**); *psen2* (**d**) mRNA in the brains of 6-dpf larvae. Maximum Z-projections of dorsal (top) and sagittal (bottom) views. A, anterior; P, posterior; R, rightwards; L, leftwards; D, dorsal; V, ventral. Larva # labels individual animals across this figure, **Fig. 1d**, and **Fig. 1**–supplement 4. See also **Fig. 1**–supplemental videos 1–9.

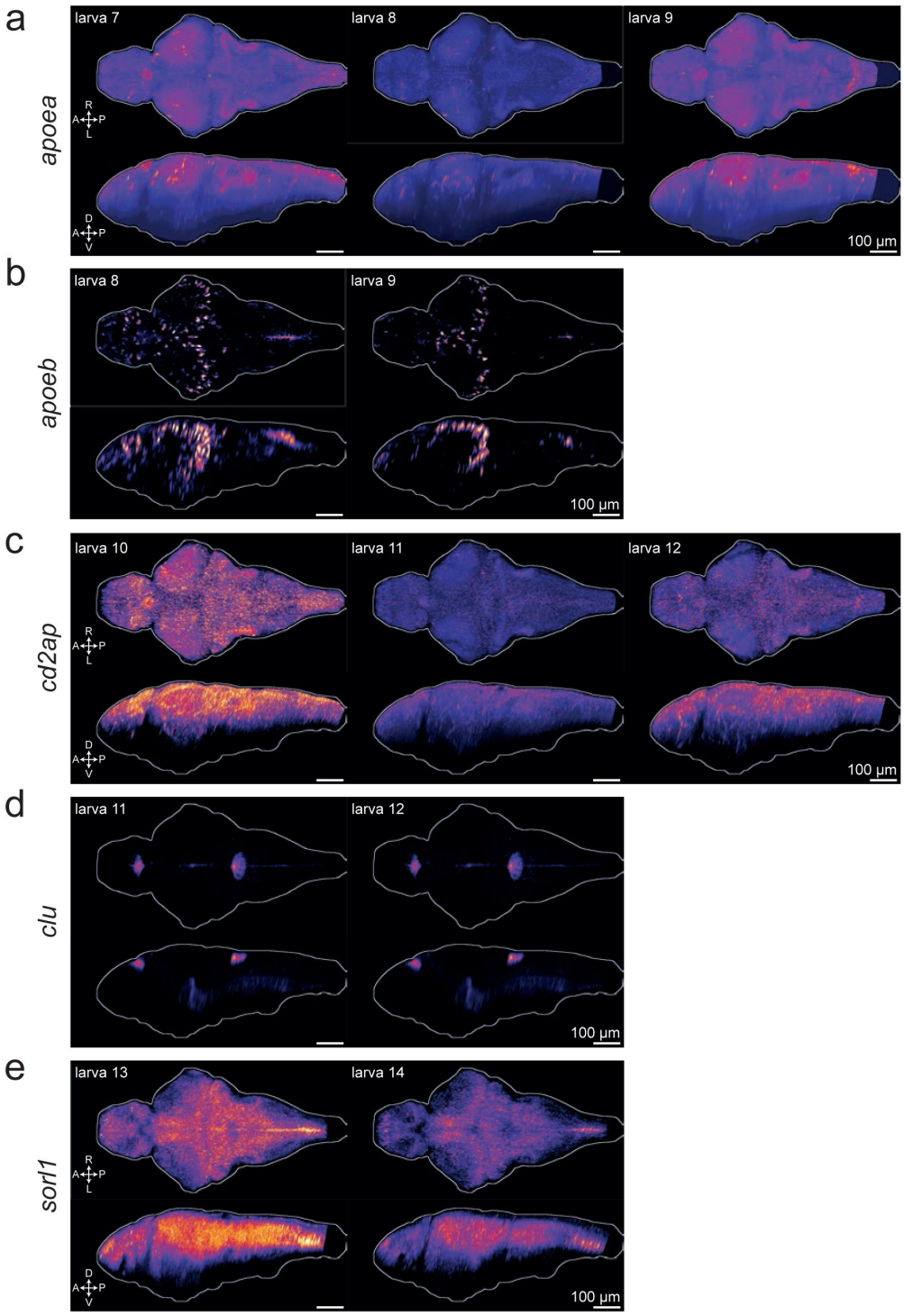

Fig. 1–suppl. 4

Expression of zebrafish orthologues of four late-onset Alzheimer's risk genes in the zebrafish brain.

In situ hybridization chain reaction labelling *apoea* (**a**); *apoeb* (**b**); *cd2ap* (**c**); *clu* (**d**); *sorl1* (**e**) mRNA in the brains of 6-dpf larvae. Maximum Z-projections of dorsal (top) and sagittal (bottom) views. A, anterior; P, posterior; R, rightwards; L, leftwards; D, dorsal; V, ventral. Larva # labels individual animals across this figure, **Fig. 1d**, and **Fig. 1**–supplement 3. See also Fig. 1–supplemental videos 1–9.

by GWAS[29,30]. At the *CD2AP* locus, *CD2AP* was highly likely to be the causal gene by colocalisation[23]. At the *CLU* locus, both *PTK2B* and *CLU* were likely causal[23], but differential splicing of *CLU* correlated with risk of AD[25]. The top variant at the *SORL1* locus was within an intron of *SORL1*[23], but rare protein-coding variants in *SORL1* were likely causal for some early-onset AD patients through haploinsufficiency or deleterious effects on protein function[31–33].

For these selected Alzheimer's risk genes, we more carefully examined their expression patterns in larval zebrafish. From the scRNA-seq dataset[27], most of these genes were broadly expressed in the 5-dpf larva in different neuronal populations and other cell types (**Fig. 1–supplement 1** and **2**). *apoeb* was highly expressed specifically in epidermis progenitors, Müller glia in the retina, and microglia (**Fig. 1c**), as observed previously[34–37]. Across clusters, the highest expression of *cd2ap* was in neurons of the thalamus (**Fig. 1– supplement 2b**, cluster 3); *clu* was enriched in radial glia (**Fig. 1–supplement 2c**, cluster 30); and *sorl1* expression was maximal in a cluster of hypothalamic neurons with enriched *tph1a* expression, a marker for serotonergic neurons (**Fig. 1–supplement 1d**, cluster 35). To confirm and extend these observations, we used in situ hybridization chain reaction (HCR) to label mRNA in 6-dpf larvae. As we observed in the scRNA-seq data, most genes tested (*appa*, *psen1*, *psen2*, *cd2ap*, *sorl1*) were broadly expressed throughout the 6-dpf brain (**Fig. 1d** and **Fig. 1–supplement 3** and **4**). HCR showed strong and widespread expression of *appb*, which contradicts the minimal expression from the Raj et al., 2018 scRNA-seq dataset but agrees with the scRNA-seq data from DanioCell[38]. *apoea* expression from HCR was unconvincing, which corroborates the negligible expression found in the scRNA-seq dataset. *apoeb* expression was restricted to cells in the forebrain and optic tectum (**Fig. 1d** and **Fig. 1–supplement 4b**). Based on the scRNA-seq dataset (**Fig. 1c**) and literature[34,39], these cells are likely *ccl34b.1*$^{+}$ amoeboid microglia derived from primitive myeloid precursors from the rostral blood island. *apoeb* was also detected in cells bordering the hindbrain ventricle, which are likely radial glia/astrocytes[40,41]. Contrary to the widespread expression found in the scRNA-seq dataset, *clu* expression was largely restricted to the diencephalic and myelencephalic choroid plexuses (**Fig. 1d** and **Fig. 1–supplement 4d**), confirming a previous report[42].

In summary, around 75% of Alzheimer's risk genes had at least one clear orthologue in zebrafish and most of these were expressed in the brain of 5–6-dpf zebrafish larvae, so they could play a role in early brain development or function.

The FramebyFrame R package for analysis of sleep/wake behaviour from high-throughput video-tracking data

The next stage in our behavioural pharmacology strategy is to measure sleep/wake behaviour of F0 knockout larvae for the genes under study. To uncover even subtle behavioural phenotypes caused by the loss of Alzheimer's risk genes, we developed a high-throughput sleep/wake tracking assay for zebrafish larvae capable of analysing behaviour at the sub-second resolution over multiple days and nights. To achieve this, we combined previous sleep/wake analysis methods[19,43,44] with some aspects of the frame-by-frame analysis developed by Ghosh and Rihel (2020)[45] into a single software tool, the FramebyFrame R package (*github.com/francoiskroll/FramebyFrame*). We also designed a 3D-printed mesh-bottom plate that supports long-term (up to 8.5 days tested) tracking of larvae with minimal intervention by regulating the water level with a small pump and delivering paramecia for feeding through the mesh from the water bath below (**Fig. 2a**,**b**).

The FramebyFrame package extracts and analyses 17 behavioural parameters from frame-by-frame Δ pixel data, which represent the number of pixels that changed intensity at each frame-to-frame transition. These parameters capture both behaviours that unfold over multiple minutes or hours, such as sleep (**Fig. 2c**), and actions at smaller time scales (< 1 sec), such as individual swimming bouts (**Fig. 2d**). The parameters are grouped into three categories: activity

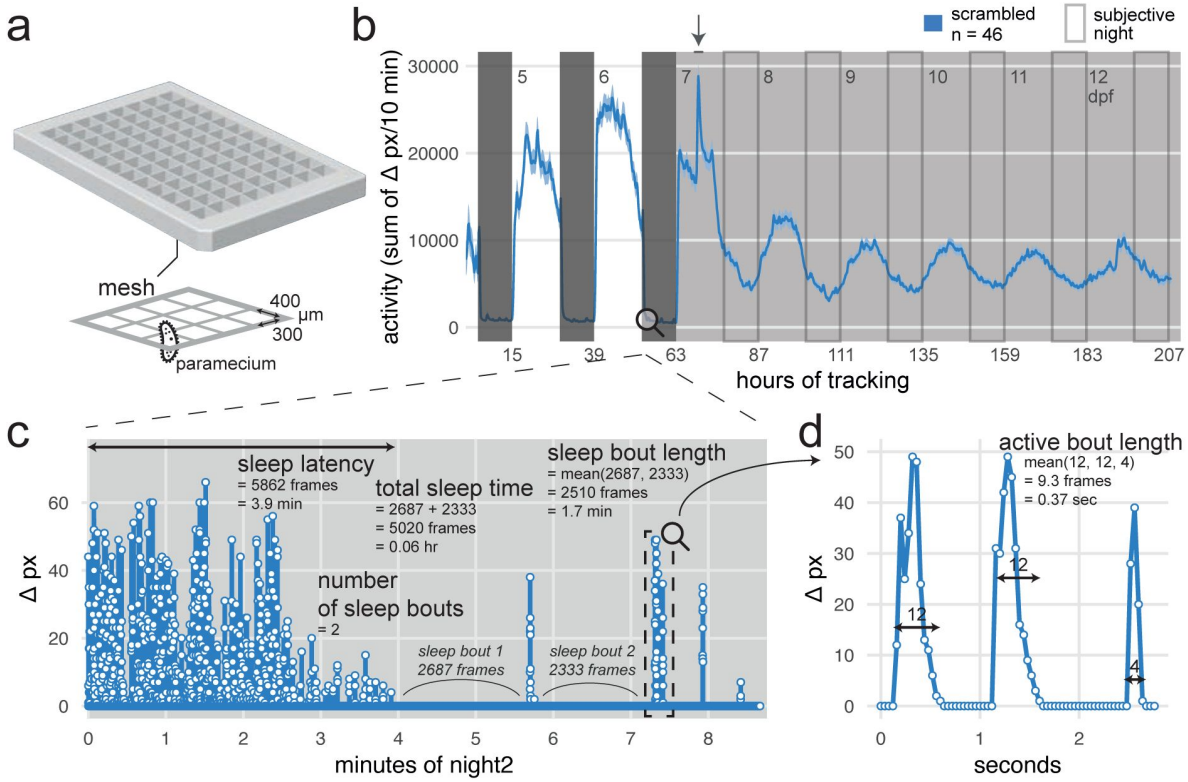

Fig. 2

Analysis of zebrafish sleep/wake behaviour at the frame-by-frame resolution with the FramebyFrame R package.

a, 3D model of the 96-square well mesh-bottom plate. Available at github.com/francoiskroll/FramebyFrame.
b, Example of an 8-day (208 hr total) video-tracking experiment. scrambled-injected control larvae were in a mesh-bottom plate placed in a water bath containing paramecia. Larvae were tracked for 63 hr on a 14 hr:10 hr light:dark cycle (white and dark grey backgrounds, respectively), then switched to constant dim light (30 lux) for 145 hr (subjective nights are framed). The larvae were tracked from 4 to 13 dpf and all appeared healthy at the end of the experiment. The trace is the mean ± SEM across larvae of the activity (sum of Δ pixels/10 minutes). The arrow indicates when the water in the bath was replaced and fresh paramecia were supplemented, causing a spike in activity.
c, The FramebyFrame R package calculates 17 parameters from the Δ pixel timeseries of each larva. The parameters are grouped in three categories: activity parameters, active bout parameters, and sleep parameters. Here, sleep parameters calculated by the FramebyFrame R package are annotated on the first ~9 min of the Δ pixel timeseries for one wild-type larva starting at lights off. These parameters describe the sleep behaviour of each larva during each day or night. Sleep parameters are also calculated for days, except for sleep latency. This plot is connected to b) for illustrative purposes only; the data was not from the same experiment.
d, Example of an active bout parameter—active bout length—annotated on the sample data from c). For all the activity and active bout parameters calculated by the FramebyFrame R package, see **Fig. 2–supplement 1**.

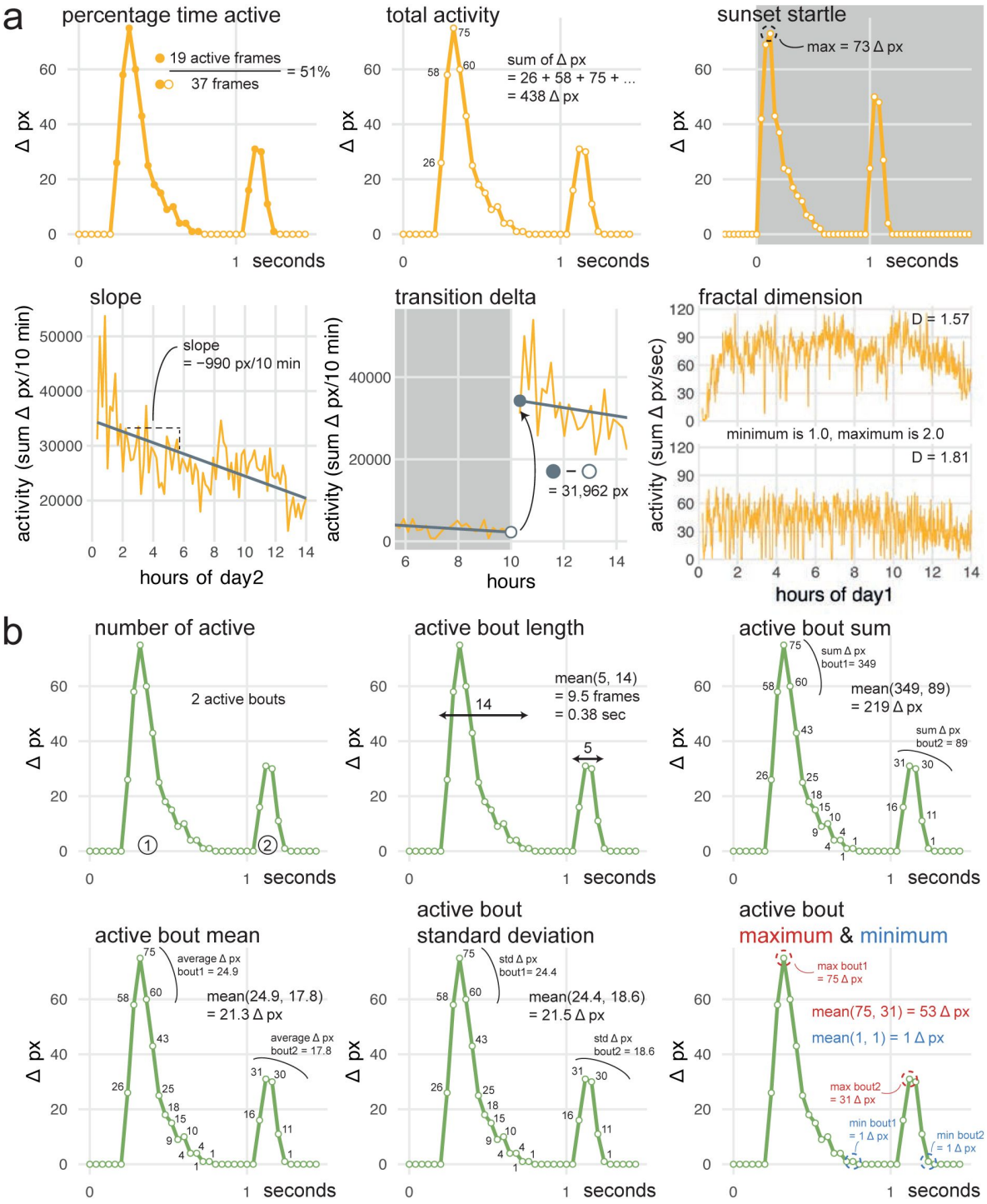

Fig. 2–suppl. 1

Behavioural parameters calculated by the FramebyFrame R package on the Δ pixel timeseries.

a, Activity parameters calculated by the FramebyFrame R package annotated on sample data from a single larva. These parameters describe the overall activity of each larva during each day or night and are calculated directly on the Δ pixel timeseries. Sunset startle describes the larva's startle response when lights abruptly switch off at the day-to-night transition, and therefore is only defined for nights. Activity tends to decrease over the course of the day; the slope parameter describes the rate of this decline. Transition delta describes the sudden jump or drop in activity which occurs at the light transitions. Fractal dimension describes the smoothness (D closer to 1.0) or roughness (D closer to 2.0) of the activity trace.
b, Active bout parameters calculated by the FramebyFrame R package annotated on sample data from a single larva. These parameters describe the average swimming bout of each larva during each day or night.

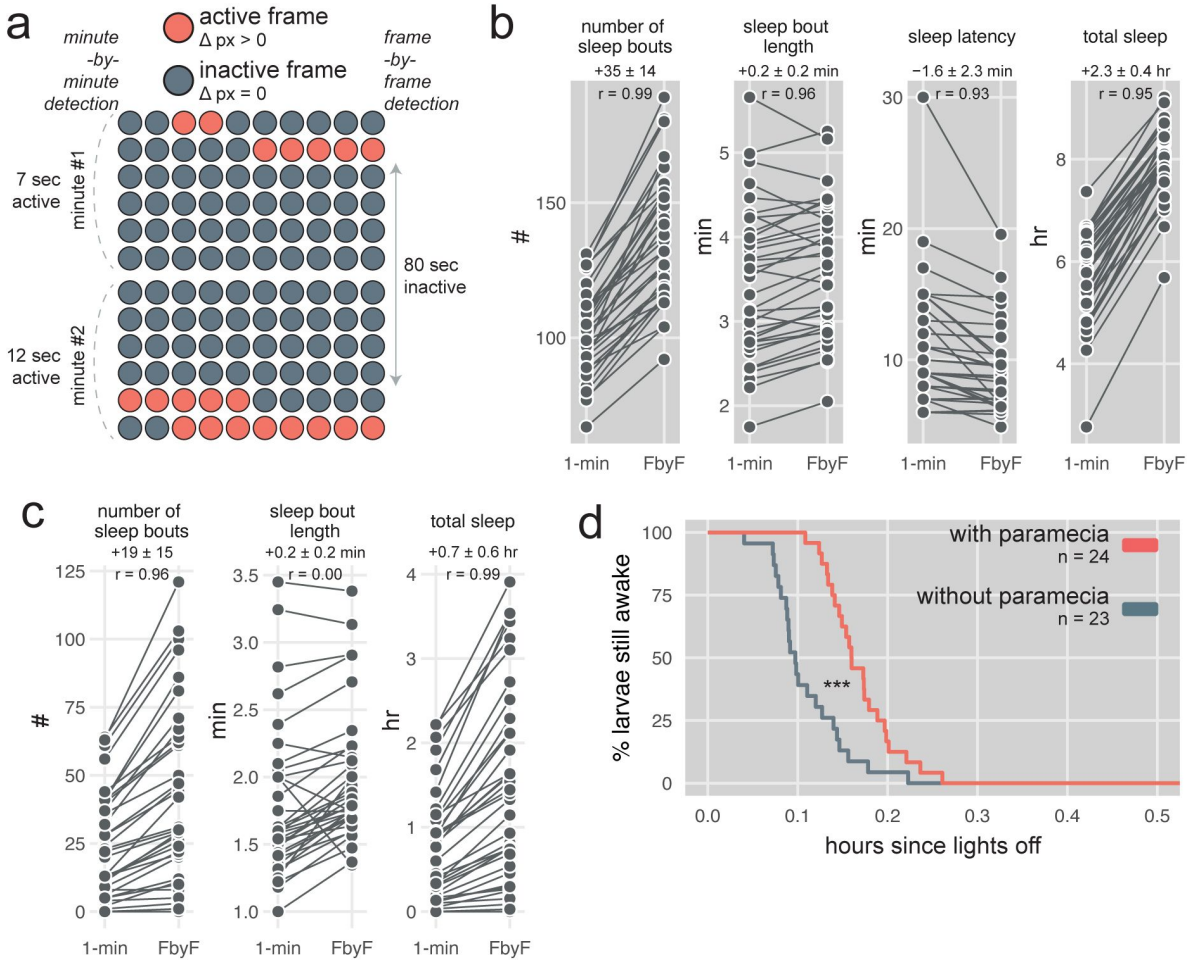

Fig. 2–suppl. 2

Sleep detection by the FramebyFrame R package.

a, Example of a sleep bout detected by the FramebyFrame R package that is missed by analysis done on one-minute epochs. In this example, the larva was inactive for 80 consecutive seconds, which represents a sleep bout as per the one-minute inactivity criterion for sleep (Rihel, Prober, and Schier 2010). Binning in one-minute epochs misses the sleep bout as it returns two active minutes with 7 and 12 sec of activity per minute, while the FramebyFrame package detects the 80-sec sleep bout.
b, Difference in sleep parameters measurements between the one-minute analysis and the frame-by-frame analysis performed on the same dataset. One line represents one wild-type larva during one night. *1-min*, results obtained with the minute-by-minute detection; *FbyF*, results obtained with the FramebyFrame R package; *r*, Pearson correlation.
c, Difference in sleep parameters measurements between the one-minute analysis and the frame-by-frame analysis, as in b). One line represents one wild-type larva during one day.
d, Example of a sleep latency survival plot generated with the FramebyFrame R package. Starting at lights-off, larvae that experienced their first sleep bout were gradually removed from the survival curve. At any timepoint, the larvae with paramecia in the well were 68 ± 31% less likely to fall asleep for the first time than larvae housed without paramecia: hazard ratio for larvae with paramecia = 0.32 ± 0.31, *** $p < 0.001$ by likelihood-ratio test.

parameters (**Fig. 2–supplement 1a**), which describe the overall activity of each larva during a complete day or night; active bout parameters (**Fig. 2–supplement 1b**), which describe the structure of individual swimming bouts; and sleep parameters (**Fig. 2c**) such as sleep latency (**Fig. 2–supplement 2d**). In zebrafish larvae, sleep is defined as any period of inactivity (Δ pixel = 0) lasting longer than one minute, a definition based on increases in arousal threshold and homeostatic rebound following deprivation[44,46]. This frame-by-frame analysis has several advantages over previous methods that analysed activity data at the one-minute resolution[19,43,44]. First, individual swimming bouts could not be resolved by these methods as single bouts last ~0.2 sec on average. Second, the one-minute methods missed around one third of all sleep bouts because of how the Δ pixel data is binned in one-minute epochs (**Fig. 2–supplement 2a**). At the frame-by-frame resolution, the start and end frame of each sleep bout can be precisely determined, which also improves the measurement accuracy of sleep bout duration and sleep latency, the delay from lights-off to first sleep bout. For example, during a sample 10-hr night (**Fig. 2– supplement 2b**), the frame-by-frame analysis detected 35 ± 14 more sleep bouts, longer average sleep bout lengths (+0.2 ± 0.2 min), and shorter sleep latencies (1.6 ± 2.3 min earlier), resulting in a 42% increase in total sleep time (+2.3 ± 0.4 hr). During the day, the FramebyFrame analysis also detected more sleep and more sleep bouts (**Fig. 2–supplement 2c**). Most behaviour plots included in this study were created using the FramebyFrame package in just a few commands from the raw frame-by-frame data.

psen2 knockouts sleep more during the day

Next, we used CRISPR-Cas9 to generate F0 knockouts for the zebrafish orthologues of the three genes that can cause early-onset AD when mutated in humans—*psen1*, *psen2*, *appa*/*appb*—and tested these mutants for behavioural and other phenotypes. We focused first on *psen1* and *psen2*.

Zebrafish Psen1 and Psen2 are highly similar to their human counterparts (~70% identical amino acid sequence, **Fig. 3a**,**b**), with the same critical amino acid at the four annotated active sites (two per presenilin). Mismatches between the human and zebrafish proteins were largely clustered into disordered domains, suggesting that the zebrafish presenilins have the same catalytic activity as in humans. The Cas9/guide RNA ribonucleoproteins (RNPs) used to generate F0 knockouts mutated virtually every copy of the genome at each of the three targeted sites. At each targeted locus of *psen1*, 99.0 ± 2.7% of reads had a small insertion and/or deletion (indel) and 78.6 ± 29.7% of all reads had a frameshift mutation (**Fig. 3c**). At each targeted locus of *psen2*, 99.9 ± 0.1% reads had indels and 82.0 ± 33.6% of all reads had a frameshift mutation (**Fig. 3d**). As each gene is mutated at three loci, the biallelic knockout probability, that is, the probability of having at least one frameshift mutation on both alleles, cumulatively reached > 98% (*francoiskroll.shinyapps.io/frameshiftmodel/*), indicating that most *psen1* and *psen2* F0 knockout larvae were complete loss-of-function mutants.

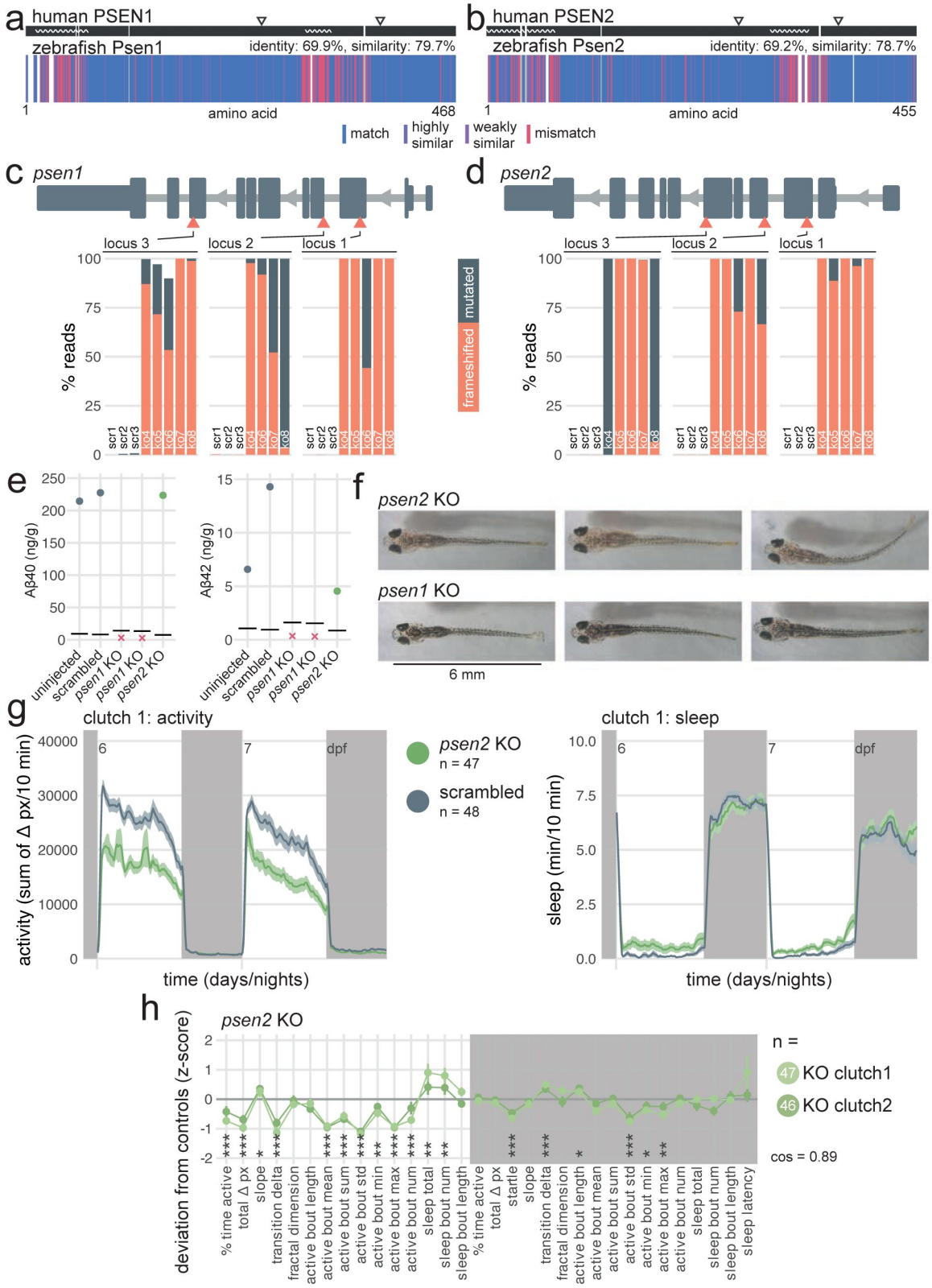
a
human PSEN1
zebrafish Psen1
identity: 69.9%, similarity: 79.7%
1
amino acid
468
match
highly similar
weakly similar
mismatch
b
human PSEN2
zebrafish Psen2
identity: 69.2%, similarity: 78.7%
1
amino acid
455
c
psen1
locus 3
locus 2
locus 1
% reads
d
psen2
mutated
frameshifted
e
Aβ40 (ng/g)
Aβ42 (ng/g)
uninjected
scrambled
psen1 KO
psen1 KO
psen2 KO
f
psen2 KO
psen1 KO
6 mm
g
clutch 1: activity
activity (sum of Δ px/10 min)
time (days/nights)
psen2 KO
n = 47
scrambled
n = 48
clutch 1: sleep
sleep (min/10 min)
h
psen2 KO
deviation from controls (z-score)
n =
47 KO clutch1
46 KO clutch2
cos = 0.89

Fig. 3

psen2 F0 knockouts initiate more sleep bouts during the day.

a, Human PSEN1 amino acid sequence (top) aligned to zebrafish Psen1 amino acid sequence (bottom). In the zebrafish protein, each amino acid (vertical bar) is coloured based on its similarity with the human protein. In the human protein, wavy lines represent disordered domains and arrowheads point to the two active sites at residues 257 and 385 (source: UniProt). White gaps are added when additional residues are present in the other sequence.

b, Human PSEN2 amino acid sequence (top) aligned to zebrafish Psen2 amino acid sequence (bottom), as in a). Active sites are at residues 263 and 366 (source: UniProt and AlphaFold).

c, (above) Schematic of *psen1* in the 5'–3' genome direction. Exons are in dark grey; tall exons are protein-coding, small are 5'-or 3'-UTR. Light grey lines are introns, and grey arrows represent the direction of transcription. Orange arrowheads mark the target loci. Exons and introns are on different scales. (below) Percentage of reads mutated (height of each bar, with orange representing percentage with a frameshift mutation) at each targeted locus of *psen1*. *scr*, scrambled-injected control larva; *ko*, *psen1* F0 knockout larva. The numbers refer to individual animals. For example, ko4 refers to an individual *psen1* F0 knockout larva for which mutations at each targeted locus are plotted. Across F0 knockout samples: 99.0 ± 2.7% mutated reads, 78.6 ± 29.7% of all reads had a frameshift mutation.

d, (above) Schematic of *psen2* in the 5'–3' genome direction, as in c). (below) Percentage of reads mutated and frameshifted at each targeted locus of *psen2*, as in c). Across F0 knockout samples: 99.9 ± 0.1% mutated reads, 82.0 ± 33.6% of all reads had a frameshift mutation.

e, Concentration of Aβ40 and Aβ42 in pools of n = 16–22 uninjected, scrambled-injected, *psen1* F0 knockout, and *psen2* F0 knockout 16-dpf larvae. Each datapoint is the mean of four technical replicates. Concentration unit is ng of Aβ40/42 per g of total protein extracted. Horizontal black line represents the limit of detection. Red crosses indicate samples for which all technical replicates were below the limit of detection. All Aβ38 measurements were below the limit of detection and are not plotted.

f, Pictures of *psen2* (top row) and *psen1* (bottom row) F0 knockout larvae at 16 dpf. Note the fainter pigmentation of *psen2* F0 knockout larvae.

g, (left) Activity (sum of Δ pixels/10 minutes) of *psen2* F0 knockout larvae and scrambled-injected siblings during 48 hr on a 14 hr:10 hr light:dark cycle (white background for days, dark grey background for nights). (right) Sleep (minutes per 10-minute epoch) during the same experiment. Traces are mean ± SEM across larvae. See also **Fig. 3–supplement 2a** for results from replicate clutch 2.

h, Behavioural fingerprints of two clutches of *psen2* F0 knockout larvae. Each dot represents the mean deviation from the same-clutch scrambled-injected mean for that parameter (z-score, mean ± SEM). Asterisks represent the p-values by likelihood-ratio test on linear mixed effects models calculated on the raw parameter values. *cos*, cosine similarity between the two clutch fingerprints.

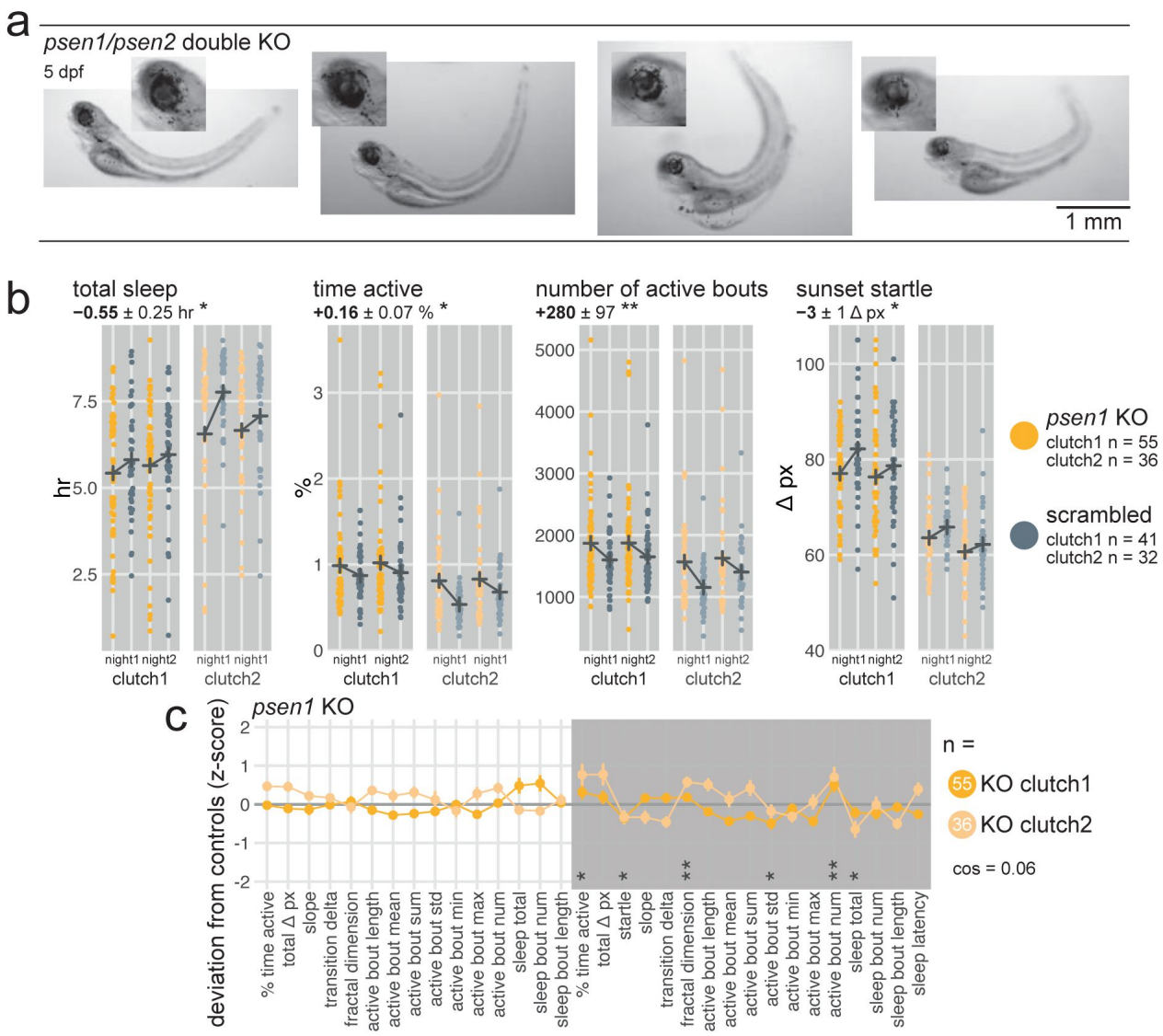

Fig. 3–suppl. 1

psen1 F0 knockouts are slightly hyperactive at night.

a, Pictures of *psen1/psen2* double F0 knockout larvae (5 dpf). Note patchy retinal pigment epithelium and eye oedema (insets).

b, Parameter plots for two clutches of *psen1* F0 knockout larvae and scrambled-injected siblings. Each dot represents one larva during one night. Black crosses mark the group means. At night, *psen1* F0 knockouts slept less (total sleep, * p = 0.030), spent more time active (time active, * p = 0.018), and initiated more swimming bouts (number of active bouts, ** p = 0.004) than scrambled-injected siblings. The startle response of *psen1* F0 knockouts was also slightly suppressed (sunset startle, * p = 0.015). Statistics by likelihood-ratio test on linear mixed effects models.

c, Behavioural fingerprints of two clutches of *psen1* F0 knockout larvae. Each dot represents the mean deviation from the same-clutch scrambled-injected mean for that parameter (z-score, mean ± SEM). Asterisks represent the p-values by likelihood-ratio test on linear mixed effects models calculated on the raw parameter values, as in b). *cos*, cosine similarity between the two clutch fingerprints.

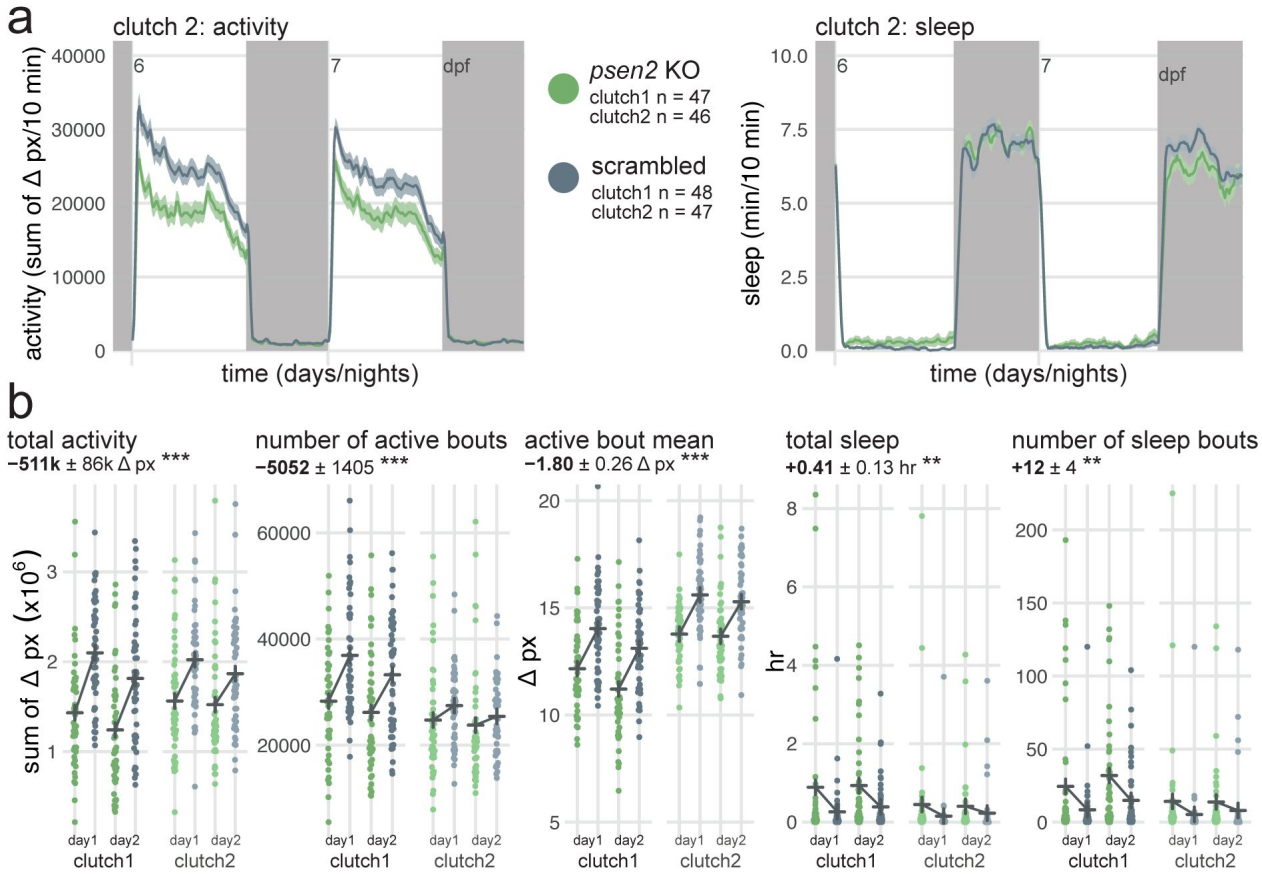
a
clutch 2: activity
activity (sum of Δ px/10 min)
40000
30000
20000
10000
0
6
7
dpf
time (days/nights)
psen2 KO
clutch1 n = 47
clutch2 n = 46
scrambled
clutch1 n = 48
clutch2 n = 47
clutch 2: sleep
sleep (min/10 min)
10.0
7.5
5.0
2.5
0.0
6
7
dpf
time (days/nights)
b
total activity
−511k ± 86k Δ px ***
sum of Δ px (x10^6)
number of active bouts
−5052 ± 1405 ***
active bout mean
−1.80 ± 0.26 Δ px ***
Δ px
total sleep
+0.41 ± 0.13 hr **
hr
number of sleep bouts
+12 ± 4 **
day1
day2
clutch1
clutch2

Fig. 3–suppl. 2

sleep/wake behaviour of *psen2* F0 knockouts.

a, (left) Activity (sum of Δ pixels/10 minutes) of *psen2* F0 knockout larvae and scrambled-injected siblings during 48 hr on a 14 hr:10 hr light:dark cycle (white background for days, dark grey background for nights). (right) Sleep (minutes per 10-minute epoch) during the same experiment. Traces are mean ± SEM across larvae. This replicate experiment is called clutch 2 in **Fig. 3h**.

b, Parameter plots for two clutches of *psen2* F0 knockout larvae and scrambled-injected siblings. Each dot represents one larva during one day. Black crosses mark the group means. Compared to scrambled-injected siblings, *psen2* F0 knockouts displaced fewer pixels (total activity, *** $p < 0.001$) and initiated fewer swimming bouts (number of active bouts, *** $p < 0.001$), each displacing fewer pixels in average (active bout mean, *** $p < 0.001$). They also spent more time asleep (total sleep, ** $p = 0.002$) and initiated more sleep bouts (number of sleep bouts, ** $p = 0.002$) than scrambled-injected siblings. Statistics by likelihood-ratio test on linear mixed effects models.

a, Pictures of *psen2* F0 knockout larvae (top row) and scrambled-injected control larvae (bottom row) at the end of the behavioural tracking (8 dpf). Note the fainter pigmentation of *psen2* F0 knockout larvae, particularly over the swim bladder (marked by black arrowheads).

b, Frame-by-frame Δ pixel timeseries of two individual larvae showing the startle response shortly after the lights turn off. (left) Startle response of a *psen2* F0 knockout larva. During the 3 seconds after lights-off, the most vigorous bout reached a maximum Δ pixel value of 75 px. (right) Startle response of a scrambled-injected larva. During the 3 seconds after lights-off, the most vigorous bout reached a maximum Δ pixel value of 85 px.

c, Maximum startle responses over the three consecutive lights-off transitions, by clutch (clutch 1 and clutch 2) and group (*psen2* KO or scrambled). Each dot represents one larva. The startle response was defined as the maximum Δ pixel during the 3 seconds directly after lights-off (see b). There were three lights-off transitions during the experiment; plotted for each larva is the largest of the three startle responses (maximum startle response). (left) Unprocessed data. scrambled-injected larvae displaced more pixels during the startle response at lights-off compared to *psen2* F0 knockout larvae, presumably because they appeared darker to the camera (clutch 1: * $p = 0.042$; clutch 2: *** $p < 0.001$, by Welch's t-test). The ratio of the means estimated how much darker *psen2* knockout larvae were compared to scrambled-injected larvae; that is, *psen2* knockout larvae were 0.89 and 0.95× as dark as scrambled-injected larvae. (right) The ratios were then used to downscale the frame-by-frame Δ pixel data of the scrambled-injected larvae, in a sense artificially making them as faint as *psen2* knockout larvae. As intended, the downscaling rendered the differences in startle response non-significant (clutch 1: ns $p = 0.78$; clutch 2: ns $p = 0.77$, by Welch's t-test).

d, The original activity trace (sum Δ pixels/10 minutes, mean ± SEM) of scrambled-injected larvae (lighter grey) compared to the downscaled one (darker grey), during the first day and night as illustration. The data of *psen2* F0 knockouts is not shown as it is not modified during the downscaling.

e, Behavioural fingerprints of two clutches of *psen2* F0 knockout larvae, before and after downscaling the Δ pixel data of the scrambled-injected larvae. Each dot represents the mean deviation from the same-clutch scrambled-injected mean for that parameter (z-score, mean ± SEM). Two parameters were excluded from the fingerprints: sunset startle, as the difference between knockouts and controls was artificially nullified by the pixel scaling procedure; and active bout minimum, because the pixel scaling procedure artefactually raised this parameter for scrambled-injected larvae. Asterisks represent the p-values by likelihood-ratio test on linear mixed effects models calculated on the raw parameter values. *cos*, cosine similarity between the two clutch fingerprints.

The pixel scaling procedure is available as a function (*pixelAdjust(...)*) in the FramebyFrame R package.

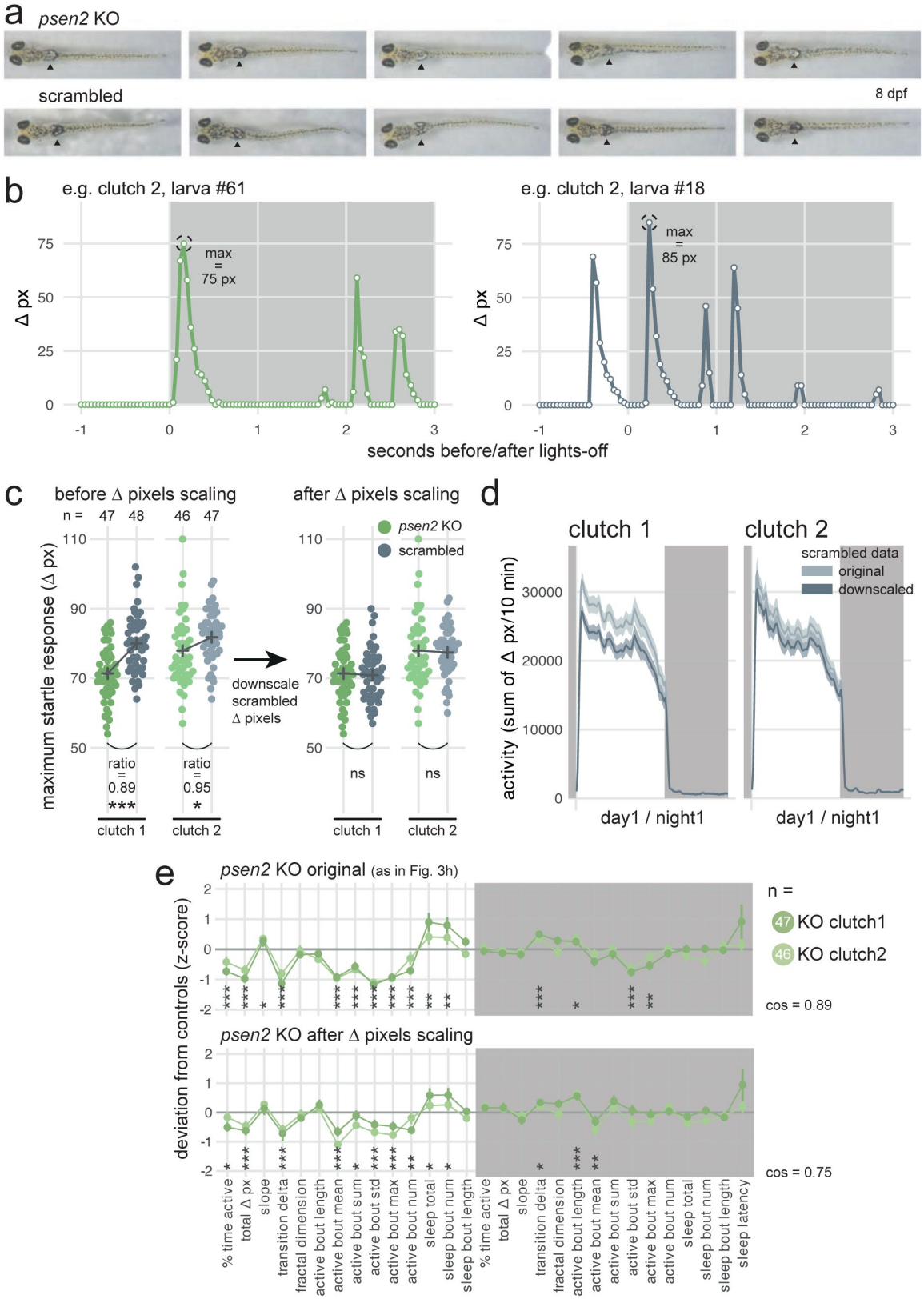
a
psen2 KO
scrambled
8 dpf
b
e.g. clutch 2, larva #61
max = 75 px
e.g. clutch 2, larva #18
max = 85 px
Δ px
seconds before/after lights-off
c
before Δ pixels scaling
after Δ pixels scaling
n = 47 48 46 47
maximum startle response (Δ px)
psen2 KO
scrambled
downscale scrambled Δ pixels
ratio = 0.89
ratio = 0.95
ns
clutch 1
clutch 2
d
clutch 1
clutch 2
scrambled data
original
downscaled
activity (sum of Δ px/10 min)
day1 / night1
e
psen2 KO original (as in Fig. 3h)
psen2 KO after Δ pixels scaling
deviation from controls (z-score)
n =
47 KO clutch1
46 KO clutch2
cos = 0.89
cos = 0.75
% time active
total Δ px
slope
transition delta
fractal dimension
active bout length
active bout mean
active bout sum
active bout std
active bout max
active bout num
sleep total
sleep bout num
sleep bout length
sleep latency

Fig. 3–suppl. 3

The behavioural phenotype of psen2 F0 knockouts is not an artefact caused by their fainter pigmentation.

a, Pictures of *psen2* F0 knockout larvae (top row) and scrambled-injected control larvae (bottom row) at the end of the behavioural tracking (8 dpf). Note the fainter pigmentation of *psen2* F0 knockout larvae, particularly over the swim bladder (marked by black arrowheads).

b, Frame-by-frame Δ pixel timeseries of two individual larvae showing the startle response shortly after the lights turn off. (left) Startle response of a *psen2* F0 knockout larva. During the 3 seconds after lights-off, the most vigorous bout reached a maximum Δ pixel value of 75 px. (right) Startle response of a scrambled-injected larva. During the 3 seconds after lights-off, the most vigorous bout reached a maximum Δ pixel value of 85 px.

c, Maximum startle responses over the three consecutive lights-off transitions, by clutch (clutch 1 and clutch 2) and group (*psen2* KO or scrambled). Each dot represents one larva. The startle response was defined as the maximum Δ pixel during the 3 seconds directly after lights-off (see b). There were three lights-off transitions during the experiment; plotted for each larva is the largest of the three startle responses (maximum startle response). (left) Unprocessed data. scrambled-injected larvae displaced more pixels during the startle response at lights-off compared to *psen2* F0 knockout larvae, presumably because they appeared darker to the camera (clutch 1: * $p = 0.042$; clutch 2: *** $p < 0.001$, by Welch's t-test). The ratio of the means estimated how much darker *psen2* knockout larvae were compared to scrambled-injected larvae; that is, *psen2* knockout larvae were 0.89 and 0.95× as dark as scrambled-injected larvae. (right) The ratios were then used to downscale the frame-by-frame Δ pixel data of the scrambled-injected larvae, in a sense artificially making them as faint as *psen2* knockout larvae. As intended, the downscaling rendered the differences in startle response non-significant (clutch 1: ns $p = 0.78$; clutch 2: ns $p = 0.77$, by Welch's t-test).

d, The original activity trace (sum Δ pixels/10 minutes, mean ± SEM) of scrambled-injected larvae (lighter grey) compared to the downscaled one (darker grey), during the first day and night as illustration. The data of *psen2* F0 knockouts is not shown as it is not modified during the downscaling.

e, Behavioural fingerprints of two clutches of *psen2* F0 knockout larvae, before and after downscaling the Δ pixel data of the scrambled-injected larvae. Each dot represents the mean deviation from the same-clutch scrambled-injected mean for that parameter (z-score, mean ± SEM). Two parameters were excluded from the fingerprints: sunset startle, as the difference between knockouts and controls was artificially nullified by the pixel scaling procedure; and active bout minimum, because the pixel scaling procedure artefactually raised this parameter for scrambled-injected larvae. Asterisks represent the p-values by likelihood-ratio test on linear mixed effects models calculated on the raw parameter values. cos, cosine similarity between the two clutch fingerprints.

The pixel scaling procedure is available as a function (*pixelAdjust*(...)) in the FramebyFrame R package.

In humans, PSEN1 or PSEN2 acts as the catalytic subunit of the γ-secretase protein complex, which is responsible for the cleavage of more than 90 substrates, such as Notch. It also performs the last cleavage of APP to release Aβ, which aggregates in the brains of patients with AD[7,9,47,48]. Do presenilins also cleave zebrafish Appa/Appb into Aβ? Using a sensitive ELISA-based assay, Aβ40 and Aβ42 were detectable in control (uninjected and scrambled-injected) larvae but not in two clutches of *psen1* F0 knockouts (**Fig. 3e**), confirming that zebrafish Psen1 is required for the cleavage of Appa/Appb into Aβ. In contrast, Aβ40 and Aβ42 were detectable in *psen2* F0 knockouts, suggesting that most Aβ is generated by Psen1 in zebrafish and that Psen2 alone cannot compensate. This result extends previous findings that Aβ production in zebrafish is blocked by the γ-secretase inhibitor DAPT[49] and matches closely observations in mice, in which loss of PSEN2 had no measurable effect on Aβ40/42 production[50,51].

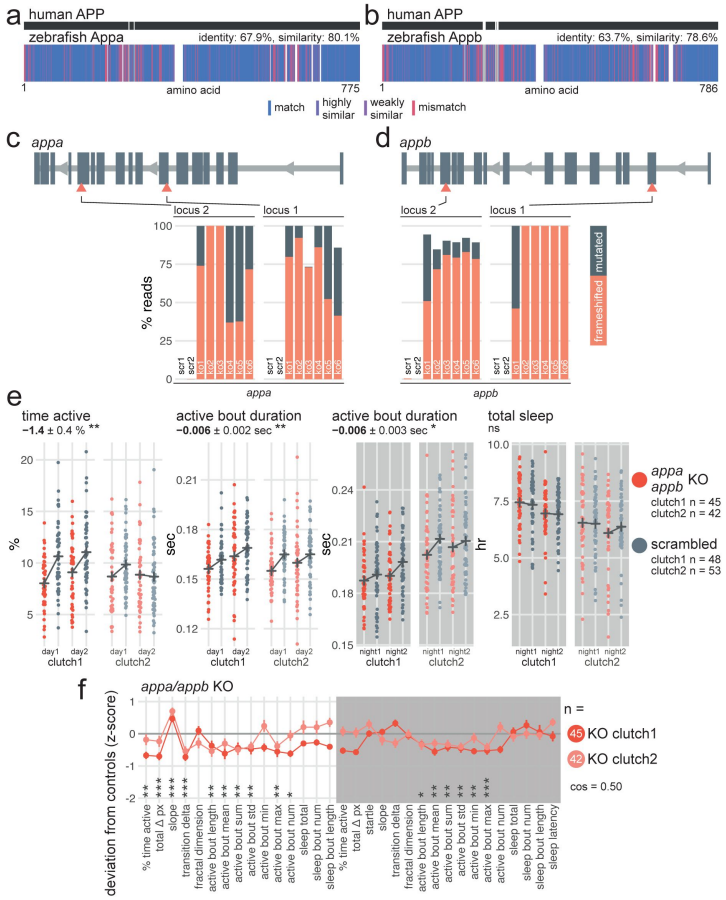

Fig. 3–suppl. 4

appa/appb F0 knockouts have subdued swimming bouts throughout the day/night cycle.

a, Human APP amino acid sequence (top) aligned to zebrafish Appa amino acid sequence (bottom). In the zebrafish protein, each amino acid (vertical bar) is coloured based on its similarity with the human protein. White gaps are added when additional residues are present in the other sequence.
b, Human APP amino acid sequence (top) aligned to zebrafish Appb amino acid sequence (bottom), as in a).
c, (top) Schematic of *appa* in the 5'–3' genome direction. Exons are in dark grey; tall exons are protein-coding, small are 5'- or 3'-UTR. Light grey lines are introns, and grey arrows represent the direction of transcription. Orange arrowheads mark the target loci. Exons and introns are on different scales. (bottom) Percentage of reads mutated (height of each bar, with orange representing percentage with a frameshift mutation) at each targeted locus of *appa*. *scr*, scrambled-injected control larva; *ko*, *appa* F0 knockout larva. Across F0 knockout samples: 96.6 ± 8.4% mutated reads, 70.4 ± 23.2% of all reads had a frameshift mutation.
d, (top) Schematic of *appb*, as in c). (bottom) Percentage of reads mutated (height of each bar, with orange representing percentage with a frameshift mutation) at each targeted locus of *appb*. *scr*, scrambled-injected control larva; *ko*, *appb* F0 knockout larva. Across F0 knockout samples: 95.0 ± 5.6% mutated reads, 82.6 ± 19.0% of all reads had a frameshift mutation. In c) and d), the numbers refer to individual animals. For example, ko5 refers to an individual *appa/appb* double F0 knockout larva for which mutations at the four targeted loci are plotted.
e, Parameter plots for two clutches of *appa/appb* F0 knockout larvae and scrambled-injected siblings. Each dot represents one larva during one day (left) or night (right). Black crosses mark the group means. Compared to scrambled-injected controls, *appa/appb* F0 knockouts spent less time active during the day (time active, ** p = 0.002) and had shorter swimming bouts across the day/night cycle (active bout duration, day: ** p = 0.003; night: * p = 0.018). Sleep was not affected (sleep total, ns p = 0.71). Statistics by likelihood-ratio test on linear mixed effects models.
f, Behavioural fingerprints of two clutches of *appa/appb* double F0 knockout larvae. Each dot represents the mean deviation from the same-clutch scrambled-injected mean for that parameter (z-score, mean ± SEM). Asterisks represent the p-values by likelihood-ratio test on linear mixed effects models calculated on the raw parameter values. *cos*, cosine similarity between the two clutch fingerprints.

In mice, knockout of *Psen1*, but not of *Psen2*, causes severe skeletal malformations and brain haemorrhages, likely because of impaired Notch signalling[51]. Homozygous animals die within minutes after birth[52]. Morphologically, our *psen1* F0 knockout larvae developed normally (tested up to 16 dpf) and were indistinguishable from their wild-type siblings, as observed in a *psen1* stable knockout line[53]. *psen2* F0 knockout larvae had a mild pigmentation defect (**Fig. 3f** and **Fig. 3–supplement 3a**), which has been previously reported in a *psen2* stable knockout line[54]. This difference suggests a specific function of Psen2 in melanophore development or function which cannot be fulfilled by Psen1. We also generated *psen1*/*psen2* double F0 knockouts but most were lethal early in development (~5 dpf) with severe defects in eye development (**Fig. 3–supplement 1a**), in which the retinal pigment epithelium appeared patchy and some larvae developed oedema around the eye. The tail was severely curved outwards, in exactly the same way as larvae treated with a high dose of the γ-secretase inhibitor DAPT[55]. Incidentally, *Psen1* knockout mice also display defects in the axial skeleton[52]. Overall, these results suggest that zebrafish presenilins are more readily capable of compensating each other during development than in mice, as only double *psen1*/*psen2* knockout larvae showed a severe morphological phenotype.

We next video-tracked two clutches of *psen1* and *psen2* F0 knockout larvae over multiple day-night cycles and applied our frame-by-frame analysis to detect behavioural phenotypes over long and short timescales. The loss of Psen1 only had mild effects on behaviour. At night, *psen1* F0 knockout larvae slept slightly less (−8% vs. scrambled, **Fig. 3–supplement 1b**) and instead spent more time active than control injected siblings (+22%), mainly because they performed more swimming bouts (+20%). The *psen1* knockouts also showed a slightly reduced startle response at lights-off (−4%), in line with some data obtained from stable *psen1* knockout larvae[53]. Behaviour during the day was not affected (**Fig. 3– supplement 1c**). In contrast, *psen2* F0 knockouts of both clutches were substantially less active than controls during the day (total activity: −26% vs. scrambled, **Fig. 3g**,**h** and **Fig. 3– supplement 2a**,**b**), performing both fewer (−17%) and more subdued swimming bouts (active bout mean: −12%). *psen2* F0 knockouts also slept more during the day than controls (**Fig. 3g**,**h**, **Fig. 3–supplement 2a**,**b**), both spending more time asleep (+178%) and initiating more frequent sleep bouts (+150%). Loss of Psen2 did not strongly affect night-time behaviour. In summary, *psen2* F0 knockout larvae were substantially less active and sleeping more than controls during the day.

Since *psen2* knockout larvae were less pigmented (Fig. 3–supplement 3a), we tested whether the reduction in activity could be an artefact due to fainter detection by the camera. We extracted the maximum Δ pixel value each larva reached during the startle response at lights off (**Fig. 3–supplement 3b**). These vigorous swimming bouts can displace the whole larva in a tenth of a second, providing a measure of how many dark pixels are detectable for each larva. *psen2* F0 knockout larvae indeed displaced fewer pixels during the startle response than scrambled-injected controls (Fig. 3–supplement 3c, clutch 1: *psen2* knockouts displaced 78 ± 10 pixels vs. 82 ± 8 pixels for scrambled-injected controls, clutch 2: 71 ± 8 pixels vs 80 ± 8 pixels). We then downscaled the Δ pixel values of the scrambled-injected larvae proportionally to the ratio of the startle response means (Fig. 3–supplement 3c,**d**), akin to artificially making the scrambled-injected larvae appear less dark. Even after this adjustment, *psen2* F0 knockouts were measurably less active and sleeping more during the day, although the parameter effect sizes were somewhat reduced (Fig. 3–supplement 3e). In summary, the *psen2* behavioural phenotype reflects a genuine difference in behaviour.

Finally, we examined the impact of loss of both Appa and Appb. While overexpression of APP causes AD[56], knockout could point to roles of APP during brain development. As described previously[49,57], zebrafish Appa and Appb are highly similar to human APP (64– 68% identical amino acid sequence, **Fig. 3–supplement 4a**,**b**). We generated *appa*/*appb* double F0 knockout larvae by mutating each gene at two loci, rather than three, to limit unviability[20]. The CRISPR-Cas9 RNPs were highly mutagenic (across all four loci: 95.8 ± 7.0% mutated reads, 76.5 ± 21.7 of all

reads had a frameshift mutation, **Fig. 3–supplement 4c**,**d**). The *appa*/*appb* double F0 knockout larvae looked morphologically normal. Behaviourally, *appa*/*appb* double knockouts were less active during the day than control siblings (–14% vs. scrambled, **Fig. 3–supplement 4e**) and showed shorter swimming bouts across the day/night cycle (active bout duration during the day: –4%; at night: –3%). Sleep was not consistently affected by the loss of *appa*/*appb* (**Fig. 3–supplement 4f**).

In summary, knockout larvae for the three genes associated with early-onset AD had distinct morphological and behavioural phenotypes, with the strongest behavioural changes observed for *psen2* knockouts. Since both presenilins are broadly expressed in the larval brain (**Fig. 1d** and **Fig. 1–supplement 3c**,**d**), these results indicate that zebrafish Psen1-and Psen2-γ-secretases likely cleave different substrates, such as Appa/Appb which is primarily cleaved into Aβ by Psen1-γ-secretase. Moreover, the behavioural phenotypes of *appa*/*appb* and *psen1* knockout larvae had little overlap while they presumably both resulted in the loss of Aβ. The *appa*/*appb* day phenotype could be primarily caused by loss of some Appa/Appb cleavage product not relying on γ-secretase. Alternatively, the net effect of loss of all other Psen1-γ-secretase products could have masked the effect of loss of Aβ.

Knockouts in all four tested late-onset Alzheimer's risk genes sleep less at night

To test whether knockout of genes associated with late-onset AD also impacted behaviour in larvae, we then generated F0 knockouts for the zebrafish orthologues of *APOE* (*apoea*/*apoeb*), *CD2AP* (*cd2ap*), *CLU* (*clu*), and *SORL1* (*sorl1*).

APOE shares 22–25% amino acid identity with its two zebrafish orthologues, Apoea and Apoeb (**Fig. 4–supplement 1a**,**b**). To make *apoea*/*apoeb* double F0 knockouts, we targeted each gene at two loci in separate exons with highly mutagenic CRISPR-Cas9 RNPs (**Fig. 4– supplement 1c**,**d**). Consistently across three clutches, double *apoea*/*apoeb* F0 knockout larvae performed slightly more subdued swimming bouts during the day than scrambled-injected siblings (active bout mean: −4%; active bout maximum: −5% vs. scrambled; **Fig. 4– supplement 1e**). This slight hypoactivity is unlikely to reflect a motor defect because at night, *apoea*/*apoeb* knockouts performed more swimming bouts (+31%) and had less sleep (−7%, **Fig. 4–supplement 1e**) than controls.

Knockout of other late-onset AD risk genes also impacted behaviour, especially at night. We mutated zebrafish *cd2ap* (44% identical amino acid sequence vs. human CD2AP; **Fig. 4–supplement 2a**), at three loci on distinct exons (**Fig. 4–supplement 2b**). While the two clutches of *cd2ap* F0 knockouts gave generally inconsistent results, knockout larvae of both clutches were more active (time active: +38%; total activity: +44% vs. scrambled) and slept less at night than control siblings (−13%), mainly because they performed more swimming bouts (+34%, **Fig. 4–supplement 2c**). Similarly, knockout of *clu* (39% identical amino acid sequence vs. human CLU, **Fig. 4–supplement 3a**) did not strongly affect behaviour during the day (**Fig. 4–supplement 3c**), despite a particularly high rate of frameshift mutations at all three targeted loci (**Fig. 4–supplement 3b**). At night, *clu* F0 knockouts were slightly more active (time active: +12% vs. scrambled) and slept less than control siblings (−7%, **Fig. 4– supplement 3c**). Finally, we generated F0 knockouts for *sorl1* (63% identical amino acid sequence vs. human SORL1, **Fig. 4–supplement 4a**) by mutating three exons (**Fig. 4– supplement 4b**). *sorl1* F0 knockout larvae were less active during the day but slept less at night (**Fig. 4–supplement 4c** and **Fig. 4–supplement 5**). Specifically, during the day (**Fig. 4– supplement 4d**), *sorl1* F0 knockouts spent less time active than scrambled-injected larvae (−15% vs. scrambled), performing fewer swimming bouts (−15%) of approximately the same duration and intensity as controls. Sleep during the day was unaffected. At night (**Fig. 4–supplement 4d**), *sorl1* F0 knockouts spent more

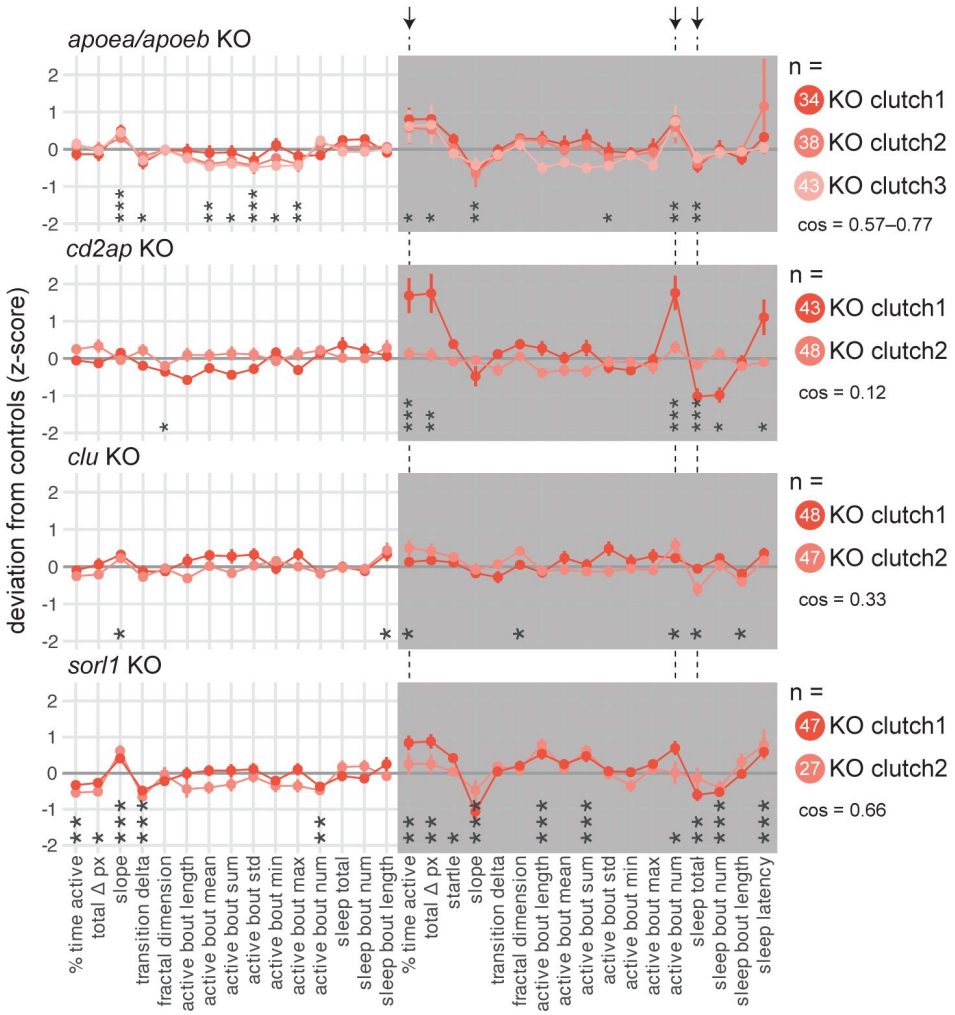

Fig. 4

F0 knockout larvae in genes associated with late-onset Alzheimer's disease slept less at night.

For each gene: behavioural fingerprints of N = 2–3 clutches of F0 knockout larvae. Each dot represents the mean deviation from the same-clutch scrambled-injected mean for that parameter (z-score, mean ± SEM). Asterisks represent the p-values by likelihood-ratio test on linear mixed effects models calculated on the raw parameter values. *cos*, cosine similarities between fingerprints. Arrows and dashed lines mark the three parameters which are significant for all four late-onset Alzheimer's risk genes tested.

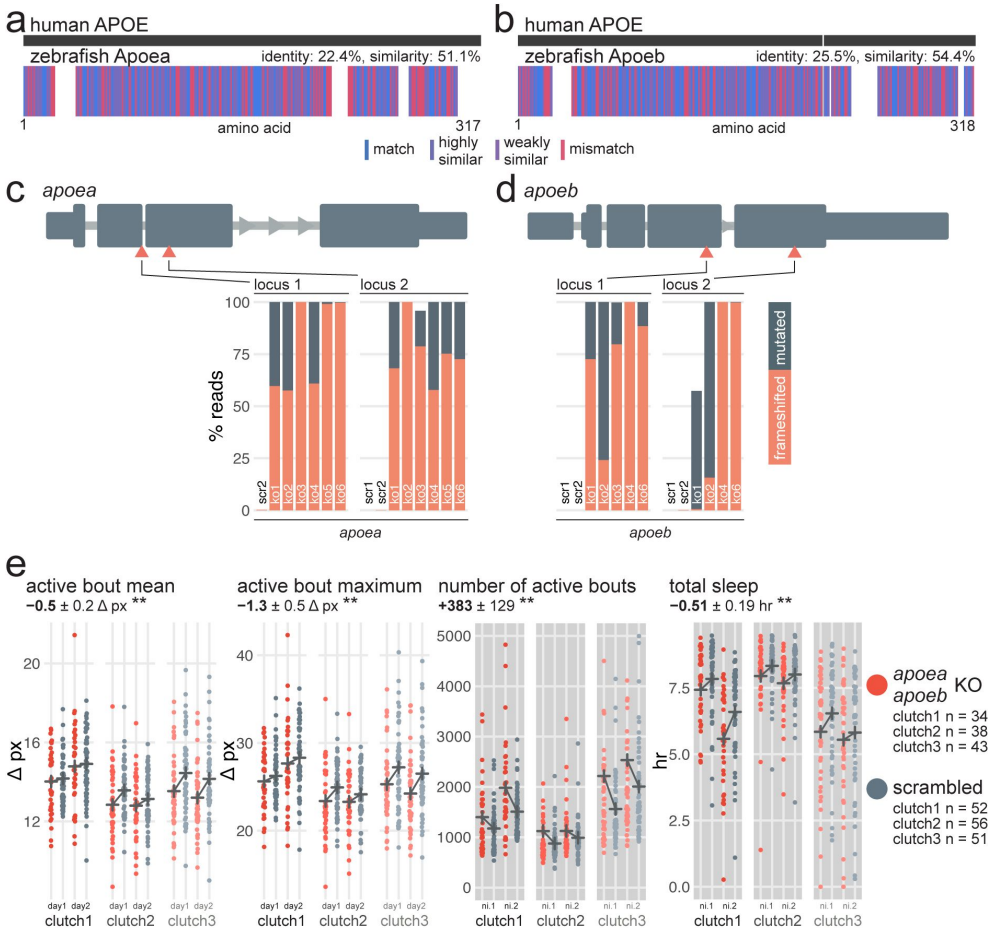

Fig. 4–suppl. 1

apoea/apoeb double F0 knockouts have subdued swimming bouts during the day and sleep less at night.

a, Human APOE amino acid sequence (top) aligned to zebrafish Apoea amino acid sequence (bottom). In the zebrafish protein, each amino acid (vertical bar) is coloured based on its similarity with the human protein. White gaps are added when additional residues are present in the other sequence.
b, Human APOE amino acid sequence (top) aligned to zebrafish Apoeb amino acid sequence (bottom), as in a).
c, (top) Schematic of *apoea* in the 5'–3' genome direction. Exons are in dark grey; tall exons are protein-coding, small are 5'- or 3'-UTR. Light grey lines are introns, and grey arrows represent the direction of transcription. Orange arrowheads mark the target loci. Exons and introns are on different scales. (bottom) Percentage of reads mutated (height of each bar, with orange representing percentage with a frameshift mutation) at each targeted locus of *apoea*. *scr*, scrambled-injected control larva; *ko*, *apoea* F0 knockout larva. Across F0 knockout samples: 99.6 ± 1.2% mutated reads, 77.5 ± 17.8% of all reads had a frameshift mutation.
d, (top) Schematic of *apoeb*, as in c). (bottom) Percentage of reads mutated (height of each bar, with orange representing percentage with a frameshift mutation) at each targeted locus of *apoeb*. *scr*, scrambled-injected control larva; *ko*, *apoeb* F0 knockout larva. Across F0 knockout samples: 95.2 ± 14.2% mutated reads, 64.6 ± 39.9% of all reads had a frameshift mutation. In c) and d), the numbers refer to individual animals. For example, ko6 refers to an individual *apoea/apoeb* double F0 knockout larva for which mutations at the four targeted loci are plotted.
e, Parameter plots for three clutches of *apoea/apoeb* double F0 knockout larvae and scrambled-injected siblings. Each dot represents one larva during one day (left) or night (right). Black crosses mark the group means. (left) During the day, *apoea/apoeb* double F0 knockout larvae had more subdued swimming bouts than scrambled-injected siblings (active bout mean, ** p = 0.006; active bout maximum, ** p = 0.004). (right) At night, *apoea/apoeb* double F0 knockout larvae were performing more swimming bouts (number of active bouts, ** p = 0.003) and sleeping less (total sleep, ** p = 0.009) than scrambled-injected siblings. Six datapoints from four *apoea/apoeb* F0 knockout larvae fall outside the Y axis limit of the number of active bouts (7,229–13,975 bouts). Statistics by likelihood-ratio test on linear mixed effects models. *ni.*, night.

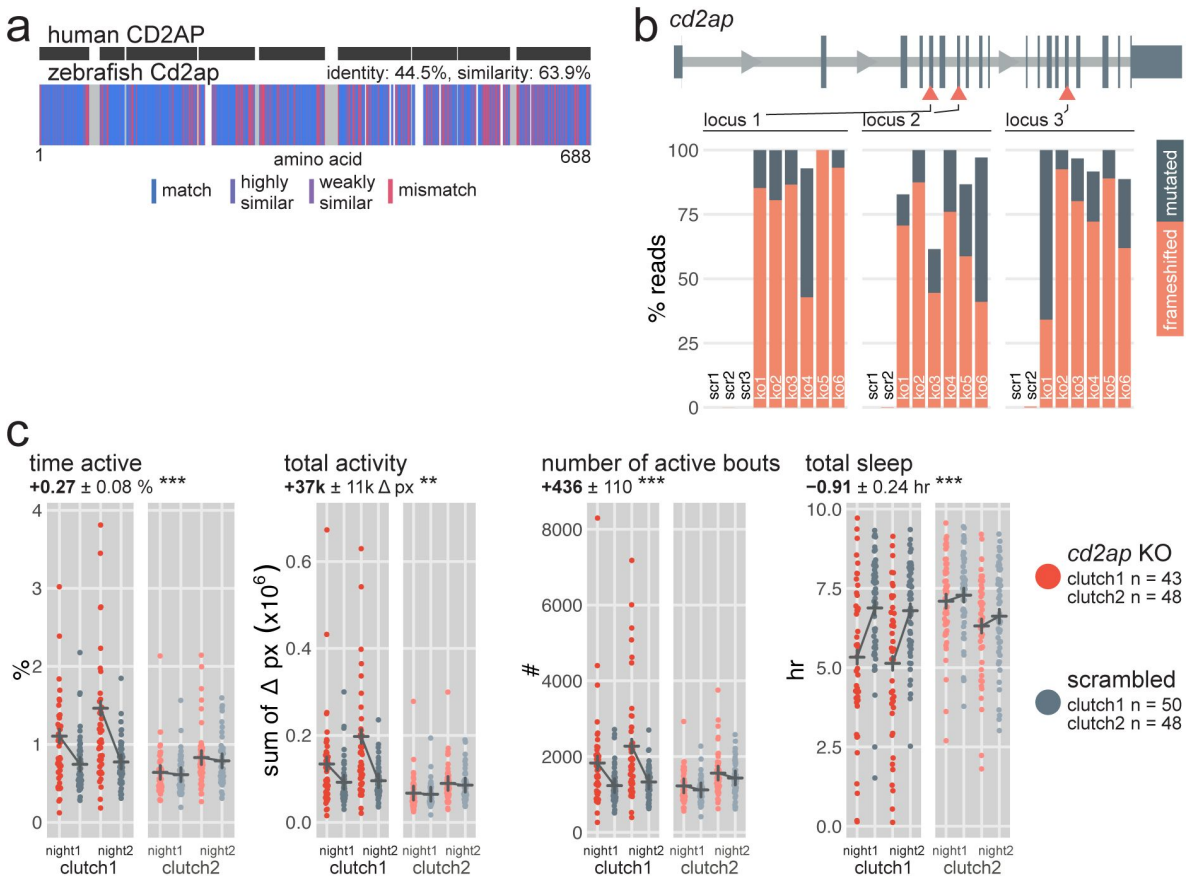

Fig. 4–suppl. 2

cd2ap F0 knockouts are hyperactive at night.

a, Human CD2AP amino acid sequence (top) aligned to zebrafish Cd2ap amino acid sequence (bottom). In the zebrafish protein, each amino acid (vertical bar) is coloured based on its similarity with the human protein. White gaps are added when additional residues are present in the other sequence.

b, (top) Schematic of *cd2ap* in the 5'–3' genome direction. Exons are in dark grey; tall exons are protein-coding, small are 5'- or 3'-UTR. Light grey lines are introns, and grey arrows represent the direction of transcription. Orange arrowheads mark the target loci. Exons and introns are on different scales. (bottom) Percentage of reads mutated (height of each bar, with orange representing percentage with a frameshift mutation) at each targeted locus of *cd2ap*. *scr*, scrambled-injected control larva; *ko*, *cd2ap* F0 knockout larva. The numbers refer to individual animals. For example, ko1 refers to an individual *cd2ap* F0 knockout larva for which mutations at each targeted locus are plotted. Across F0 knockout samples: 94.3 ± 9.8% mutated reads, 72.1 ± 20.3% of all reads had a frameshift mutation.

c, Parameter plots for two clutches of *cd2ap* F0 knockout larvae and scrambled-injected siblings. Each dot represents one larva during one night. Black crosses mark the group means. At night, *cd2ap* F0 knockouts spent more time active (time active, *** $p < 0.001$), displaced more pixels in total (total activity, ** $p = 0.001$), initiated more swimming bouts (number of active bouts, *** $p < 0.001$), and slept less (total sleep, *** $p < 0.001$) than scrambled-injected siblings.

Three datapoints from two *cd2ap* F0 knockout larvae (clutch1) fall outside the Y axis limit of the time active plot (5.1–5.8 hr). One datapoint from a *cd2ap* F0 knockout larvae (clutch1) falls outside the Y axis limit of the total activity plot (1.2×10^6 Δ px).

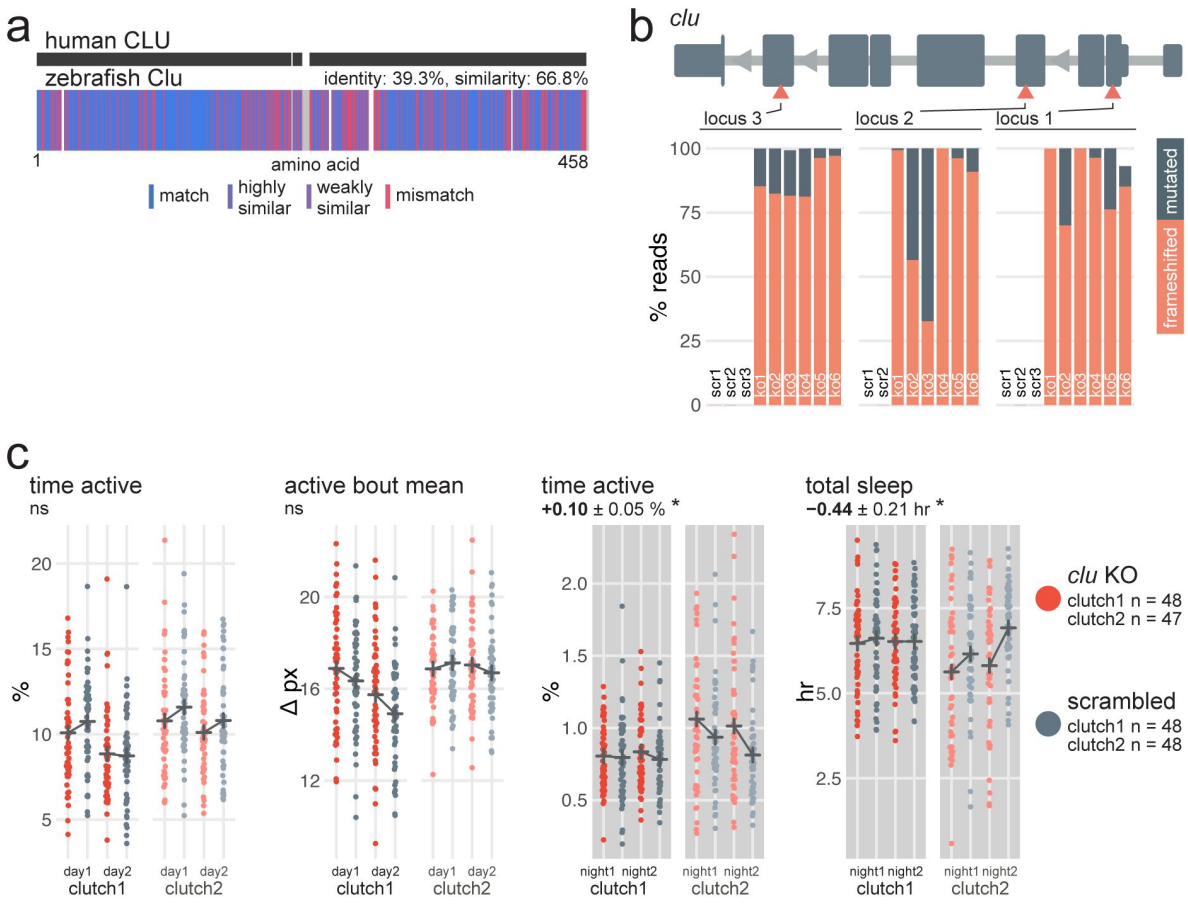

Fig. 4–suppl. 3

clu F0 knockouts sleep slightly less at night.

a, Human CLU amino acid sequence (top) aligned to zebrafish Clu amino acid sequence (bottom). In the zebrafish protein, each amino acid (vertical bar) is coloured based on its similarity with the human protein. White gaps are added when additional residues are present in the other sequence.

b, (top) Schematic of *clu* in the 5'–3' genome direction. Exons are in dark grey; tall exons are protein-coding, small are 5'- or 3'-UTR. Light grey lines are introns, and grey arrows represent the direction of transcription. Orange arrow-heads mark the target loci. Exons and introns are on different scales. (bottom) Percentage of reads mutated (height of each bar, with orange representing percentage with a frameshift mutation) at each targeted locus of *clu*. *scr*, scrambled-injected control larva; *ko*, *clu* F0 knockout larva. The numbers refer to individual animals. For example, ko2 refers to an individual *clu* F0 knockout larva for which mutations at each targeted locus are plotted. Across F0 knockout samples: 99.6 ± 1.6% mutated reads, 84.9 ± 17.7% of all reads had a frameshift mutation.

c, Parameter plots for two clutches of *clu* F0 knockout larvae and scrambled-injected siblings. Each dot represents one larva during one day (left) or night (right). Black crosses mark the group means. Loss of Clu did not consistently affect locomotor activity during the day (time active, ns p = 0.18; active bout mean, ns p = 0.21). At night, *clu* F0 knockouts were slightly more active (time active, * p = 0.047) and slept less (total sleep, * p = 0.033) than scrambled-injected siblings, although the effect sizes were not well replicated across clutches. One datapoint from a *clu* F0 knockout larvae (clutch2) falls outside the Y axis limit of the night time active plot (3.3%).

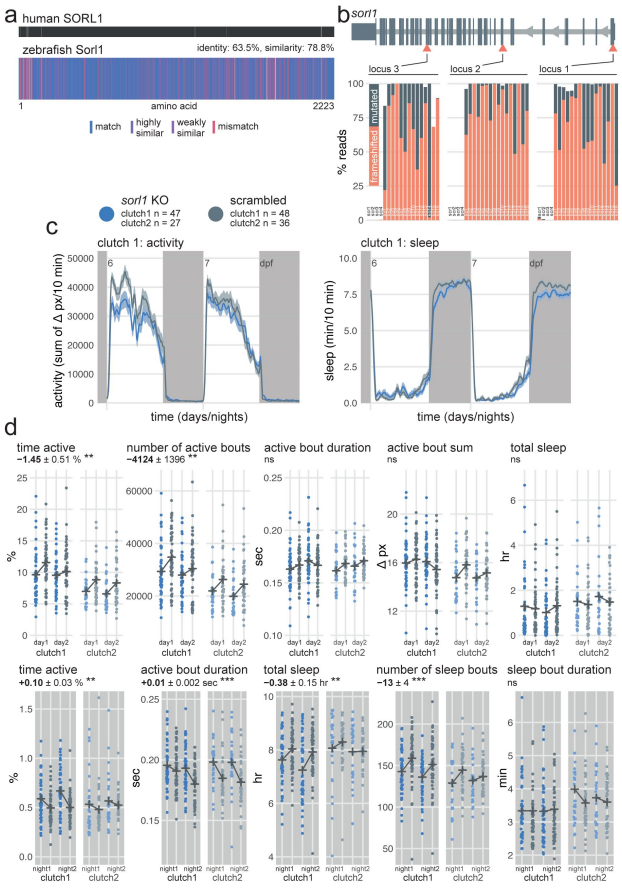

Fig. 4–suppl. 4

sorl1 F0 knockouts are hypoactive during the day but hyperactive at night.

a, Human SORL1 amino acid sequence (top) aligned to zebrafish Sorl1 amino acid sequence (bottom). In the zebrafish protein, each amino acid (vertical bar) is coloured based on its similarity with the human protein. White gaps are added when additional residues are present in the other sequence.
b, (top) Schematic of *sorl1* in the 5'–3' genome direction. Exons are in dark grey; tall exons are protein-coding, small are 5'- or 3'-UTR. Light grey lines are introns, and grey arrows represent the direction of transcription. Orange arrowheads mark the target loci. Exons and introns are on different scales. (bottom) Percentage of reads mutated (height of each bar, with orange representing percentage with a frameshift mutation) at each targeted locus of *sorl1*. *scr*, scrambled-injected control larva; *ko*, *sorl1* F0 knockout larva. The numbers refer to individual animals. For example, ko6 refers to an individual *sorl1* F0 knockout larva for which mutations at each targeted locus are plotted. Across F0 knockout samples: 98.2 ± 5.4% mutated reads, 73.9 ± 23.8% of all reads had a frameshift mutation.
c, (left) Activity (sum of Δ pixels/10 minutes) of *sorl1* F0 knockout larvae and scrambled-injected siblings during 48 hr on a 14 hr:10 hr light:dark cycle (white background for days, dark grey background for nights). (right) Sleep (minutes per 10-minute epoch) during the same experiment. Traces are mean ± SEM across larvae. See also **Fig. 4** –supplement 5 for results from replicate clutch 2.
d, Parameter plots for two clutches of *sorl1* F0 knockout larvae and scrambled-injected siblings. Each dot represents one larva during one day (top row) or night (bottom row). Black crosses mark the group means. (top row) During the day, *sorl1* F0 knockouts spent less time active (time active, ** p = 0.005) and initiated fewer swimming bouts (number of active bouts, ** p = 0.004) than scrambled-injected controls. The average duration and number of pixels each swimming bout displaced were not affected by the loss of Sorl1 (active bout duration, ns p = 0.40; active bout sum, ns p = 0.84). Sleep was also not affected (total sleep, ns p = 0.98). (bottom row) During the night, *sorl1* F0 knockouts spent more time active (time active, ** p = 0.002) and their swimming bouts lasted longer on average (active bout duration, *** p < 0.001) than scrambled-injected siblings. *sorl1* F0 knockouts also slept less (total sleep, ** p = 0.001), mainly because they initiated fewer sleep bouts (number of sleep bouts, *** p < 0.001), while the duration of each sleep bout remained broadly unchanged (sleep bout duration, ns p = 0.69). One scrambled-injected larva from clutch 2 falls outside the Y axis limit of sleep bout duration (night1: 16.1 min, night2: 12.3 min). Statistics by likelihood-ratio test on linear mixed effects models.

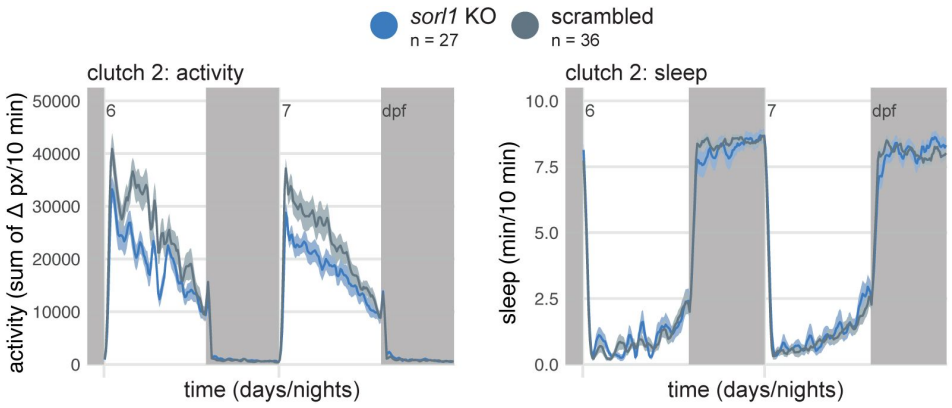

Fig. 4–suppl. 5

Replicate clutch of *sorl1* F0 knockouts.

(left) Activity (sum of Δ pixels/10 minutes) of *sorl1* F0 knockout larvae and scrambled-injected siblings during 48 hr on a 14 hr:10 hr light:dark cycle (white background for days, dark grey background for nights). (right) Sleep (minutes per 10-minute epoch) during the same experiment. Traces are mean ± SEM across larvae. This replicate experiment is called clutch 2 in **Fig. 4** –supplement 4d.

time active than control siblings (+20%), largely because their swimming bouts tended to last longer (+6%). They also slept less (−5%), initiating fewer sleep bouts (−9%) of roughly the same duration.

In summary, we video-tracked the sleep/wake behaviours of F0 knockout larvae in four genes associated with late-onset AD: *apoea*/*apoeb*, *cd2ap*, *clu*, and *sorl1*. Remarkably, loss of all four genes produced a fairly consistent phenotype at night (**Fig. 4**), with all knockout larvae spending 5–13% less time asleep and instead spending 12–38% more time active because they were moving 13–34% more often. In contrast, each mutant had distinct day-time behavioural alterations. Comparing with early-onset genes, *psen1* knockouts had similar night-time phenotypes, but knockout of *psen2* or *appa*/*appb* had no effect on night-time sleep. Therefore, at least some late-onset (and one early-onset) Alzheimer's risk genes have common effects on sleep from an early age, despite being expressed in different tissues and having distinct biochemical properties.

From behavioural fingerprint to causal process: serotonin signalling disruption by the loss of Sorl1

From genomic studies of AD, we know that mutations in genes such as *SORL1* modify risk by disrupting some biological processes[23,31–33]. Presumably, the same processes are disrupted in zebrafish *sorl1* knockouts, and some caused the behavioural alterations we observed. Can we now follow the thread backwards and predict some of the biological processes in which Sorl1 is involved based on the behavioural profile of *sorl1* knockouts?

To predict disrupted biological processes from the *sorl1* knockout behavioural profile, we developed a behavioural pharmacology approach based on a database of 5,756 small molecule behavioural fingerprints (3,677 unique compounds) obtained in wild-type larvae[19]. First, we used information from the Therapeutic Target Database[58] to annotate each compound with its indications (e.g. triprolidine is used to treat hay fever), targets (e.g. triprolidine targets the histamine H1 receptor), and the pathways it affects through its targets (e.g. triprolidine affects the "inflammatory mediator regulation of TRP channels"). Second, we converted the frame-by-frame behavioural fingerprint of *sorl1* knockouts to the one-minute format used by the database. We then compared the mean *sorl1* knockout fingerprint with each small molecule behavioural fingerprint, creating a ranked list from the small molecule fingerprint most similar to the *sorl1* fingerprint (SU6656: cosine similarity = 0.83) to the small molecule fingerprint most opposite to the *sorl1* fingerprint (nitrocaramiphen HCl: cos = −0.78). Third, we tested using a custom permutation test whether specific indication, target, or pathway annotations were significantly enriched at the top and/or the bottom of the ranked list. More present among the small molecules most correlating and/or anti-correlating with the *sorl1* fingerprint were drugs used to treat depression (**Fig. 5**–supplement 1a, simulated p-value = 0.049), targeting the serotonin transporter SLC6A4 (**Fig. 5a,b**, simulated p-value = 0.015), and affecting the "serotonergic synapse" pathway (**Fig. 5**–supplement 1b, simulated p-value = 0.027). Thus, *sorl1* knockout larvae behaved similarly to larvae treated with small molecules targeting serotonin signalling, suggesting that the loss of Sorl1 altered serotonin signalling.

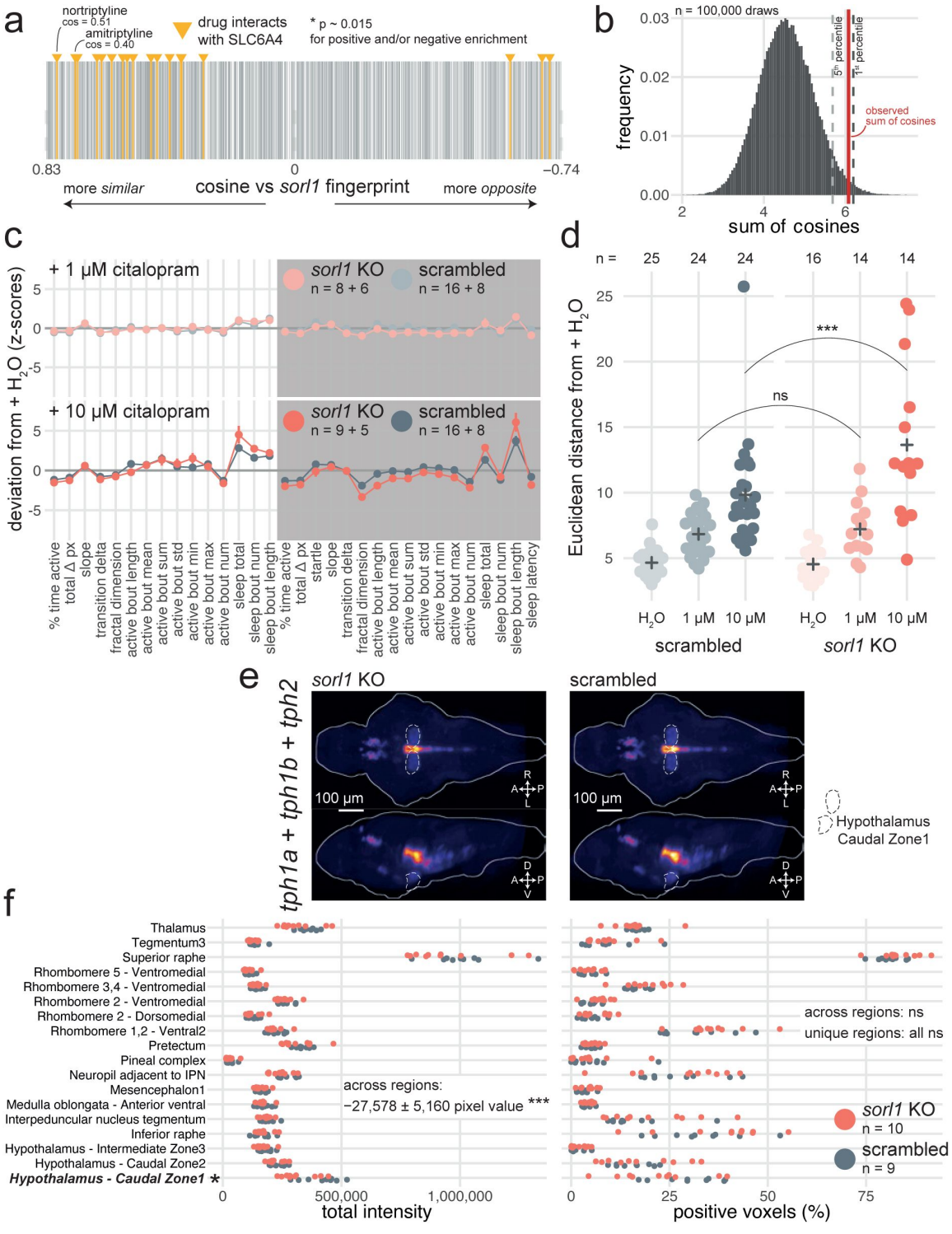
a
nortriptyline
cos = 0.51
amitriptyline
cos = 0.40
drug interacts
with SLC6A4
* p ~ 0.015
for positive and/or negative enrichment
0.83
0
−0.74
more similar
cosine vs sorl1 fingerprint
more opposite
b
n = 100,000 draws
frequency
5th percentile
1st percentile
observed
sum of cosines
sum of cosines
c
+ 1 µM citalopram
sorl1 KO
n = 8 + 6
scrambled
n = 16 + 8
+ 10 µM citalopram
sorl1 KO
n = 9 + 5
scrambled
n = 16 + 8
deviation from + H2O (z-scores)
% time active
total Δ px
slope
transition delta
fractal dimension
active bout length
active bout mean
active bout sum
active bout std
active bout min
active bout max
active bout num
sleep total
sleep bout num
sleep bout length
sleep latency
d
n = 25 24 24 16 14 14
Euclidean distance from + H2O
***
ns
H2O
1 µM
10 µM
scrambled
sorl1 KO
e
sorl1 KO
scrambled
tph1a + tph1b + tph2
100 µm
Hypothalamus
Caudal Zone1
f
Thalamus
Tegmentum3
Superior raphe
Rhombomere 5 - Ventromedial
Rhombomere 3,4 - Ventromedial
Rhombomere 2 - Ventromedial
Rhombomere 2 - Dorsomedial
Rhombomere 1,2 - Ventral2
Pretectum
Pineal complex
Neuropil adjacent to IPN
Mesencephalon1
Medulla oblongata - Anterior ventral
Interpeduncular nucleus tegmentum
Inferior raphe
Hypothalamus - Intermediate Zone3
Hypothalamus - Caudal Zone2
Hypothalamus - Caudal Zone1 *
across regions:
−27,578 ± 5,160 pixel value ***
total intensity
across regions: ns
unique regions: all ns
sorl1 KO
n = 10
scrambled
n = 9
positive voxels (%)

Fig. 5

Predictive behavioural pharmacology identifies impaired serotonin signalling in *sorl1* knockouts.

a, Compounds interacting with the serotonin transporter SLC6A4 tend to generate behavioural phenotypes similar to the *sorl1* F0 knockout fingerprint. 2,674 compound–target protein pairs (vertical bars; 1,552 unique compounds) are ranked from the fingerprint with the most positive cosine to the fingerprint with the most negative cosine in comparison with the mean *sorl1* F0 knockout fingerprint. Fingerprints of compounds that interact with SLC6A4 are coloured in yellow (source: Therapeutic Target Database). Simulated p-value = 0.015 for enrichment of drugs interacting with SLC6A4 at the top (positive cosine) and/or bottom (negative cosine) of the ranked list by a custom permutation test.

b, Result of the permutation test for top and/or bottom enrichment of drugs interacting with SLC6A4 in the ranked list. The absolute cosines of the fingerprints of drugs interacting with SLC6A4 (n = 18, one fingerprint per compound) were summed, giving sum of cosines = 6.1. To simulate a null distribution, 18 fingerprints were randomly drawn 100,000 times, generating a distribution of 100,000 random sum of cosines. Here, only 1,470 random draws gave a larger sum of cosines, so the simulated p-value was p = 1,470/100,000 = 0.015 *.

c, (top) Behavioural fingerprints of *sorl1* F0 knockouts and scrambled-injected siblings treated with 1 µM citalopram. (bottom) Behavioural fingerprints of *sorl1* F0 knockouts and scrambled-injected siblings treated with 10 µM citalopram. In both plots, each dot represents the mean deviation from the mean of the same-group (F0 knockout or scrambled-injected) untreated (H_2O) siblings (z-score, mean ± SEM); therefore, the baseline (z-scores = 0) does not represent the same larvae for *sorl1* F0 knockouts and scrambled-injected controls. Z-scores from two clutches were averaged.

d, Euclidean distance from same-group controls' mean across the 32 parameters. ns p = 0.71, *** p < 0.001 by Welch's t-test.

e, HCRs labelling transcripts encoding serotonin transporters *(slc6a4a* and *slc6a4b*) in 6-dpf *sorl1* F0 knockouts and scrambled-injected controls. The images are maximum Z-projections of dorsal (top) and sagittal (bottom) views of the median stack of all larvae in each group. A, anterior; P, posterior; R, rightwards; L, leftwards; D, dorsal; V, ventral.

f, Quantification of HCRs from c). (left) Total grey pixel intensity per anatomical region in *sorl1* F0 knockouts and scrambled-injected controls. Across regions: ns p = 0.98; unique regions: ns p > 0.25. (right) Number of voxels with positive signal per anatomical region in *sorl1* F0 knockouts and scrambled-injected controls. ** p = 0.001, unique regions: ns p > 0.07. Statistics across regions by likelihood-ratio test on linear mixed effects models; statistics on unique regions by Welch's t-test without p-value adjustment. The same larvae are plotted in **Fig. 5**–supplement 1e,f.

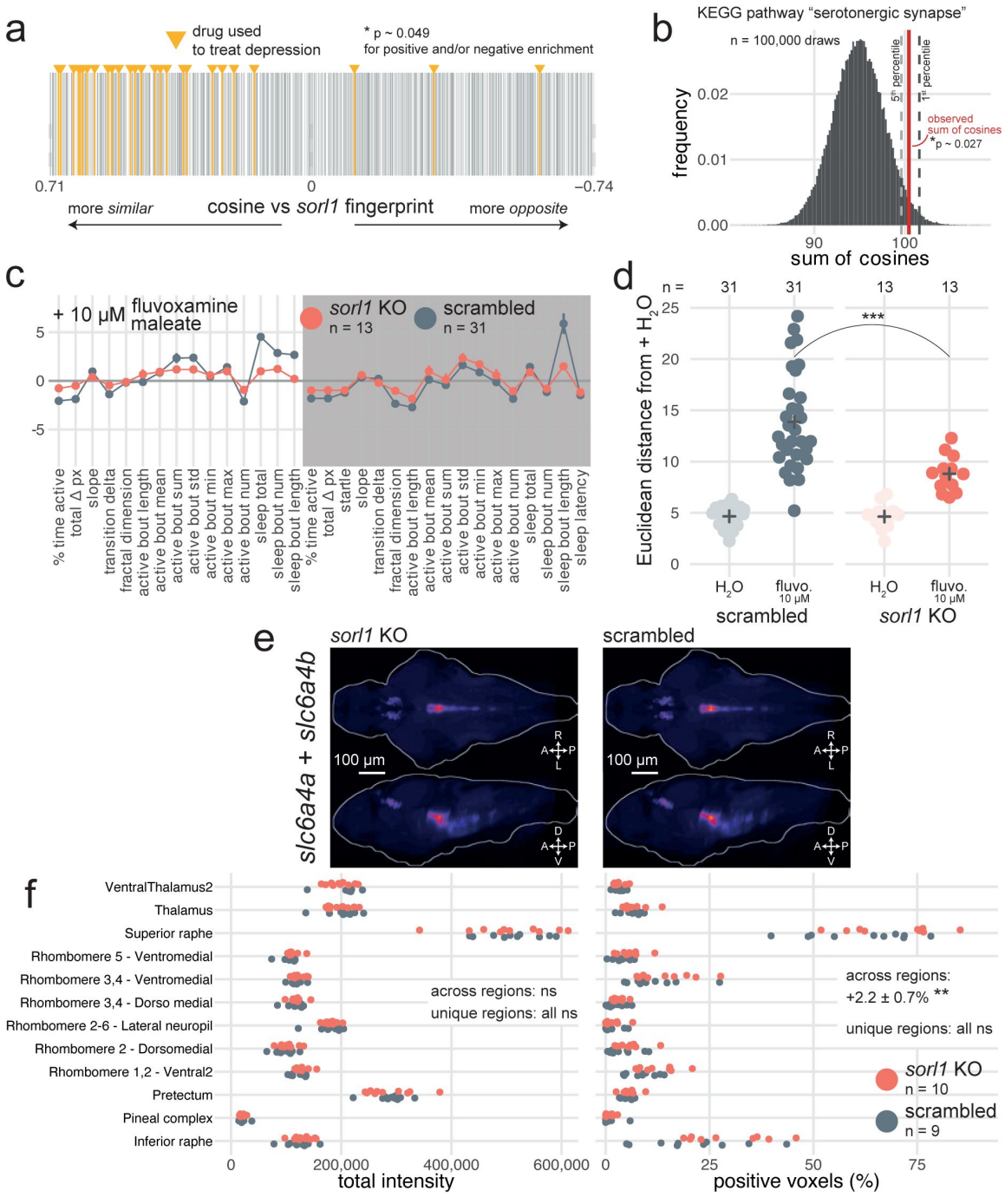
a
drug used
to treat depression
* p ~ 0.049
for positive and/or negative enrichment
0.71
0
–0.74
more similar
cosine vs sorl1 fingerprint
more opposite
b
KEGG pathway "serotonergic synapse"
n = 100,000 draws
5th percentile
1st percentile
observed
sum of cosines
*p ~ 0.027
frequency
0.02
0.01
0.00
90
100
sum of cosines
c
+ 10 µM fluvoxamine maleate
sorl1 KO
n = 13
scrambled
n = 31
5
0
-5
% time active
total Δ px
slope
transition delta
fractal dimension
active bout length
active bout mean
active bout sum
active bout std
active bout min
active bout max
active bout num
sleep total
sleep bout num
sleep bout length
sleep latency
d
n =
31
31
13
13
Euclidean distance from + H2O
25
20
15
10
5
0
***
H2O
fluvo.
10 µM
scrambled
sorl1 KO
e
sorl1 KO
scrambled
slc6a4a + slc6a4b
100 µm
R
A
P
L
D
V
f
VentralThalamus2
Thalamus
Superior raphe
Rhombomere 5 - Ventromedial
Rhombomere 3,4 - Ventromedial
Rhombomere 3,4 - Dorso medial
Rhombomere 2-6 - Lateral neuropil
Rhombomere 2 - Dorsomedial
Rhombomere 1,2 - Ventral2
Pretectum
Pineal complex
Inferior raphe
across regions: ns
unique regions: all ns
across regions:
+2.2 ± 0.7% **
unique regions: all ns
sorl1 KO
n = 10
scrambled
n = 9
0
200,000
400,000
600,000
total intensity
0
25
50
75
positive voxels (%)

Fig. 5–suppl. 1

Predictions of disrupted processes in *sorl1* knockouts based on indications and KEGG pathways.

a, Drugs used to treat depression tend to generate behavioural phenotypes similar to the *sorl1* F0 knockout fingerprint. 1,401 pairs of one compound and one therapeutic indication (vertical bars; 1,123 unique compounds) are ranked from the fingerprint with the most positive cosine to the fingerprint with the most negative cosine in comparison with the mean *sorl1* F0 knockout fingerprint. Fingerprints of drugs used to treat depression are coloured in yellow (source: Therapeutic Target Database). Simulated p-value = 0.049 for enrichment of drugs used to treat depression at the top (positive cosine) and/or bottom (negative cosine) of the ranked list by a custom permutation test.

b, Result of the permutation test for top and/or bottom enrichment of drugs affecting the "serotonergic synapse" KEGG pathway. The absolute cosines of the fingerprints of drugs which affect the "serotonergic synapse" (n = 374, one fingerprint per compound) were summed, giving sum of cosines = 100.4. To simulate a null distribution, 374 fingerprints were randomly drawn 100,000 times, generating a distribution of 100,000 random sum of cosines. Here, only 2,662 random draws gave a larger sum of cosines, so the simulated p-value was p = 2,662/100,000 = 0.027 *.

c, Behavioural fingerprints of *sorl1* F0 knockouts and scrambled-injected siblings treated with 10 µM fluvoxamine maleate. In both plots, each dot represents the mean deviation from the mean of the same-group (F0 knockout or scrambled-injected) untreated (H_2O) siblings (z-score, mean ± SEM), therefore the baseline (z-scores = 0) does not represent the same larvae for *sorl1* F0 knockouts and scrambled-injected controls.

d, Euclidean distance from same-group controls' mean across the 32 parameters. *** p < 0.001 by Welch's t-test.

e, HCRs labelling transcripts encoding tryptophan hydroxylases (*tph1a*, *tph1b*, *tph2*) in 6-dpf *sorl1* F0 knockouts and scrambled-injected controls. The images are maximum Z-projections of dorsal (top) and sagittal (bottom) views of the median stack of all larvae in each group. A, anterior; P, posterior; R, rightwards; L, leftwards; D, dorsal; V, ventral.

f, Quantification of HCRs from e). (left) Total grey pixel intensity per anatomical region in *sorl1* F0 knockouts and scrambled-injected controls. *** p < 0.001, * p = 0.012. (right) Number of voxels with positive signal per anatomical region in *sorl1* F0 knockouts and scrambled-injected controls. Across regions: ns p = 0.08; unique regions: ns p > 0.07. Statistics across regions by likelihood-ratio test on linear mixed effects models; statistics on unique regions by Welch's t-test without p-value adjustment. The same larvae are plotted in **Fig. 5e,f**.

If serotonin signalling is altered in *sorl1* knockouts, they should react differently to serotonergic drugs than wild-type animals. To test this hypothesis, we treated *sorl1* F0 knockouts and controls with citalopram, a selective serotonin reuptake inhibitor (SSRI) used to treat depression[59]. Citalopram binds the serotonin transporter SLC6A4, preventing the reuptake of serotonin from the synaptic cleft. At a low dose of citalopram (1 µM, added directly to the fish water), *sorl1* F0 knockouts and scrambled-injected controls reacted similarly, sleeping about 1.1 hr more during both day and night (**Fig. 5c**). In contrast, at a higher dose of citalopram (10 µM), *sorl1* F0 knockouts had a stronger reaction than their control siblings. For example, sleep during the day increased 2.5× in *sorl1* knockouts, while it only increased 2.2× in controls. The heightened sensitivity of *sorl1* knockouts to citalopram was also apparent when taking all parameters into account by measuring each larva's Euclidean distance from the average H_2O-treated sibling of same genotype (**Fig. 5d**). Indeed, 10 µM citalopram displaced the *sorl1* knockout larvae further from their behavioural baseline than it pushed controls from theirs. In a second experiment, we treated knockouts and controls with fluvoxamine maleate (10 µM), another commonly prescribed SSRI[60]. *sorl1* F0 knockouts had a weaker reaction to fluvoxamine than their control siblings, the opposite effect than for citalopram. For example, fluvoxamine doubled (2.1×) sleep bout length at

night in *sorl1* knockouts but tripled it (3.4×) in controls (**Fig. 5** – supplement 1c). Measuring each larva's Euclidean distance from its H_2O-treated siblings confirmed the reduced sensitivity of *sorl1* knockouts to fluvoxamine (**Fig. 5** –supplement 1d). While it is surprising that the *sorl1* knockout larvae reacted oppositely to the two SSRIs, they reacted differently than control larvae in both cases, demonstrating that our behavioural pharmacology approach correctly predicted from behaviour alone that serotonin signalling was in some way altered in *sorl1* knockouts.

There are at least two ways *sorl1* knockouts could react differently to SSRIs. First, compared to wild types, *sorl1* knockouts could undergo a smaller or larger spike of serotonin in the synaptic cleft when reuptake is blocked. This may be because *sorl1* knockouts synthesise serotonin at a different rate, either because they have a different number of serotonergic neurons or a different expression of the enzymes required to make serotonin; or because they do not produce the same amount of serotonin transporter, which would change their sensitivity to SSRIs as a given dose would inhibit a smaller or larger proportion of the transporter than in wild-type animals. Second, *sorl1* knockouts may have a different sensitivity to serotonin itself because post-synaptic neurons have different densities of serotonin receptors.

To distinguish between these two hypotheses, we used HCR to label serotonergic neurons by tagging mRNA coding for tryptophan hydroxylases (in zebrafish: *tph1a*, *tph1b*, *tph2*; **Fig. 5e**), an enzyme required for the synthesis of serotonin, and serotonin transporters by tagging *slc6a4a* and *slc6a4b* mRNA[61] (**Fig. 5** –supplement 1e). We registered the brain stacks to a common atlas (Zebrafish Brain Browser) and segmented them into 168 anatomical regions. In each region with expression, we counted the number of positive voxels and measured the total signal intensity in each channel (channel 1: *tph1a* + *tph1b* + *tph2*; channel 2: *slc6a4a* + *slc6a4b*). *sorl1* F0 knockouts had slightly more (+2%) *slc6a4a*/*b* positive voxels than controls across regions, but this difference was not definite for any one region and not replicated when looking at total signal intensity (**Fig. 5** –supplement 1f). *sorl1* F0 knockouts had on average 18% lower *tph1a*/*1b*/*2* signal intensities across regions, particularly in the hypothalamus (hypothalamus – caudal zone 1: –24%, **Fig. 5e,f**). Incidentally, of 94 clusters from the 5-dpf scRNA-seq dataset, *sorl1* expression was highest in hypothalamic neurons enriched for *tph1a* expression (**Fig. 1** –supplement 2). These small differences can help explain the reduced sensitivity of *sorl1* knockouts to fluvoxamine, but do not explain the heightened sensitivity to citalopram. Additionally, at least one study did not find significant changes in serotonin levels in the striatum of *SORL1* knockout mice[62], and we did not find genes related to serotonin signalling to be differentially expressed in a bulk RNA-seq dataset of *sorl1* knockout zebrafish brains[63]. Support for our first hypothesis is therefore not overwhelming. Alternatively, different levels of serotonin receptors on the post-synaptic neurons could also contribute.

From behavioural fingerprint to candidate therapeutic: betamethasone rescues the *psen2* behavioural phenotype

In addition to pointing to the disrupted pathways, behavioural pharmacology can also predict small molecules that may normalise mutant behavioural phenotypes by pointing to compounds that generate the opposite behavioural fingerprint in wild-type larvae.

Using this approach, we sought to identify compounds capable of normalising the behavioural alterations of *psen2* knockouts, such as the increased day-time sleep. We ranked the 5,756 small molecule behavioural fingerprints in comparison with the mean *psen2* F0 knockout fingerprint and focused on compounds that generated the most opposite (anti-correlating) fingerprint when applied on wild-type larvae. This identified three compounds with a high negative cosine compared to *psen2* knockouts (**Fig. 6a** and **Fig. 6** – supplement 1a): tinidazole (minimum cos = −0.89), fenoprofen (minimum cos = −0.79), and betamethasone (minimum cos = −0.79). These compounds were also selected because they were each replicated at least once in the database, lending confidence to the prediction. We then applied the three compounds on *psen2* F0 knockouts

and measured their effects on sleep/wake parameters. For each treatment, we grouped the behavioural parameters into four categories: “rescue” if the parameter was significantly altered in DMSO-treated *psen2* knockout larvae but got normalised by the drug; “missed rescue” if the *psen2* knockout parameter remained altered after drug treatment; “side effect” if a parameter was unaffected in *psen2* knockouts but got altered by the drug; and “no effect” if the parameter was unaffected in *psen2* knockouts and remained unchanged by the drug.

All three compounds normalised at least some aspects of the *psen2* knockout behavioural phenotype. Tinidazole did not reduce the abnormally high day-time sleep characteristic of *psen2* knockouts (**Fig. 6c** left). It rescued the swimming bout alterations (active bout parameters) during the day but not at night. Overall, the compound barely caused any side effects but only rescued a small aspect of the *psen2* knockout phenotype (9/18 altered parameters rescued). Fenoprofen performed worse (**Fig. 6c** middle, 8/18 altered parameters rescued), rescuing some of the swimming bout alterations during the day but aggravating them at night. Furthermore, fenoprofen worsened the day-time hypoactivity of *psen2* knockout larvae, causing sleep to increase further and activity to decrease. Strikingly, betamethasone completely resolved the excess day-time sleep without causing hyperactivity (**Fig. 6b** and **Fig. 6**–supplement 1b). Betamethasone rescued most, but not all, of the swimming bout alterations during both the day and night (**Fig. 6c** right, 14/18 altered parameters rescued). Betamethasone did cause a few side effects, likely by making *psen2* knockout larvae overly aroused at the start of the night, extending sleep latency, steepening the slope in activity, and decreasing the startle response. Therefore, of the three drugs we selected using behavioural pharmacology, one almost completely normalised the *psen2* knockout phenotype, albeit with a few side effects.

Discussion

The F0 knockout and behavioural pharmacology approach successfully predicted the different sensitivity of *sorl1* mutants to serotonin drugs and identified a drug capable of normalising the *psen2* knockout behavioural phenotype. To allow researchers to generate pharmacological predictions from their own sleep/wake datasets, we built an online app (*francoiskroll.shinyapps.io/zoltar/*) that can plot behavioural fingerprints, rank all 5,756 small molecule fingerprints in the database in comparison to the query fingerprint, and perform permutation tests for enrichment of indications, drug targets, and KEGG pathways (**Fig. 7–supplement 1**). While we used genes associated with AD as a case study, predictive behavioural pharmacology provides a generalisable framework that can be applied to any set of disease risk genes.

Disrupted sleep and serotonin signalling—causal processes of Alzheimer’s disease?

Of the seven genes tested, *psen1* and all four late-onset Alzheimer’s risk genes decreased sleep duration at night when mutated in zebrafish larvae. Could disrupted sleep itself be a causal process in AD? AD patients often take longer to fall asleep, have higher sleep fragmentation, and spend sharply less time in NREM sleep[64,65]. Sleep disruption can be present before the onset of cognitive deficits. For example, very high sleep fragmentation in elderly people is associated with subsequent diagnosis of AD[66]. Experiments on humans and animal models also point to disrupted sleep being a causal process in some cases. In healthy adults, one night of sleep deprivation was sufficient to cause a 25–30% increase in Aβ signal on PET scans[67], a ~30% increase in CSF concentrations of Aβ[68], and a ~50% increase in CSF concentrations of tau[69]. In wild-type rats and in mice overexpressing mutated human *APP* and *PSEN1*, restricting sleep for 21 days increased Aβ deposits in the cortex[70,71]. Conversely, pharmaceutically or chemogenetically consolidating sleep in AD mouse models for 1–2 months delayed Aβ plaque formation[70,72]. Disrupted sleep is therefore likely to be a causal process in AD. Can it become

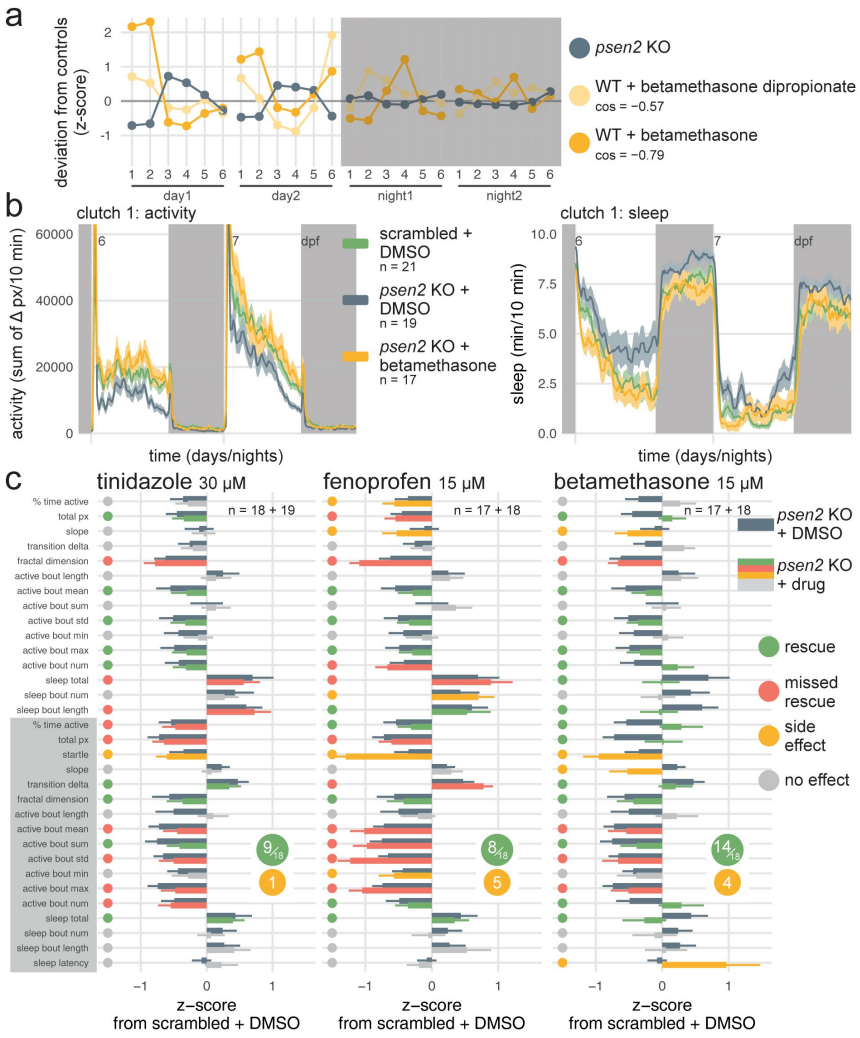

Fig. 6

Betamethasone normalises the *psen2* knockout behavioural phenotype.

a, The *psen2* F0 knockout fingerprint was used as query to identify small molecules that generate the opposite behavioural phenotype when applied on wild-type larvae, returning betamethasone as candidate therapeutic. Plotted are the query *psen2* fingerprint (mean of two clutches, dark grey) and the two betamethasone fingerprints from the drug database with the largest negative cosine similarities (yellow). Parameters: 1, average activity (sec active/min); 2, average waking activity (sec active/min, excluding inactive minutes); 3, total sleep (hr); 4, number of sleep bouts; 5, sleep bout length (min); 6, sleep latency (min until first sleep bout). *cos*, cosine similarity between each betamethasone fingerprint and the *psen2* F0 knockout fingerprint.

b, (left) Activity (sum of Δ pixels/10 minutes) of scrambled-injected larvae treated with DMSO and *psen2* F0 knockout larvae treated with DMSO or 15 µM betamethasone during 48 hr on a 14 hr:10 hr light:dark cycle (white background for days, dark grey background for nights). (right) Sleep (minutes per 10-minute epoch) during the same experiment. Traces are mean ± SEM across larvae. See also **Fig. 6**—supplement 1 for results from replicate clutch 2.

c, Survey of behavioural parameters for each drug treatment. Bars represent the mean deviation from scrambled-injected siblings treated with DMSO (z-score, mean ± SEM). Dark grey bars represent the *psen2* knockouts treated with DMSO, i.e. the phenotype to be treated (same population of *psen2* knockouts treated with DMSO for all the drug treatments, n = 19 + 18). Other bars are colour-coded by the effect of each drug on *psen2* knockouts: “rescue” (green) if the drug normalised the parameter; “missed rescue” (red) if the drug failed to normalise the parameter; “side effect” (yellow) if the drug significantly altered a parameter which was unaffected in *psen2* knockouts; and “no effect” (grey). Calls were decided based on significance by likelihood-ratio test on linear mixed effects models calculated on the raw parameter values from both clutches (n is sample size of drug-treated *psen2* knockouts of clutch1 + clutch2).

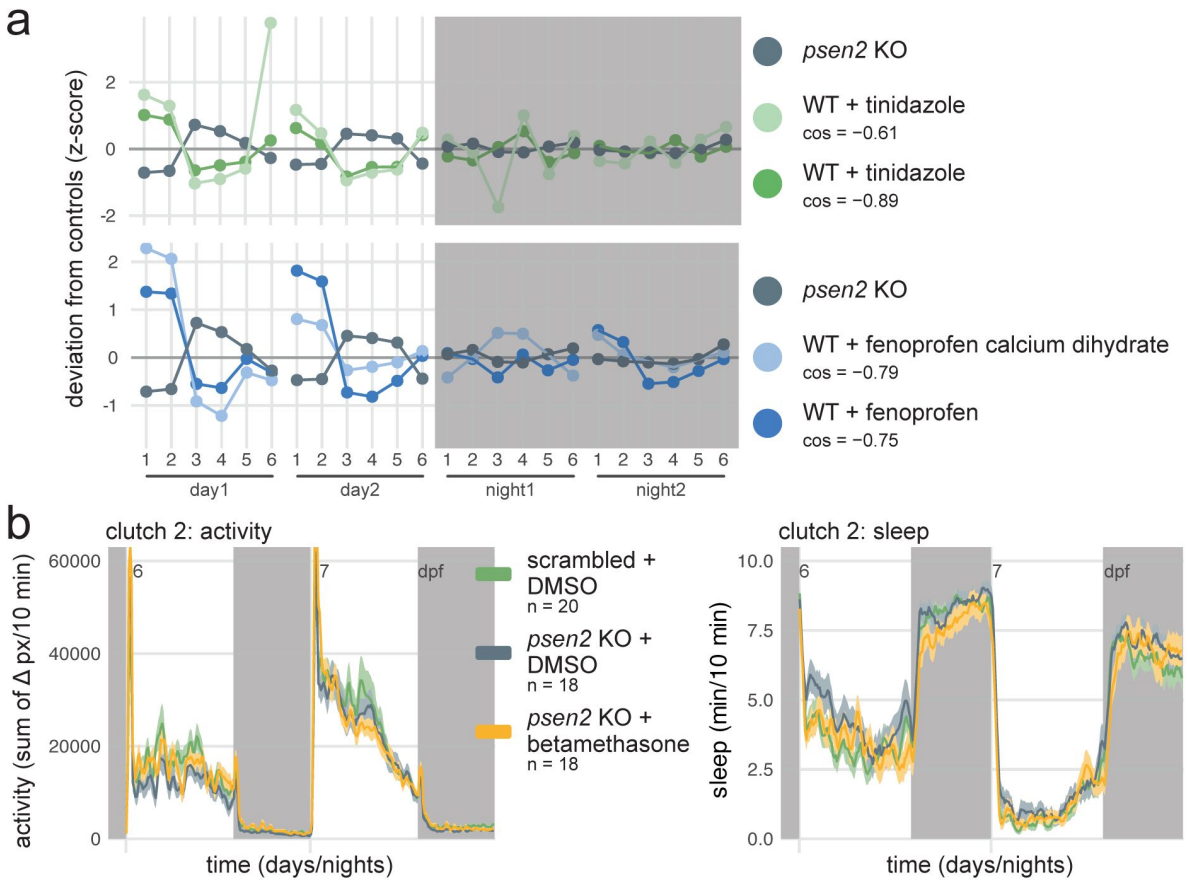

Fig. 6–suppl. 1

Selection of candidate therapeutics to normalise the *psen2* behavioural phenotype by predictive behavioural pharmacology.

a, The *psen2* F0 knockout fingerprint was used as query to identify small molecules that generate the opposite behavioural phenotype when applied on wild-type larvae, returning tinidazole and fenoprofen as candidate therapeutics. Plotted are the query *psen2* fingerprint (mean of two clutches, dark grey) and the tinidazole (green) and fenoprofen (blue) fingerprints from the drug database. Parameters: 1, average activity (sec active/min); 2, average waking activity (sec active/min, excluding inactive minutes); 3, total sleep (hr); 4, number of sleep bouts; 5, sleep bout length (min); 6, sleep latency (min until first sleep bout). *cos*, cosine similarity between the drug fingerprint and the *psen2* F0 knockout fingerprint.
b, (left) Activity (sum of Δ pixels/10 minutes) of scrambled-injected larvae treated with DMSO and *psen2* F0 knockout larvae treated with DMSO or 15 µM betamethasone during 48 hr on a 14 hr:10 hr light:dark cycle (white background for days, dark grey background for nights). (right) Sleep (minutes per 10-minute epoch) during the same experiment. Traces are mean ± SEM across larvae.

a therapeutic target? An ongoing clinical trial (NCT04629547) is underway to test whether suvorexant, an orexin receptor antagonist that increases sleep, can reduce Aβ accumulation by consolidating sleep in older adults without dementia[73]. Our observation that disruption of genes associated with AD diagnosis after 65 years reduces sleep in 7-day zebrafish larvae suggest that disrupted sleep may be a common mechanism through which these genes exert an effect on risk. Impaired sleep early in life may be especially deleterious as it is likely essential for brain development: infants spend most of their time asleep during the first year of life[74]. Incidentally, infants who carry the risk allele of *APOE, ε4*, show differences in grey matter volume and myelin content in multiple brain regions[75]. Differences are also present in children 9–17 years old who carry the disease-causing *PSEN1* E280A mutation[76]. In adults without dementia, higher genetic risk of AD correlate with some sleep phenotypes, sometimes as early as their early twenties[77–79]. Future work should directly assess whether sleep is impaired in infants at higher genetic risk of AD and whether it is related to these brain structural differences.

Our behavioural pharmacology approach also predicted that loss of Sorl1 impaired serotonin signalling. *sorl1* knockouts did respond differently to SSRIs, but the exact mechanism is unclear. SORL1 acts as an adaptor protein between retromer and several cargo proteins, such as APP[80], GDNF receptor α1[62], and glutamate receptor 1 (GLUA1)[81]. Retromer is a large protein complex which 'rescues' proteins from endosomes, targeting them to recycling instead of lysosomal digestion[82]. By disrupting retromer function, mutations in SORL1 disrupt endosomal recycling, which appears as swelling of early endosomes[83]. As a result, APP remains in endosomes for longer, where it is more likely to be cleaved by β-secretase, the first step towards production of Aβ[84]. Similarly, retromer dysfunction also lowers the level of GLUA1 receptors on the neuron membrane, likely because endocytosed receptors are not recycled back to the membrane, which can result in both increased or decreased firing rates *in vitro*[81]. We speculate that some serotonin (5-hydroxytryptamine, 5-HT) receptors are also recycled via retromer and SORL1. Consequently, *sorl1* knockouts would react differently to a large spike in serotonin (SSRI treatment) as they have different levels of 5-HT receptors on the post-synaptic membrane. In support for this idea, both 5-HT type 4 receptor[85] and SORL1[86] interact with sorting nexin 27, a subunit of retromer. Incidentally, the 5-HT receptor type 4 was also an enriched target for *sorl1* (simulated p-value = 0.016). Other observations are consistent with serotonin signalling being a causal process of AD. For example, treatment of an AD mouse model with citalopram caused a rapid decrease in Aβ concentrations in the ISF and eventually reduced amyloid plaque load. Additionally, humans treated with SSRIs within the past 5 years had significantly lower cortical amyloid plaque load on PET scans, suggesting a causal relationship[87]. While much work remains to be done, SSRIs can generally be used safely for many years, so modulating serotonin signalling may be an attractive approach to reduce Aβ levels years before the onset of cognitive symptoms[87].

Limitations and future directions for predictive behavioural pharmacology

Currently, the hypotheses that our behavioural pharmacology approach can test are limited by the small molecule screen dataset[19], which was biased towards specific themes and targets. For example, of 1,552 compounds with an annotated target, 60 (3.9%) target the dopamine D2 receptor but only 1 (0.06%) targets mitochondrial uncoupling proteins (UCP1, 2, 3). Consequently, the approach presumably has high sensitivity for disruptions in dopamine signalling, while some hypotheses, such as impairment in mitochondrial coupling, are never formally tested. Broadly, this means that a negative (non-significant) result may not be meaningful if the biological process in question is underrepresented. Additionally, about 30% of the annotated compounds in the database have more than one target. While this is not necessarily an issue when the goal is to find any small molecule which rescues the phenotype, this lack of specificity likely blurs the signal from modulation of a specific target to effect on behaviour. For example, all five compounds which target the histamine H4 receptor also target the histamine H3 receptor, so if the H3 receptor

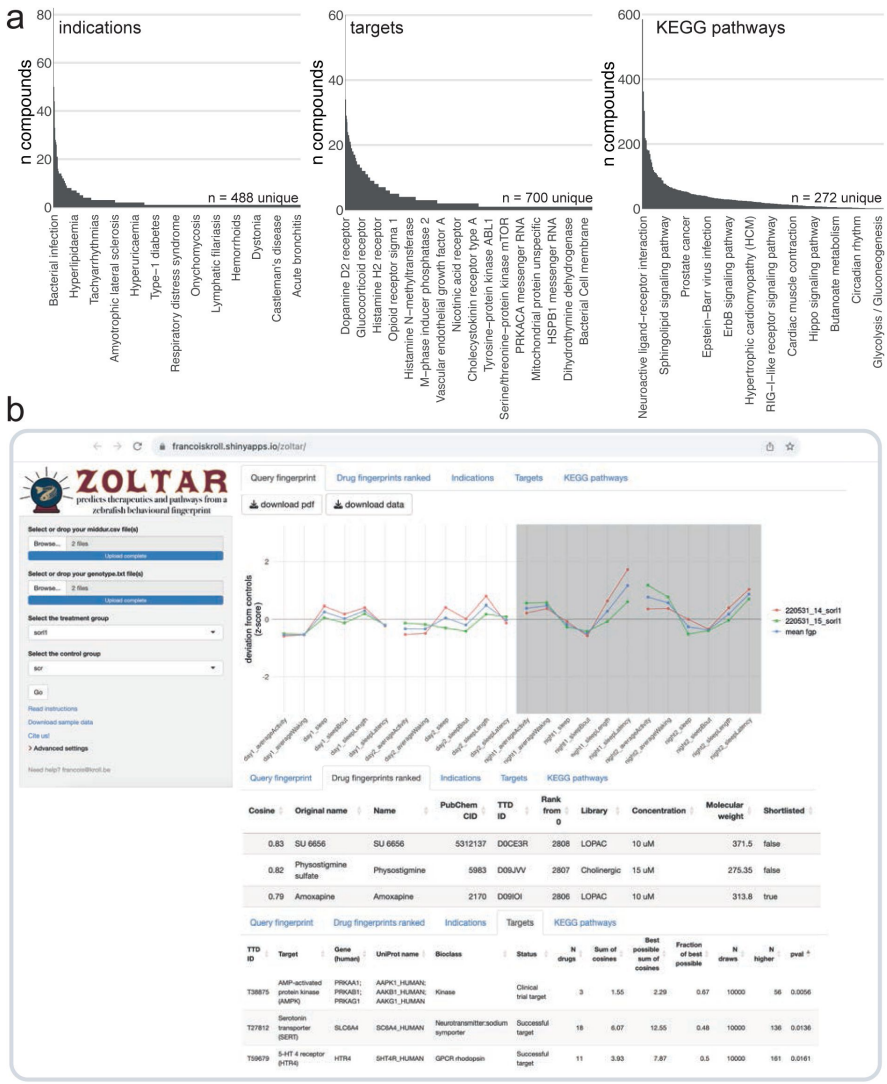

Fig. 7–suppl. 1

The ZOLTAR online app for prediction of therapeutics and disrupted processes from behavioural fingerprints.

a, Datasets currently available to the ZOLTAR online app for predictions. The height of each bar represents the number of unique compounds with this annotation. Some annotations are labelled as examples. Of 3,677 unique compounds labelled with a PubChem ID, 1,123 were annotated with one or more indications; 1,552 were annotated with one or more target proteins; and 1,140 were annotated with one or more KEGG pathways through their targets. Source of annotations: Therapeutic Target Database.

b, Screenshot showing some of the features of the ZOLTAR online app. User drags and drops data file(s) (*middur* = sec active/min for each larva) and file(s) labelling each well with a condition (called "genotype file", but can be any group assignments). The app reads the groups from the genotype file(s) and the user selects the treatment and control groups in a dropdown menu. The app calculates and plots the fingerprint(s) (tab *Query fingerprint*), then ranks the 5,756 small molecule fingerprints (tab *Drug fingerprints ranked*) from maximum positive cosine to maximum negative cosine. Clicking on a row in the table of ranked compounds plots all the fingerprints of this compound (all fingerprints with the same PubChem ID) in comparison with the query fingerprint, as in **Fig. 6a**. The app tests, for each annotation, enrichment towards the top and/or bottom of the ranked list with a custom permutation test. Current annotations are clinical indications (tab *Indications*), target proteins (tab *Targets*), and the KEGG pathways each target protein is associated with (tab *KEGG pathways*). Clicking on a row in a table of annotation results generates the "barcode plot" for this annotation, as in **Fig. 5a**. The tables can be downloaded as .csv files and the plots as .pdf files.

is detected as significantly enriched, the H4 receptor is certain to be significant too, regardless of whether the H4 receptor is indeed specifically disrupted. To develop the biological process prediction, future work should focus on selecting specific agonists and antagonists for a set list of targets, such as the compound VUF-6002 to selectively target the histamine H4 receptor without also activating H3[88]. Alternatively, ZOLTAR could weigh the evidence for a target based on the compound's affinity constant, such that a weak inhibitor (high Ki) could only contribute proportionally weak evidence for its target in the analysis.

A way to improve the specificity of the approach is to enhance the resolution of the behaviour tracking so that targets which give similar but unique effects on behaviour can be distinguished. We introduced the FramebyFrame R package to enable analysis at sub-second resolution, but the original small molecule screen dataset was collected at the one-minute resolution[19], so comparing a new behavioural profile to the small molecule database first involves losing resolution to make the fingerprints comparable. During a new small molecule screen, one could use SLEAP[89] or DeepLabCut[90] to extract additional behavioural parameters from video recordings such as speed or position in the well. A faster and higher definition camera could be introduced to allow fine tracking of tail and eye movements. Exposing the larvae to various stimuli is also a way to increase the number of parameters while avoiding redundancy[91]. With more behavioural parameters, the prediction of therapeutics using behavioural pharmacology would also be more precise and the detection of possible behavioural side effects more thorough. Analytically, an improvement could be to represent larval behaviour as a sequence of movements, rather than parameter averages. For example, the Δ pixel time course from our experiments can be encoded as a sequence of bout types termed modules, themselves organised in motifs which are 2–20-module long[45]. Alternatively, behaviour could be represented as sequences of known types of swimming bouts[92] or automatically discovered 'syllables'[93]. In mouse, this sequence representation was better than a fingerprint at differentiating similar compounds or even doses[93], so should also improve the predictive power of the behavioural pharmacology approach.

This leads to a thought experiment: assuming absolute resolution in behaviour tracking, does every knockout give a unique effect on behaviour? In other words, are there ~26,000 distinct knockout fingerprints or do multiple genes converge on a smaller set of possible fingerprints? How much resolution is required to distinguish every possible fingerprint?

Conclusion

In summary, we present a behavioural pharmacology approach which uses the sleep/wake behaviour of zebrafish larvae as a tool to translate genomic findings into druggable biological processes and candidate therapeutics. We used Alzheimer's risk genes, especially *SORL1* and *PSEN2*, as case studies and correctly predicted mutant-drug interactions from behaviour alone. Our strategy is both scalable thanks to the F0 knockout method and the FramebyFrame analysis package and generalisable beyond AD through the *ZOLTAR 0app*. Other neurological conditions for which many risk genes are known, such as autism, epilepsy, or schizophrenia, are prime candidates for the application of the strategy.

Methods

Animals

Adult zebrafish were reared by University College London's Fish Facility on a 14 hr:10 hr light:dark cycle. To obtain eggs, pairs of one female and one male were isolated in breeding boxes overnight, separated by a divider. Around 9 AM (lights on) the next day, the dividers were removed and eggs were collected 7–10 min later. The embryos were then raised in 10-cm Petri dishes filled with fish water (0.3 g/L Instant Ocean) in a 28.5°C incubator on a 14 hr:10 hr light:dark cycle. Debris and dead or dysmorphic embryos were removed every other day with a Pasteur pipette under a bright-field microscope and the fish water replaced. At the end of the experiments, larvae were euthanised with an overdose of 2-phenoxyethanol (ACROS Organics). Experimental procedures were in accordance with the Animals (Scientific Procedures) Act 1986 under Home Office project licences PA8D4D0E5 and PP6325955 awarded to Jason Rihel. Adult zebrafish were kept according to FELASA guidelines[94].

Wild types refer to AB × Tup LF zebrafish, except for the fluvoxamine experiment (**Fig. 5** – supplement 1) which used TL larvae. Throughout, F0 knockouts refer to wild-type embryos that were injected with gRNA/Cas9 RNPs at the single-cell stage.

Generation of F0 knockout larvae

crRNA selection

The crRNA was the only component of the Cas9/gRNA RNP specific to the target locus.

In previous work[20], we selected predesigned crRNAs from the Integrated DNA Technologies (IDT) database (*eu.idtdna.com*) based on predicted on-target and off-target scores calculated by a proprietary IDT algorithm. Subsequent benchmarking in zebrafish of various crRNA design algorithms revealed that the IDT on-target scores did not predict mutagenesis rates *in vivo*[95]. All crRNAs used in F0 knockout experiments were therefore designed using CHOPCHOP (chopchop.cbu.uib.no)[96] implementing both the on-target score calculation by CRISPRScan[97], which benchmarking determined was the best predictor of mutagenesis[95], and inDelphi[98], which predicts to some extent the generated mutations in zebrafish embryos[99].

We prioritised targeting asymmetrical exons and only selected crRNAs without any off-targets with 0, 1, 2, or 3 mismatches, as off-targets with up to 3 mismatches may undergo mutation[20,100]. We then selected the crRNAs based on their on-target score and the prediction of frameshift mutations by inDelphi (crRNAs used had 82.8 ± 5.7% predicted frameshift mutation rate). We also used SNPfisher, an online database of common single-nucleotide polymorphisms (SNP) in zebrafish wild-type strains, to check that putative target sites did not contain any SNP[101].

A protocol describing how to select crRNAs based on these developments is available at *dx.doi.org/10.17504/protocols.io.81wgb6r5qlpk/v1*. Sequences of the crRNAs and information about the targeted loci are provided in Supplementary file 1.

Cas9/gRNA preparation

A protocol describing how to generate F0 knockout larvae is available at *dx.doi.org/10.17504/protocols.io.5qpvo52wdl4o/v3*.

The CRISPR-Cas9 RNP was made of three components bought from IDT: the crRNA (Alt-R® CRISPR-Cas9 crRNA) and tracrRNA (Alt-R® CRISPR-Cas9 tracrRNA), together forming the gRNA, and the Cas9 (Alt-R® S.p. Cas9 Nuclease V3). The crRNA and tracrRNA were received as pellets, which were individually resuspended in Duplex buffer (IDT, received with the tracrRNA) to form 200 µM

stocks. Stocks of crRNA and tracrRNA were stored at −70°C before use. Cas9 was stored at –20°C before use. Each crRNA was annealed separately with the tracrRNA by mixing 1 µL crRNA 200 µM; 1 µL tracrRNA 200 µM; 1.28 µL Duplex buffer. The mix was heated to 95°C for 5 min, then cooled on ice, to obtain a 61 µM gRNA solution. The gRNA solutions were then mixed in equal volumes with Cas9 (1 µL gRNA 61 µM; 1 µL Cas9 61 µM directly from the IDT vial), incubated at 37°C for 5 min then cooled on ice, generating three 30.5 µM RNP solutions. The three RNP solutions were pooled; the final concentration of each RNP in the pool was thus 10.2 µM and the total RNP concentration 30.5 µM.

The RNPs were usually kept overnight in a 4°C fridge on ice before injections the following day. Some experiments used RNPs stored at –70°C for a few weeks.

For experiments targeting two genes simultaneously (*appa*/*appb*, *psen1*/*psen2*, *apoea*/*apoeb*), we targeted each gene at two loci to potentially reduce unviability[20]. While mutating two loci instead of three is predicted to reduce rates of complete biallelic knockout animals, given the high rate of frameshift mutations achieved with the RNPs that were used, ~90% of injected animals were still expected to be complete biallelic knockouts. Across loci that were mutated during double F0 knockout experiments, 97.5 ± 7.0% of the reads were mutated, and 78.9 ± 24.0% of all reads had a frameshift mutation; see *francoiskroll.shinyapps.io/frameshiftmodel/* for the theoretical knockout rate prediction. The preparation followed the same steps as above. The four RNP solutions were pooled, so the final concentration of each RNP in the pool was 7.6 µM and the total RNP concentration was 30.5 µM.

Injections

Approximately 1 nL of the three-RNP pool was injected into the yolk at the single-cell stage before cell inflation. This amounts to ~30.5 fmol of RNP (30.5 fmol [5029 pg] of Cas9 and 30.5 fmol [1070 pg] of total gRNA). Each unique RNP was present in equal amounts in the pool. Therefore, in the case of three RNPs, ~10.2 fmol of each RNP were co-injected.

When targeting two genes simultaneously, approximately 1.3 nL of the four-RNP mix were injected so the amount of RNP per gene would remain equal to when a single gene is targeted at three loci.

The injected eggs were kept at ~20°C for ~50 min after injection before transfer to a 28.5°C incubator, as delaying the first cell division by lowering the temperature was tentatively shown to increase mutagenesis and reduce the diversity of alleles[102].

Scrambled RNPs

In all F0 knockout experiments, three or four non-targeting, 'scrambled', crRNAs were prepared into RNPs and injected following the same steps as above. These were created by shuffling the spacer sequence of existing crRNAs until the only predicted targets had 4 or more mismatches in protein-coding sequences, or 3 or more in non-coding sequences. Sequences of the scrambled crRNAs are available in Supplementary file 1.

Preparation of samples for Illumina MiSeq

We sequenced every targeted locus in samples of F0 knockout larvae using Illumina MiSeq. For *psen1*, *psen2*, *apoea*, and *apoeb*, the samples were from video-tracked larvae. The *appa*, *appb*, *cd2ap*, *clu*, and *sorl1* (scr1–2 and ko1–6) larvae were generated expressly to be sequenced. The other *sorl1* samples (scr3–4 and ko7–16) were from video-tracked larvae of the fluvoxamine experiment. For each locus, we generally prepared 5–6 F0 knockout samples and 2–3 scrambled-injected samples. Individual larvae were sequenced at the three or four mutated loci.

The larvae were anaesthetised and their genomic DNA extracted by HotSHOT[103] as follows. Individual larvae were transferred to a 96-well PCR plate or strips of 12 tubes. Excess liquid was removed from each well before adding 50 µL of 1× base solution (25 mM KOH, 0.2 mM EDTA in water). Plates were sealed and incubated at 95°C for 30 min then cooled to room temperature before the addition of 50 µL of 1× neutralisation solution (40 mM Tris-HCl in water). Genomic DNA was then stored at –20°C.

PCR primers were designed for each target locus using Primer-BLAST (NCBI) to amplify a window of 150–200 bp with at least 30 bp between each primer binding site and the predicted double-strand break site, as this is where most deletions are found[20]. PCR primers were ordered with a Nextera overhang at the 5'-end of each primer to allow indexing (see Supplementary file 1).

Each PCR well contained: 7.98 µL PCR mix (2 mM MgCl2, 14 mM pH 8.4 Tris-HCl, 68 mM KCl, 0.14% gelatine in water, autoclaved for 20 min, cooled to room temperature, chilled on ice, then added 1.8% 100 mg/mL BSA and 0.14% 100 mM d[A, C, G, T]TP), 3 µL 5× Phusion HF buffer (New England Biolabs), 2.7 µL dH2O, 0.3 µL forward primer (100 µM), 0.3 µL reverse primer (100 µM), 0.12 µL Phusion High-Fidelity DNA Polymerase (New England Biolabs), 1.0 µL genomic DNA; for a total of 15.4 µL. The PCR plate was sealed and placed into a thermocycler. The PCR program was: 95°C – 5 min, then 40 cycles of: 95°C – 30 sec, 60°C – 30 sec, 72°C – 30 sec, then 72°C – 10 min, then cooled to 10°C until collection. The PCR product's concentration was quantified with Qubit (dsDNA High Sensitivity or Broad Range Assay) and its length was verified on a 2.5% agarose gel with GelRed (Biotium). Excess primers and dNTPs were removed by ExoSAP-IT (ThermoFisher) following the manufacturer's instructions. The samples were then sent for Illumina MiSeq, which used MiSeq Reagent Nano Kit v2 (300 Cycles).

Illumina MiSeq data analysis

Illumina MiSeq data was received as two fastq files for each well, one forward and one reverse. The paired-end reads were aligned to the reference amplicon with bwa v0.7.17 and the resulting bam alignment file was sorted and indexed with samtools v1.11[104]. Alignments were then filtered to keep only reads with less than 20% of its length soft-clipped and spanning at least 20 bp on each side of the predicted Cas9 double-strand break site, 4 bp upstream of the 'N' of the NGG protospacer adjacent motif. Whenever necessary, bam alignment files were visualised with IGV v2.16.0. The resulting filtered bam file was converted back to a forward and a reverse fastq file using bedtools v2.30.0[105]. The filtered fastq files were used as input to the R package ampliCan v1.20.0[106], together with a csv configuration file containing metadata information about the samples. AmpliCan was run with settings min_freq = 0.005 (any mutation at a frequency below this threshold was considered as a sequencing error), cut_buffer = 12 (any insertion/deletion starting within ±12 bp of the PAM may be Cas9-generated), and event_filter = FALSE (no filtering of reads), as the reads were already filtered. AmpliCan can normalise mutation counts by ignoring any insertion/deletion found in control samples. On rare occasions, this could artefactually decrease mutation counts in F0 knockout samples because of low-level contamination in control samples (e.g. **Fig. 4**–supplement 4b, locus 1, sample scr1) so we turned this feature off. Instead, we manually checked the scrambled-injected samples in IGV to confirm that there were no insertions or deletions already present in the wild-type background. AmpliCan detected and counted mutations in the reads and wrote results files that were used for subsequent analysis. Any sample with less than 20× paired-end (40× single-read) coverage were excluded from plots and subsequent analysis, which is why some samples are missing from plots (e.g. locus2, ko5 is missing in **Fig. 3c**). Figures like **Fig. 3c,d** plot the proportion of mutated reads and the proportion of reads with a frameshift mutation at each locus, as computed by ampliCan. A read was counted as mutated if it contained one or more insertions or deletions (indels), base substitutions were not considered. If a read contained multiple indels, ampliCan summed them to conclude whether the read had a frameshift mutation or not.

3D-printed 96-well mesh-bottom plate

The 96-square well mesh-bottom plate (**Fig. 2a**) was designed using Fusion 360 and PrusaSlicer. Multiple copies were 3D-printed in clear polylactic acid (PLA) with a Creality Ender-3 3D printer. The 3D model is available at *github.com/francoiskroll/FramebyFrame*.

Behavioural video-tracking

In F0 knockout experiments, wild-type embryos from separate clutches were injected at the single-cell stage with CRISPR-Cas9 RNPs. Each clutch was from a unique pair of parents allowed to mate for 7–10 min. For each clutch, about half of the embryos were injected with non-targeting 'scrambled' RNPs to generate control siblings. Clutch-to-clutch variability in locomotor activity is substantial in zebrafish larvae, even between wild-type clutches of the same strain[107]. Therefore, keeping clutches from different parents/mating events separate is predicted to increase sensitivity of the assay by reducing variability. More generally, it is crucial never to perform comparisons where treatment larvae (e.g. mutant, transgenic, drug-treated) are from one clutch and the control larvae are from another (i.e. controls are not siblings), as any difference discovered with such an experimental design could be caused by clutch-to-clutch variability.

At 5 dpf, individual larvae were transferred to the wells of 3D-printed mesh-bottom plates (see *3D-printed 96-well mesh-bottom plate*), each sitting in the water bath of a Zebrabox (ViewPoint Behavior Technology). To avoid any potential localisation bias during the tracking, F0 knockout and scrambled-injected larvae were plated in alternating columns of the 96-well plate. From each well, the video-tracking software (ZebraLab, ViewPoint Behavior Technology) recorded the number of pixels that changed intensity between successive frames. To be counted, a pixel must have changed grey value above a sensitivity threshold, which was set at 20. The metric, termed Δ pixel, describes each animal's behaviour over time as a sequence of zeros and positive values, denoting if the larva was still or moving. In ZebraLab, the *freeze* setting was set to 3 and the *burst* setting was set to 200. However, note that these settings determine how the Δ pixel data is summarised into number of seconds active per minute by the software (*middur* parameter, see *One-minute vs. frame-by-frame*); therefore, their values are irrelevant when analysing the data using the FramebyFrame package. Tracking was performed at 25 frames per second on a 14 hr:10 hr light:dark cycle for ~65 hours, generating sequences of roughly 5,850,000 Δ pixel values per animal. During the experiment, a pump on a timer (Kollea Automatic Watering System, Amazon UK) injected fish water from a reservoir to the bath every morning around 9 AM (lights on) to counteract water evaporation. Water could overflow through an exit pipe, whose height was adjusted to set the water level in the bath. The day light level was calibrated at 555 lux with a RS PRO RS-92 light meter (RS Components). Night was in complete darkness with infrared lighting for video recording. Temperature and light transitions were recorded with a HOBO Pendant (Onset Data Loggers) immersed in the water bath. Temperature throughout the experiment was 23–26°C.

At the end of the tracking, we inspected the larvae under a bright-field microscope and excluded from analysis any larva that did not appear healthy or was not responsive to a light touch with a P10 tip. We then randomly selected 2–3 scrambled-injected and 5–6 F0 knockout larvae for sequencing of the targeted loci (see *Preparation of samples for Illumina MiSeq*).

Behavioural video-tracking with drug treatment

This refers to the experiments treating *sorl1* F0 knockouts with citalopram (**Fig. 5c,d**) or fluvoxamine (**Fig. 5**–supplement 1c,d) and the experiment treating *psen2* F0 knockouts with tinidazole, fenoprofen, and betamethasone (**Fig. 6b,c** and **Fig. 6**–supplement 1b). Broadly, video-tracking was performed as above (see *Behavioural video-tracking*) but larvae were housed in standard 96-square well plates (Whatman) in fish water with drug. Water was topped up every morning shortly after 9 AM (lights on).

Citalopram hydrobromide (Fisher Scientific, #15732987) was stored at room temperature before use. We chose the treatment concentrations (1 µM and 10 µM) based on previous work in zebrafish larvae[108] that found that the minimum dose which had a discernible effect on locomotor activity was 373 µg/L (0.92 µM). A 500× stock (5 mM) for the 10 µM treatment was prepared by diluting 0.0203 g in 10 mL dH2O (molecular weight = 405.3 g/mol). The 5 mM solution was then diluted 1:10 (100 µL citalopram 5 mM + 900 µL dH2O) to obtain a 500× stock (500 µM) for the 1 µM treatment. Using a P1000 pipet with a tip whose end was cut-off, individual 5-dpf larvae were transferred in 650 µL fish water to the wells of clear 96-square well plates (Whatman). 1.3 µL of each 500× stock was added on top of each well, effectively diluting each stock 1:500 (5 mM stock diluted to 10 µM and 500 µM stock diluted to 1 µM). Control wells were topped-up with 1.3 µL dH2O.

Fluvoxamine maleate (MedChemExpress HY-B0103A) was stored at −20°C before use. We chose 10 µM as the treatment concentration to match the citalopram experiment. A 500× stock (5 mM) was prepared by diluting the 5 mg received from the vendor in 3.14 mL dH2O (molecular weight = 318.3 g/mol). Aliquots of this stock were kept at −20°C before the experiment. Treatment was then performed as for citalopram.

Tinidazole (Fisher Scientific, #16594384) was stored at room temperature before use. We chose the treatment concentration (30 µM) based on a preliminary experiment where we video-tracked wild-type larvae treated with 10 µM, 30 µM, 100 µM tinidazole (data not shown). A 50 mM solution was prepared by diluting 0.0247 g in 2 mL DMSO (molecular weight = 247.27 g/mol), we then diluted this solution to 15 mM in DMSO as 500× stock.

Fenoprofen calcium salt hydrate (Sigma-Aldrich, #F1517) was stored at room temperature before use. We chose 15 µM as the treatment concentration based on the results from the Rihel et al., 2010 small molecule behavioural screen database[19]. A 200 mM solution was prepared by diluting 0.1114 g in 1065 µL DMSO (molecular weight = 522.6 g/mol), then diluting this solution to 7.5 mM in DMSO as 500× stock.

Betamethasone (Cayman Chemical, #20363) was stored at –20°C before use. We chose 15 µM as the treatment concentration based on the results from the Rihel et al., 2010 small molecule behavioural screen database. A 33 mM solution was prepared by diluting 0.0204 g in 1,575 µL DMSO (molecular weight = 393.5 g/mol), then diluting this solution to 7.5 mM in DMSO as 500× stock.

For tinidazole, fenoprofen, and betamethasone, 100 µL of each 500× stock was then mixed in 20 mL fish water in a Falcon, and the solution transferred to one Petri dish per drug. A Petri dish for control larvae was prepared by mixing 100 µL of DMSO in 20 mL fish water. Using a P1000 pipet with a tip whose end was cut-off, individual 5-dpf larvae were transferred in 500 µL fish water to the Petri dishes. Each Petri dish was then topped-up with fish water to 50 mL final volume, which effectively diluted each drug to the final treatment concentration (100 µL 500× stock in 50 mL fish water). The final DMSO concentration was 0.2% (100 µL 100% DMSO in 50 mL fish water). Using a P1000 pipet with a tip whose end was cut-off, individual larvae were then transferred in 650 µL to the 96-square well plates. This process was to avoid adding drug in DMSO directly to the well as the solution sinks in water and may not mix properly.

Video-tracking was then performed with the same settings as above (see *Behavioural video-tracking*). Both mornings shortly after 9 AM (lights on), the wells were manually topped-up with fish water (no drug), which assumes that the drug does not evaporate and was stable in fish water at 23–26°C for a few days.

A protocol for behavioural video-tracking with drug treatment is available at *dx.doi.org/10.17504/protocols.io.4r3l27p6pg1y/v1*.

Behavioural data analysis

Behavioural data analysis was performed using the FramebyFrame R package v0.11.0. A tutorial and documentation are available at *github.com/francoiskroll/FramebyFrame*. The important steps of the analysis are summarised below.

The raw file generated by the ZebraLab software was exported into hundreds of xls files each containing 1 million rows of data. Each row of data represented the Δ pixel of one larva at one frame transition. Using the vpSorter(…) function, these data were re-organised in a large csv file where each column was a well, each row was a frame transition, and each cell a Δ pixel value. To visualise activity over time, we smoothed the Δ pixel time course for each larva with a 60-min (~90,000 rows) rolling average then binned the data by summing Δ pixels in 10-min epochs. We generated the activity trace of individual larvae using ggActivityTraceGrid(…) and excluded from subsequent analysis any larva that had an obviously aberrant behaviour, defined as having missed entirely a day-night transition (no jump/drop in the activity trace) or having shown activity during a day lower than the previous night. Each well was assigned to a group using a metadata file generated by genotypeGenerator(…). For each 10-min epoch, we calculated the mean and standard error of the mean (SEM) across larvae in each group to build the activity traces (e.g. **Fig. 3g** left).

Sleep was measured on the large csv file containing all the frame-by-frame Δ pixel data. A 60-second (~1,500 rows) rolling sum was applied on the Δ pixel time course of each larva, so that any data point that became zero indicated that the previous 60 seconds of Δ pixels were all zeros, that is, a sleep bout started exactly 60 seconds ago. The data after the rolling sum was converted into a series of Booleans: *true* if the data point was 0 (i.e. that frame was part of a sleep bout); *false* if the data point was positive (i.e. that frame was not part of a sleep bout, as the larva moved at some point in the preceding 60 seconds). At this stage, the first 0 of each sleep bout marked the frame at the 60th second of each sleep bout. Therefore, a correction was then applied to extend each sleep bout 60 seconds in the past by switching the ~1,500 frames of *false* before each sleep bout start to *true*. The time spent asleep in 10-min epochs (~15,000 rows) was calculated by counting the number of *true* frames in each epoch and multiplying the counts by 1/frame rate (typically 1/25 frames per second), which was converted into minutes for the sleep trace. For example, if larva #3 had 5,000 out of 15,000 frames marked *true* (i.e. these frames are part of a sleep bout) from minute 20 to 30 of tracking, that represented $5{,}000 \times {}^{1}/_{25} \times {}^{1}/_{60} = 3.33$ *minutes asleep* for that epoch. As for the activity trace, the mean and SEM across larvae in each group were calculated for each 10-min epoch to build the sleep traces (e.g. **Fig. 3g** right).

15 behavioural parameters were then calculated for each larva and day/night. Two additional parameters, startle response at sunset and sleep latency, were only defined for nights, for a total of 32 unique parameters (15 day parameters and 17 night parameters). Full days/nights during the experiment were: night0, day1, night1, day2, night2. Larvae were 5 dpf during night0, 6 dpf during day1/night1, 7 dpf during day2/night2, and the experiment was stopped in the morning of 8 dpf. Night0 (5 dpf) was excluded from the analysis as a habituation period; therefore, two day data points and two night data points were calculated for each larva and behavioural parameter. Definitions of the behavioural parameters can be found in the documentation of the FramebyFrame package (*github.com/francoiskroll/FramebyFrame*).

To build the behavioural fingerprints, a z-score was calculated for each day/night, each larva, and each unique parameter. For example, to calculate the z-score for parameter active bout length of larva #5 for day1, we first calculated the mean and standard deviation of all active bout length data points for control larvae during day1. These were then used to calculate larva #5's z-score as:

$$z_{day1} = \frac{x - \mu_{con}}{\sigma_{con}}$$

Where x was larva #5's day1 data point, μ_{con} was the mean of control day1 data points, μ_{con} was the standard deviation of control day1 data points. The calculation was repeated for day2. The day1 and day2 z-scores were then averaged to produce a common day z-score for active bout length of larva #5. The process was repeated for each unique parameter, producing 32 z-scores for each larva, which we term each larva's behavioural fingerprint. To draw the fingerprint plots (e.g. **Fig. 3h**), the mean and SEM of all z-scores were calculated for each unique parameter and group of larvae. By definition of the z-score, the mean z-score for the control larvae was always 0 and the SEM constant for each experiment (dependent on the number of control larvae), so the controls' fingerprint was omitted from the plot.

In **Fig. 6c**, for each parameter, the mean and SEM of all z-scores from each clutch were calculated separately. The two z-score means and SEMs were then averaged to draw each bar. See *Statistics on behavioural parameters* for the definition of each category.

Each larva's fingerprint can be conceptualised as the coordinates of one data point in a 32-dimension space where each dimension represents one behavioural parameter. In **Fig. 5d** and **Fig. 5**–supplement 1d, the centre of the H2O-treated scrambled-injected larvae or the centre of the H2O-treated *sorl1* F0 knockout larvae was set as the origin of this 32-dimension space (point at coordinates 0, 0, 0, …) by the z-scoring procedure. We then measured the Euclidean distance between each larva's fingerprint and the origin.

Statistics on behavioural parameters

Each behavioural parameter was statistically compared between F0 knockout and scrambled-injected larvae using linear mixed effects (LME) modelling implemented in the lmer function of the R package lme4 v1.1.31[109]. The data were parameter values per larva per time window, for example larva #3 slept 4 hr during night2. We always tracked one unique clutch in each ZebraBox run; therefore, the replicate experiment(s) provided both technical and biological replication. The data collected during nights or during days were analysed separately. The fixed effect was the group assignment (genotype or treatment). Random effects were intercepts for clutch assignment (experiment), larva number, and the larva's age (dpf). Random effects of clutch assignment and larva number were modelled as nested, as data points between larvae of the same clutch were expected to be more similar than between larvae of different clutches; and within each clutch, the day 1 (or night 1) data point of one larva was expected to be similar to its day 2 (or night 2) data point. The command to create the day or night model was:

$$lmer(parameter \sim group + (1|experiment/larva) + (1|dpf), data = night\ or\ day)$$

The model provided the slope and its standard error reported on top of the parameter plots (e.g. **Fig. 3**–supplement 1b). A model without the fixed effect group was then created, as:

$$lmer(parameter \sim 1 + (1|experiment/larva) + (1|dpf), data = night\ or\ day)$$

This null model was compared with the full model created above with a likelihood-ratio test, which provided the p-value reported in the figures and legends.

The LME analysis was informed by a published tutorial[110]. The FramebyFrame R package performs the above LME analysis when generating parameter plots with ggParameterGrid(…) or writing a report of LME statistics using LMEreport(…).

The main likelihood-ratio test (see above) tested the null hypothesis that group assignment had no effect on parameter values. In experiments with more than two groups, each group was also compared to the reference group using estimated marginal means implemented in the R package emmeans, which provided the p-value.

In **Fig. 6c**, the LME analysis was performed on data from both clutches, as described above. The colour for each parameter was based on two p-values obtained using estimated marginal means: the p-value when comparing DMSO-treated scrambled-injected controls with DMSO-treated *psen2* F0 knockouts ("knockout p-value"), and the p-value when comparing DMSO-treated scrambled-injected controls with drug-treated *psen2* F0 knockouts ("drug p-value"), such that:

- if knockout p-value < 0.05 and drug p-value > 0.05, parameter was a "rescue";
- if knockout p-value < 0.05 and drug p-value < 0.05, parameter was a "missed rescue";
- if knockout p-value > 0.05 and drug p-value < 0.05, parameter was a "side effect";
- if knockout p-value > 0.05 and drug p-value > 0.05, parameter was a "no effect".

One-minute vs. frame-by-frame

The one-minute analyses developed previously[19,43,44] use the *middur* parameter calculated by ZebraLab. The *middur* parameter reports, for each minute, the number of seconds each larva spent above the *freeze* threshold (set by the user, typically 3 Δ pixel) and below the *burst* threshold (set by the user, typically 200 Δ pixel). In **Fig. 2**–supplement 2b,c, to better focus the comparisons on the effect of the one-minute binning, we re-calculated the *middur* dataset of the experiment using the FramebyFrame R package (function rawToMiddur(…)) setting the *freeze* threshold to 0. Larvae plotted were the scrambled-injected larvae from *sorl1* F0 knockout clutch 2 (**Fig. 4**–supplement 5).

Pilot long-term video-tracking in 96-well plate

For the experiment in **Fig. 2b**, we placed 4-dpf scrambled-injected larvae in the wells of a mesh-bottom plate and added to the water bath 50 mL of paramecia culture filtered through a 40-µm cell strainer nylon mesh (Fisherbrand) to remove the large debris which may be detected by the camera of the ZebraBox. Larvae were video-tracked for a total of 208 hr, first on a 14 hr:10 hr light:dark cycle for 63 hr then in constant dim light at 30 lux for 145 hr for the free-running segment. In the afternoon of the first day in constant dim conditions, we removed most of the water from the bath using a 10 mL Pasteur pipette, replaced with fresh fish water, and added another 50 mL of filtered paramecia. As can be seen in **Fig. 2b**, this created a sharp rise in activity. We did not intervene for the rest of the experiment. The activity trace was generated as above (see *Behavioural data analysis*).

Sleep latency in presence of paramecia

We video-tracked wild-type 6-dpf larvae as described above (see *Behavioural video-tracking*) for 24 hr, including a 14-hr night. Larvae were in the wells of a standard 96-square well plate (Whatman), and we added two drops of filtered paramecia in half of the wells. There was no water bath and the light level at night was 0 lux.

Zebrafish orthologues of Alzheimer's risk genes

We used the GWAS meta-analysis and list of most likely causal genes from Schwartzentruber et al. (2021)[23]. We downloaded from Ensembl the list of all zebrafish orthologues of human genes (accessed 27/04/2023). More details about GWAS loci, causal genes, and zebrafish orthologues can be found in Supplementary file 1.

Single-cell RNA sequencing data

We downloaded single-cell RNA sequencing (scRNA-seq) data generated by Raj et al. (2020)[27] from GEO repository GSE158142 (.rds.gz files, Seurat data structure). In **Fig. 1b**, each gene was considered expressed if it was detected in at least three cells at this developmental stage. In

Supplementary file 1, we manually grouped the clusters from Raj et al. (2020) in broad categories to add colours. The expression data plotted (e.g. **Fig. 1c**) were normalised from raw counts by the authors using the "LogNormalize" method implemented in Seurat[111].

In situ hybridization chain reaction

In situ hybridization chain reaction (HCR) probes were designed as described by Choi et al. (2018)[112] using a custom Python script. HCR split initiator sequences B1, B3, and B5 were obtained from Choi et al. (2018). To generate probe sets, probe pairs were excluded if they fell below melting temperature and %GC thresholds. Probe pairs with strong sequence similarity to off-target transcripts were also excluded. For each target transcript, we generated sets of 15–25 probe pairs. Multiple transcripts were often stained in the same individual larvae. HCR probes were purchased as custom DNA oligos from Thermo Fisher Scientific. HCR amplifiers (B1-Alexa Fluor 488, B3-Alexa Fluor 546, and B5-Alexa Fluor 647) and buffers were purchased from Molecular Instruments. More details about HCR probes can be found in Supplementary file 1.

The HCR protocol we used was adapted from MI-Protocol-RNAFISH-Zebrafish (Rev10) (Molecular Instruments). Proteinase K and methanol permeabilisation steps from the protocol were skipped. HCR to label Alzheimer's risk genes was performed in *Tg(elavl3:H2b-GCaMP6s)* larvae homozygous for the *mitfa*^{w2} allele (*nacre*)[113,114]. 6-dpf larvae were euthanised and fixed in 4% paraformaldehyde (PFA)/Dulbecco's phosphate-buffered saline (DPBS) overnight at 4°C. Following fixation, larvae were washed three times 5 min in phosphate-buffered saline (PBS). Larvae were then transferred to a SYLGARD-coated Petri dish and the eyes were removed using forceps. Sample preparation was completed by two brief PBST (1× DPBS + 0.1% Tween 20) washes. For the probe hybridization stage, larvae were first incubated in hybridization buffer at 37°C for 30 min. Meanwhile, a probe solution was prepared by adding 4 µL of each 1 µM probe set (4 pmol) to 500 µL hybridization buffer. Hybridization buffer was replaced by the probe solution, and larvae were incubated at 37°C overnight (12–16 hr).

The next day, excess probe solution was removed by washing larvae four times 15 min with 500 µL of probe wash buffer preheated to 37°C. Larvae were then washed twice 5 min with 5× SSCT at room temperature. Samples were kept at room temperature for subsequent amplification steps. First, larvae were transferred to amplification buffer at room temperature for 30 min. 3 µM stocks of hairpin H1 and hairpin H2 were individually heated to 95°C for 90 sec then left to cool at room temperature in the dark for 30 min. For HCR on up to 8 larvae together, a hairpin solution was prepared by adding 4 µL (12 pmol) of hairpin H1 and 4 µL of hairpin H2 (12 pmol) to 200 µL amplification buffer. Finally, amplification buffer was removed and the hairpin solution was added to the larvae which were incubated overnight (12–16 hr) in the dark at room temperature. After overnight incubation, excess hairpins were removed by washing in 5× SSCT for twice 5 min, then twice 30 min and finally once 5 min at room temperature. Larvae were transferred to PBS and kept at 4°C protected from light for up to 3 days.

For a subset of transcripts (*appa*, *appb*, *slc6a4a*, *slc6a4b*, *tph1a*, *tph1b*, *tph2*), HCR was not carried out in *nacre*, *elavl3:H2b-GCaMP6s* larvae. Instead, *gad1b* was labelled as a reference channel. We proceeded as above, with some amendments at the sample preparation stage. Larvae were fixed in 4% PFA with 4% (w/v%) sucrose overnight at 4°C. Brains were dissected with forceps, removing the eyes and the skin that covers the brain. After dissection, there was a 20-min postfix in 4% PFA with 4% (w/v%) sucrose followed by three washes in PBST to remove the fixative. When performing HCR on *sorl1* F0 knockout and scrambled-injected larvae (**Fig. 5e** and **Fig. 5** – supplement 1e), larvae from both conditions were pooled in a single Eppendorf tube prior to the hybridization steps. Using a scalpel, a portion of the tail was removed from the scrambled-injected larvae to differentiate the genotypes during imaging.

For imaging, larvae were mounted in 1% low melting point agarose (Sigma-Aldrich) in fish water and imaged with a ZEISS LSM 980 equipped with an Airyscan 2 detector (CO-8Y multiplex mode, confocal resolution) and a ZEISS C-Aprochromat 10×/0.45 W M27 objective. The whole brain was imaged without tiling. The image size was 844.29 µm (3188 pixels) × 846.41 µm (3196 pixels). Each pixel was 0.265 × 0.265 × 1.5 µm. The laser wavelength was 639 nm for B5-Alexa Fluor 647; 561 nm for B3-Alexa Fluor 546; 488 nm for GCaMP6s.

Samples in **Fig. 1**–supplement 3a,b, **Fig. 5e,f**, and **Fig. 5**–supplement 1e,f were imaged with a lightsheet ZEISS Z.1 microscope equipped with a W Plan-Aprochromat 10×/0.5 M27 75 mm objective. The image size was 889.56 µm (1920 pixels) × 889.56 µm (1920 pixels). Each pixel was 0.46 × 0.46 × 1.0 µm. The laser wavelength was 638 nm for B5-Alexa Fluor 647; 561 nm for B3-Alexa Fluor 546; 488 nm for GCaMP6s or B1-Alexa Fluor 488 to image *gad1b*.

Brains were registered to the reference brain from the Zebrafish Brain Browser[115,116] with *elavl3:H2B-GCaMP6s* or *gad1b* as reference channel using ANTs toolbox version 2.1.0[117], as described previously[118].

We prepared **Fig. 1d**, and **Fig. 1**–supplement 3 and 4 using Fiji[119]. The minimum/maximum and contrast of each stack/channel were adjusted before generating a maximum Z-projection. We created the sagittal views using Image > Stacks > Reslice before generating a maximum Z-projection. Whole-brain dorsal and sagittal outlines were from the Zebrafish Brain Browser.

In the *sorl1* experiments, masks for anatomical regions were from the Zebrafish Brain Browser. To measure total signal intensity in different anatomical regions (**Fig. 5f** left and **Fig. 5**–supplement 1f left), we summed the grey pixel values of every voxel within each mask on the stacks after registration. To count the number of positive voxels in different anatomical regions (**Fig. 5f** right and **Fig. 5**–supplement 1f right), we first rescaled each stack to the maximum grey value of the stack. We then applied a threshold at grey pixel value 15 (8bit image, so grey pixel value 0–255) so that the grey value of any voxel with signal below 15 was turned to 0. The threshold value was decided using the multi-Otsu algorithm with two classes implemented in the scikit-image Python package[120]. We then counted for each anatomical region the number of voxels with grey pixel value > 0.

To prepare **Fig. 5e** and **Fig. 5**–supplement 1e, we calculated each median stack using MATLAB R2022b. The maximum of all four median stacks were then adjusted to the same value in Fiji to keep intensities comparable. The dorsal and sagittal Z-projections were prepared as above.

Amyloid beta measurements on psen1 and psen2 F0 knockouts

psen1, *psen2*, and double *psen1*/*psen2* F0 knockout larvae were generated as described above (see *Generation of F0 knockout larvae*). Most double *psen1*/*psen2* F0 knockout larvae died or were severely dysmorphic by 5 dpf. The other larvae were raised until 16 dpf to increase the amount of tissue available for the assay. Larvae were euthanised by an overdose of tricaine then decapitated with a scalpel. Heads were snap-frozen in liquid nitrogen then homogenized using a mechanical homogenizer in 100 µL TBS (50mM Tris-HCl, pH 8.0) containing 1:200 protease inhibitor cocktail set III (Calbiochem). Homogenates were centrifuged at 16,000 g at 4°C for 30 min. The supernatant was then collected and stored at –70°C. We measured total protein concentration of each sample using the Pierce Detergent Compatible Bradford Assay Kit (ThermoFisher). Aβ38, Aβ40, and Aβ42 concentrations were measured on the Meso Scale Discovery platform (Meso Scale Diagnostics) using the V-PLEX Plus Aβ Peptide Panel 1 (4G8) kit.

Each pool of larvae was measured in four technical replicates: two at the original concentration and two diluted 1:1 in TBS. Meso Scale returned concentrations of Aβ38, Aβ40, Aβ42 in pg/mL. All Aβ38 measurements were below the detection limit. We converted the Aβ concentrations to pg Aβ/

µg total protein using the total protein content measured with the Bradford assay. The limit of detection (LOD) for each Aβ species was the concentration of the most diluted standard in pg/mL. We calculated a sample-specific LOD by calculating the Aβ concentration (pg Aβ/µg total protein) that would have given exactly the LOD in pg/mL. For example, the LOD for Aβ40 was 39.79 pg/mL. Therefore, for a sample whose total protein content was 3788 µg/mL, Aβ40 concentration should have been 0.0105 pg Aβ40/g total protein to give exactly the LOD (39.79 pg/mL). Each data point represents the mean of the four technical replicates, except if both diluted replicates were below the sample-specific LOD, in which case the data point represents the mean of the two undiluted technical replicates. If one undiluted sample was below the LOD but not the other, we replaced the below-LOD measurement by the sample-specific LOD itself. If all four technical replicates (undiluted and diluted) were below the sample-specific LOD, the sample was marked with a cross in the plot.

Annotation of the Rihel et al., 2010 small molecule behavioural database

From the Rihel et al., 2010 small molecule zebrafish behavioural database[19], we extracted the name of each compound tested and the 5,756 behavioural fingerprints, which are the mean z-score for each sleep/wake parameter (see **Fig. 6a** for the one-minute parameters). The same compound could have alternate database names (e.g. “Dopamine hydrochloride” and “Dopamine HCl”), and could vary by its stereochemistry or salts (e.g. atropine sulfate vs. atropine methyl nitrate). Therefore, we first simplified as much as possible each compound name by removing various stereochemistry and salt information. This reduced the number of unique compound names from 5,149 to 4,731. We then used the webchem R package[121] to automatically search each name in the PubChem database and return the PubChem CID. CID could be retrieved automatically for 4,365 (92%) of the names. We manually searched the remaining 366 compound names, eventually leaving only 8 of 4,731 compound names without a CID. The final number of unique CIDs was 3,677. The Therapeutic Target Database (TTD) uses a custom TTD Drug ID but provided a file for cross-matching PubChem CIDs to TTD Drug IDs (*P1-03-TTD_crossmatching.txt*). We found a TTD Drug ID for 1,740 of the 3,677 CIDs (47%). Using each TTD Drug ID as query, we then extracted indications and target proteins from databases provided by the TTD using TTD Drug IDs as queries (*P1-05-Drug_disease.txt* and *P1-01-TTD_target_download.txt*). Proteins are given a target ID by the TTD, which we then used as query to extract the KEGG pathways each protein was associated with (*P4-01-Target-KEGGpathway_all.txt*).

As TTD Drug IDs were used to extract annotations but that only 47% of compounds were assigned one, the ZOLTAR app currently uses less than half of the dataset by Rihel et al., 2010 for prediction of disrupted pathways. In the future, other sources could be used to enrich the annotations, for example using machine learning to predict target proteins[122].

Behavioural pharmacology from sorl1 F0 knockout’s fingerprint

We first simplified the Rihel et al., 2010 behavioural database[19] so that each compound (unique PubChem CID) would be present as a single average fingerprint. Without this adjustment, a single compound could in theory drive a significant enrichment because it is present as several replicate fingerprints (e.g. propranolol has 10 fingerprints) all positively or negatively correlating with the query fingerprint. We then measured the cosine similarity (range −1.0–1.0) between the mean fingerprint of the two *sorl1* F0 knockout clutches and each of the 3,677 average small molecule fingerprints (one per PubChem CID) from the Rihel et al., 2010 database, ranking them from the small molecule fingerprint with the most positive cosine (SU6656: cos = 0.83) to the one with the most negative cosine (nitrocaramiphen HCl: cos = −0.78).

At this stage, the general goal of the analysis is to detect whether compounds with a given annotation (indication, target, or KEGG pathway) are found more towards the top and/or bottom of the ranked list than expected by chance. For example, two cases suggest that inhibition of a pathway is what causes the knockout behavioural phenotype: all compounds *inhibiting* this

pathway are found towards the top of the list (positive cosines); or all compounds *activating* this pathway are found towards the bottom of the list (negative cosines). The database may include both agonists and antagonists for a given pathway, so we also want to detect cases where compounds interacting with the pathway are found both towards the top *and* towards the bottom of the ranked list. Therefore, the null hypothesis for a given annotation is specifically that fingerprints with this annotation are found across the ranked list in a pattern that can be explained by chance, or that they are mostly found around the centre of the list (cos ~ 0 position).

We swapped each compound in the ranked list for its annotations, for example its target(s), keeping for each the original cosine of the compound. If a compound had no annotated target (or indication or KEGG pathway), it was simply deleted. If a compound had multiple annotated targets (or indications or KEGG pathways), all targets received the compound's cosine. For example, aspirin had cos = −0.41 and two annotated targets: HMG-CoA reductase and prostaglandin G/H synthase. Therefore, swapping aspirin for its targets generated two rows with the same cosine −0.41.

To measure enrichment of a given annotation towards the top and/or bottom of the list, we summed the absolute cosines of all its instances. For example, 18 compounds in the database are annotated as binding the serotonin transporter (SLC6A4). In the ranked list of fingerprints for *sorl1*, the sum of those 18 cosines was 6.07. Was this sum of cosines surprising or could it be explained by chance? To test this, we randomly drew 18 positions and measured the sum of cosines 100,000 times to generate a null distribution of sum of cosines (e.g. **Fig. 5b**). We counted how many random draws gave a larger sum of cosines than the observed sum of cosines (6.07) to calculate a simulated p-value. In the case of SLC6A4, 1,470 random draws gave a larger sum of cosines; therefore, the probability that a sum of cosines as high as 6.07 was obtained by chance was estimated at 1,470/100,000 = 0.0147, which we reported as the simulated p-value.

Behavioural pharmacology from psen2 F0 knockout's fingerprint

We measured the cosine similarity between the mean fingerprint of the two *psen2* F0 knockout clutches and each of the 5,756 small molecule fingerprints from the Rihel et al., 2010 database. We then ranked the 5,756 small molecule fingerprints from the most positive cosine (3-3-Acetoxypregn-16-en-12,20-dione: cos = 0.82) to the most negative cosine (isogedunin: cos = −0.87). We searched within the ~100 fingerprints with the most negative cosines (range of cosines: −0.72–−0.87) for compounds which Rihel et al., 2010 labelled as shortlisted because it affected one behavioural parameter with a large effect size and/or affected the same parameter in the same direction across the two days/nights. From these compounds, we selected fenoprofen and betamethasone because they both had a replicate fingerprint with cosine < −0.50. Tinidazole was selected based on a preliminary experiment in wild-type larvae (data not shown), although it was not shortlisted by Rihel et al., 2010.

To simplify this selection process in the ZOLTAR app (*francoiskroll.shinyapps.io/zoltar/*), the shortlisted compounds are labelled, and clicking on a candidate compound automatically plots all the fingerprints from this compound (same PubChem CID).

Protein alignment plots

This refers to the plots as in **Fig. 3a,b**. Amino acid sequences were obtained from UniProt. The ClustalOmega algorithm, implemented in R by the msa package, was used to align the sequences. Definitions of "highly similar" and "weakly similar" groups of amino acids were taken from the ClustalOmega online documentation. The following groups of amino acids were considered highly similar: STA, NEQK, NHQK, NDEQ, QHRK, MILV, MILF, HY, FYW. The following groups of amino acids were considered weakly similar: CSA, ATV, SAG, STNK, STPA, SGND, SNDEQK, NDEQHK, NEQHRK, FVLIM, HFY. Identity was the number of positions where the zebrafish amino acid matched the human amino acid divided by the total length of the alignment. Similarity was the

number of positions where the zebrafish amino acid matched or was highly similar to the human amino acid divided by the total length of the alignment. UniProt IDs of the amino acid sequences used were (human vs. zebrafish): *appa*, P05067 vs. Q6NUZ1; *appb*, P05067 vs. B0V0E5; *psen1*, P49768 vs. Q9W6T7; *psen2*, P49810 vs. Q90ZE4; *apoea*, P02649 vs. Q503V2; *apoeb*, P02649 vs. O42364; *cd2ap*, Q9Y5K6 vs. F1R1N9; *clu*, P10909 vs. Q6PBL3; *sorl1*, Q92673 vs. Q90ZE4.

Gene schematics

This refers to the plots as in **Fig. 3c,d**. Coordinates of 5'-UTRs, 3'-UTRs, and exon boundaries were obtained from Ensembl accessed through R using the biomaRt package v2.54.1[123]. For each gene, we drew the transcript that was used as reference when selecting the crRNAs, usually the longest coding transcript annotated in Ensembl. Ensembl IDs of transcripts drawn were: *appa*, ENSDART00000166786; *appb*, ENSDART00000077908; *psen1*, ENSDART00000149864; *psen2*, ENSDART00000006381; *apoea*, ENSDART00000172219; *apoeb*, ENSDART00000058965; *cd2ap*, ENSDART00000102611; *clu*, ENSDART00000127173; *sorl1*, ENSDART00000156995.

Pictures

For the pictures of the *psen2* F0 knockout larvae and scrambled-injected siblings (**Fig. 3f** and **Fig. 3**–supplement 3a), larvae were anaesthetised and mounted in 1% low melting point agarose (Sigma-Aldrich) in fish water. Pictures were then taken with a Nikon SMZ1500 brightfield microscope with illumination from above the sample.

Pictures of the *psen1/psen2* double F0 knockout larvae (**Fig. 3**–supplement 1a) were taken with an Olympus MVX10 microscope connected to a computer with the software cellSens (Olympus).

Statistics

For statistics on behavioural parameters, see *Statistics on behavioural parameters*. For the permutations procedure used in **Fig. 5a,b** and **Fig. 5**–supplement 1a,b, see *Behavioural pharmacology from sorl1 F0 knockout's fingerprint*.

Threshold for statistical significance was $\alpha = 0.05$. In figures, ns refers to $p > 0.05$, * to $p \leq 0.05$, ** to $p \leq 0.01$, and *** to $p \leq 0.001$. In text, data distributions are reported as mean ± standard deviation, unless stated otherwise.

In text, estimates of behavioural parameter effect sizes are often reported in % vs. scrambled-injected controls. To calculate those, we first calculated, for each clutch and day or night, the mean of all control data points for this parameter, typically returning four averages (e.g. clutch1 controls, night1 and night2; clutch2 controls, night1 and night2). To each average, the slope from the LME model (see *Statistics on behavioural parameters*) was added/subtracted to estimate the knockout averages. An effect size in % vs. controls (*ef*%) was then calculated for each clutch and day or night as:

$$ef\% = 100 \times (-1 + \frac{ko}{con})$$

if the slope was positive; or

$$ef\% = -100 \times (1 - \frac{ko}{con})$$

if the slope was negative; where *ko* and *con* is the knockout or control average for one clutch and one day or night. The effect sizes were then averaged to return one effect size representing the estimated % increase or decrease vs. scrambled controls.

In **Fig. 2**–supplement 2d, the data were 47 observations, one per larva. Each observation was the time in hours when the larva had its first sleep bout (status 2). Every larva slept at least once during the experiment, so there were no censored (status 1) observations. We calculated the hazard ratio with a Cox proportional-hazards model and the p-value with a likelihood-ratio test. The functions we used were implemented in the R package survival v3.4.0. The FramebyFrame R package automatically performs this survival analysis when generating sleep latency survival plots with the function ggSleepLatencyGrid(...).

In **Fig. 5f** and **Fig. 5**–supplement 1f, we compared values between groups (*sorl1* F0 knockouts vs. scrambled-injected) in each anatomical region using Welch's t-test. To test the null hypothesis that group assignment had no effect on values across regions, we used LME modelling implemented in the lmer function of the R package lme4 v1.1.31[109]. Taking total signal intensity as an example, the command to create the LME model was:

$$lmer(total\ signal\ intensity \sim group + (1|larva) + (1|anatomical\ region)$$

The model provided the slope and its standard error reported in the figures. We then created a model without the fixed effect group, as:

$$lmer(total\ signal\ intensity \sim 1 + (1|larva) + (1|anatomical\ region)$$

We compared this null model with the full model created above with a likelihood-ratio test, which provided the p-value reported in the figures.

Software

Data analysis was performed in R v4.2.2 ran through RStudio 2023.06.0+421. Analysis of HCR on *sorl1* F0 knockouts used Jupyter notebooks written in Python 3 and a MATLAB script ran in MATLAB R2022b. Figures were prepared with Adobe Illustrator 2019. Videos were prepared with Adobe Premiere Pro 2020.

Code availability

Source code of the FramebyFrame R package is available at *github.com/francoiskroll/FramebyFrame*. The package can be installed directly into R. The GitHub repository includes installation instructions, tutorial, and documentation.

The ZOLTAR online app (*francoiskroll.shinyapps.io/zoltar/*) was written in R using the Shiny package. Source code is available at *github.com/francoiskroll/ZOLTAR*.

The online app illustrating the simplified model of knockout by frameshift (*francoiskroll.shinyapps.io/frameshiftmodel/*) was written in R using the Shiny package. Source code is available *github.com/francoiskroll/frameshiftShiny*.

Other code used for analysis is available at *github.com/francoiskroll/ZFAD*.

Data availability

Data is available on Zenodo at *https://doi.org/10.5281/zenodo.11673115*.

Acknowledgements

We thank the members of the Rihel lab and other zebrafish groups at University College London (UCL) for helpful discussions. We thank Daniel J. Stein and Douglas A. Lauffenburger (MIT) for inspiration. We thank Alexandra Lubin and Katie-Jo Thorpe for the Illumina MiSeq runs; Chintan Trivedi for code used to design HCR probes and advice on analysis of the HCR images; Tom Ryan for help raising the *psen1*/*psen2* knockout larvae used for the Aβ measurements; Alizée Kastler for the *slc6a4b* HCR probes; Stephen Carter for his assessment of the *psen1*/*psen2* double knockout eye phenotype; Declan Lyons for the measurements of the 3D-printed plate's mesh. We thank all supporting staff at UCL including Fish Facility staff for fish care and husbandry. FK thanks Filippo Del Bene for the time spent in his lab working on the manuscript and Sophie Nunes Figueiredo and Camille Lejeune (PHENO-Zfish platform, Institut du Cerveau, Paris) for kindly giving access to their Zebrabox. Most of the behavioural small molecule dataset was generated by JR and David Prober in Alexander F Schier's lab at Harvard University. FK was supported and funded by the Leonard Wolfson PhD Programme in Neurodegeneration. The work was also funded by a Wellcome Trust Investigator Award awarded to JR (217150/Z/19/Z).

Additional files

Supplemental File 1

Fig. 1–suppl. video 1. *Expression of appa in the larval zebrafish brain.**A**verage stack (n = 3 larvae), from dorsal to ventral, of the brain of 6-dpf wild-type larvae stained for appa mRNA by in situ hybridization chain reaction. gad1b mRNA was also stained as background channel (grey scale).*

Fig. 1–suppl. video 2. *Expression of appb in the larval zebrafish brain.Average stack (n = 3 larvae), from dorsal to ventral, of the brain of 6-dpf wild-type larvae stained for appb mRNA by in situ hybridization chain reaction. gad1b mRNA was also stained as background channel (grey scale).*

Fig. 1–suppl. video 3. *Expression of psen1 in the larval zebrafish brain.Average stack (n = 3 larvae), from dorsal to ventral, of the brain of 6-dpf elavl3:H2b-GCaMP6s larvae stained for psen1 mRNA by in situ hybridization chain reaction.*

Fig. 1–suppl. video 4. *Expression of psen2 in the larval zebrafish brain.Average stack (n = 3 larvae), from dorsal to ventral, of the brain of 6-dpf elavl3:H2b-GCaMP6s larvae stained for psen2 mRNA by in situ hybridization chain reaction.*

Fig. 1–suppl. video 5. *Expression of apoea in the larval zebrafish brain.Average stack (n = 3 larvae), from dorsal to ventral, of the brain of 6-dpf elavl3:H2b-GCaMP6s larvae stained for apoea mRNA by in situ hybridization chain reaction.*

Fig. 1–suppl. video 6. *Expression of apoeb in the larval zebrafish brain.Average stack (n = 3 larvae), from dorsal to ventral, of the brain of 6-dpf elavl3:H2b-GCaMP6s larvae stained for apoeb mRNA by in situ hybridization chain reaction.*

Fig. 1–suppl. video 7. *Expression of cd2ap in the larval zebrafish brain.Average stack (n = 3 larvae), from dorsal to ventral, of the brain of 6-dpf elavl3:H2b-GCaMP6s larvae stained for cd2ap mRNA by in situ hybridization chain reaction.*

Fig. 1–suppl. video 8. *Expression of clu in the larval zebrafish brainAverage stack (n = 3 larvae), from dorsal to ventral, of the brain of 6-dpf elavl3:H2b-GCaMP6s larvae stained for clu mRNA by in situ hybridization chain reaction.*

Fig. 1–suppl. video 9. *Expression of sorl1 in the larval zebrafish brain.Average stack (n = 2 larvae), from dorsal to ventral, of the brain of 6-dpf elavl3:H2b-GCaMP6s larvae stained for sorl1 mRNA by in situ hybridization chain reaction.*

References

1. Schellenberg G. D., et al. (1992) **Genetic linkage evidence for a familial Alzheimer's disease locus on chromosome 14** *Science* **258**:668–671

2. Levy E., et al. (1990) **Mutation of the Alzheimer's Disease Amyloid Gene in Hereditary Cerebral Hemorrhage, Dutch Type** *Science* **248**:1124–1126

3. Van Broeckhoven C., et al. (1990) **Amyloid β Protein Precursor Gene and Hereditary Cerebral Hemorrhage with Amyloidosis (Dutch)** *Science* **248**:1120–1122

4. Campion D., et al. (1995) **Mutations of the presenilin I gene in families with early-onset Alzheimer's disease** *Human Molecular Genetics* **4**:2373–2377

5. Rogaev E. I., et al. (1995) **Familial Alzheimer's disease in kindreds with missense mutations in a gene on chromosome 1 related to the Alzheimer's disease type 3 gene** *Nature* **376**:775–778

6. Glenner G. G., Wong C. W (1984) **Alzheimer's disease and Down's syndrome: sharing of a unique cerebrovascular amyloid fibril protein** *Biochem Biophys Res Commun* **122**:1131–1135

7. Haass C., Selkoe D. J (1993) **Cellular processing of β-amyloid precursor protein and the genesis of amyloid β-peptide** *Cell* **75**:1039–1042

8. Shoji M., et al. (1992) **Production of the Alzheimer amyloid beta protein by normal proteolytic processing** *Science* **258**:126–129

9. De Strooper B., et al. (1998) **Deficiency of presenilin-1 inhibits the normal cleavage of amyloid precursor protein** *Nature* **391**:387–390

10. Wolfe M. S., et al. (1999) **Two transmembrane aspartates in presenilin-1 required for presenilin endoproteolysis and gamma-secretase activity** *Nature* **398**:513–517

11. Hardy J., Selkoe D. J (2002) **The amyloid hypothesis of Alzheimer's disease: progress and problems on the road to therapeutics** *Science* **297**:353–356

12. van Dyck C. H., et al. (2023) **Lecanemab in Early Alzheimer's Disease** *New England Journal of Medicine* **388**:9–21

13. Hardy J., Mummery C (2023) **An anti-amyloid therapy works for Alzheimer's disease: why has it taken so long and what is next?** *Brain* **146**:1240–1242

14. Lu Q., et al. (2017) **Systematic tissue-specific functional annotation of the human genome highlights immune-related DNA elements for late-onset Alzheimer's disease** *PLOS Genetics* **13**

15. Tansey K. E., Cameron D., Hill M. J (2018) **Genetic risk for Alzheimer's disease is concentrated in specific macrophage and microglial transcriptional networks** *Genome Medicine* **10**

16. Bellenguez C., et al. (2022) **New insights into the genetic etiology of Alzheimer's disease and related dementias** *Nat Genet* **54**:412–436

17. Kroll F. (2022) **From disease genes to behavioural screen in zebrafish: early onset Alzheimer's as case study** (University College London). (UCL (University College London)

18. Verschuur C. V. M., et al. (2019) **Randomized Delayed-Start Trial of Levodopa in Parkinson's Disease** *N Engl J Med* **380**:315–324

19. Rihel J., et al. (2010) **Zebrafish Behavioral Profiling Links Drugs to Biological Targets and Rest/Wake Regulation** *Science* **327**:348–351

20. Kroll F., et al. (2021) **A simple and effective F0 knockout method for rapid screening of behaviour and other complex phenotypes** *eLife* **10**

21. Ashlin T. G., Blunsom N. J., Ghosh M., Cockcroft S., Rihel J (2018) **Pitpnc1a Regulates Zebrafish Sleep and Wake Behavior through Modulation of Insulin-like Growth Factor Signaling** *Cell Reports* **24**:1389–1396

22. Hoffman E. J., et al. (2016) **Estrogens Suppress a Behavioral Phenotype in Zebrafish Mutants of the Autism Risk Gene, CNTNAP2** *Neuron* **89**:725–733

23. Schwartzentruber J., et al. (2021) **Genome-wide meta-analysis, fine-mapping and integrative prioritization implicate new Alzheimer's disease risk genes** *Nat Genet* **53**:392–402

24. Giambartolomei C., et al. (2014) **Bayesian Test for Colocalisation between Pairs of Genetic Association Studies Using Summary Statistics** *PLoS Genet* **10**

25. Raj T., et al. (2018) **Integrative transcriptome analyses of the aging brain implicate altered splicing in Alzheimer's disease susceptibility** *Nat Genet* **50**:1584–1592

26. Meyer A., Mélaga-Trillo E (1999) **Vertebrate genomics: More fishy tales about Hox genes** *Current Biology* **9**:R210–R213

27. Raj B., et al. (2020) **Emergence of Neuronal Diversity during Vertebrate Brain Development** *Neuron* **108**:1058–1074

28. Yamazaki Y., Zhao N., Caulfield T. R., Liu C.-C., Bu G (2019) **Apolipoprotein E and Alzheimer disease: pathobiology and targeting strategies** *Nat Rev Neurol* **15**:501–518

29. Kunkle B. W., et al. (2019) **Genetic meta-analysis of diagnosed Alzheimer's disease identifies new risk loci and implicates Aβ, tau, immunity and lipid processing** *Nat Genet* **51**:414–430

30. Lambert J.-C., et al. (2013) **Meta-analysis of 74,046 individuals identifies 11 new susceptibility loci for Alzheimer's disease** *Nat Genet* **45**:1452–1458

31. Nicolas G., et al. (2016) **SORL1 rare variants: a major risk factor for familial early-onset Alzheimer's disease** *Mol Psychiatry* **21**:831–836

32. Pottier C., et al. (2012) **High frequency of potentially pathogenic SORL1 mutations in autosomal dominant early-onset Alzheimer disease** *Mol Psychiatry* **17**:875–879

33. Thonberg H., et al. (2017) **Identification and description of three families with familial Alzheimer disease that segregate variants in the SORL1 gene** *Acta Neuropathologica Communications* **5**

34. Herbomel P., Thisse B., Thisse C (2001) **Zebrafish Early Macrophages Colonize Cephalic Mesenchyme and Developing Brain, Retina, and Epidermis through a M-CSF Receptor-Dependent Invasive Process** *Developmental Biology* **238**:274–288

35. Kudoh T., et al. (2001) **A Gene Expression Screen in Zebrafish Embryogenesis** *Genome Res* **11**:1979–1987

36. Raymond P. A., Barthel L. K., Bernardos R. L., Perkowski J. J (2006) **Molecular characterization of retinal stem cells and their niches in adult zebrafish** *BMC Dev Biol* **6**

37. Thiel W. A., Esposito E. J., Findley A. P., Blume Z. I., Mitchell D. M (2022) **Modulation of retinoid-X-receptors differentially regulates expression of apolipoprotein genes apoc1 and apoeb by zebrafish microglia** *Biology Open* **11**

38. Farrell J. A., et al. (2018) **Single-cell reconstruction of developmental trajectories during zebrafish embryogenesis** *Science* **360**

39. Wu S., et al. (2020) **Two phenotypically and functionally distinct microglial populations in adult zebrafish** *Sci. Adv* **6**

40. Lowery L. A., Sive H. (2005) **Initial formation of zebrafish brain ventricles occurs independently of circulation and requires the nagie oko and snakehead/atp1a1a.1 gene products** *Development* **132**:2057–2067

41. Mu Y., et al. (2019) **Glia Accumulate Evidence that Actions Are Futile and Suppress Unsuccessful Behavior** *Cell* **178**:27–43

42. Jiao S., et al. (2011) **The Conserved Clusterin Gene Is Expressed in the Developing Choroid Plexus Under the Regulation of Notch But Not IGF Signaling in Zebrafish** *Endocrinology* **152**:1860–1871

43. Lee D., Oikonomou G., Prober D (2022) **Large-scale Analysis of Sleep in Zebrafish** *Bio-protocol* **12**

44. Rihel J., Prober D. A., Schier A. F (2010) **Monitoring Sleep and Arousal in Zebrafish** *Methods in Cell Biology* **100**:281–294

45. Ghosh M., Rihel J (2020) **Hierarchical Compression Reveals Sub-Second to Day-Long Structure in Larval Zebrafish Behavior** *eNeuro* **7**

46. Prober D. A., Rihel J., Onah A. A., Sung R.-J., Schier A. F (2006) **Hypocretin/Orexin Overexpression Induces An Insomnia-Like Phenotype in Zebrafish** *J. Neurosci* **26**:13400–13410

47. Haapasalo A., Kovacs D. M (2011) **The Many Substrates of Presenilin/γ-Secretase** *Jad* **25**:3–28

48. Kang J., et al. (1987) **The precursor of Alzheimer's disease amyloid A4 protein resembles a cell-surface receptor** *Nature* **325**:733–736

49. Özcan G. G., Lim S., Rihel J. (2022) **Genetic and chemical disruption of Amyloid Precursor Protein processing impairs zebrafish sleep maintenance** *bioRxiv* https://doi.org/10.1101/2022.06.08.495312

50. Frånberg J., Svensson A. I., Winblad B., Karlström H., Frykman S (2011) **Minor contribution of presenilin 2 for γ-secretase activity in mouse embryonic fibroblasts and adult mouse brain** *Biochemical and Biophysical Research Communications* **404**:564–568

51. Herreman A., et al. (1999) **Presenilin 2 deficiency causes a mild pulmonary phenotype and no changes in amyloid precursor protein processing but enhances the embryonic lethal phenotype of presenilin 1 deficiency** *Proceedings of the National Academy of Sciences* **96**:11872–11877

52. Shen J., et al. (1997) **Skeletal and CNS Defects in Presenilin-1-Deficient Mice** *Cell* **89**:629–639

53. Sundvik M., Chen Y.-C., Panula P (2013) **Presenilin1 Regulates Histamine Neuron Development and Behavior in Zebrafish, Danio rerio** *J. Neurosci* **33**:1589–1597

54. Jiang H., Newman M., Lardelli M (2018) **The zebrafish orthologue of familial Alzheimer's disease gene PRESENILIN 2 is required for normal adult melanotic skin pigmentation** *PLoS ONE* **13**

55. Yang T., Arslanova D., Gu Y., Augelli-Szafran C., Xia W (2008) **Quantification of gamma-secretase modulation differentiates inhibitor compound selectivity between two substrates Notch and amyloid precursor protein** *Molecular Brain* **1**

56. Sleegers K., et al. (2006) **APP duplication is sufficient to cause early onset Alzheimer's dementia with cerebral amyloid angiopathy** *Brain* **129**:2977–2983

57. Musa A., Lehrach H., Russo V. E (2001) **Distinct expression patterns of two zebrafish homologues of the human APP gene during embryonic development** *Dev Genes Evol* **211**:563–567

58. Zhou Y., et al. (2022) **Therapeutic target database update 2022: facilitating drug discovery with enriched comparative data of targeted agents** *Nucleic Acids Res* **50**:D1398–D1407

59. Andersen J. S., Kristensen A., Bang-Andersen B., Strømgaard K. (2009) **Recent advances in the understanding of the interaction of antidepressant drugs with serotonin and norepinephrine transporters** *Chemical Communications* 0:3677–3692

60. Omori I. M., et al. (2010) **Fluvoxamine versus other anti-depressive agents for depression** *Cochrane Database Syst Rev C* https://doi.org/10.1002/14651858.CD006114.pub2

61. Lillesaar C (2011) **The serotonergic system in fish** *Journal of Chemical Neuroanatomy* **41**:294–308

62. Glerup S., et al. (2013) **SorLA Controls Neurotrophic Activity by Sorting of GDNF and Its Receptors GFRα1 and RET** *Cell Reports* **3**:186–199

63. Barthelson K., Pederson S. M., Newman M., Lardelli M (2020) **Brain transcriptome analysis reveals subtle effects on mitochondrial function and iron homeostasis of mutations in the SORL1 gene implicated in early onset familial Alzheimer's disease** *Molecular Brain* **13**

64. D'Atri A., et al. (2021) **EEG alterations during wake and sleep in mild cognitive impairment and Alzheimer's disease** *iScience* **24**

65. Prinz P. N., et al. (1982) **Sleep, EEG and mental function changes in senile dementia of the Alzheimer's type** *Neurobiol Aging* **3**:361–370

66. Lim A. S. P., Kowgier M., Yu L., Buchman A. S., Bennett D. A (2013) **Sleep Fragmentation and the Risk of Incident Alzheimer's Disease and Cognitive Decline in Older Persons** *Sleep* **36**:1027–1032

67. Shokri-Kojori E., et al. (2018) **β-Amyloid accumulation in the human brain after one night of sleep deprivation** *Proc Natl Acad Sci U S A* **115**:4483–4488

68. Lucey B. P., et al. (2018) **Effect of sleep on overnight cerebrospinal fluid amyloid β kinetics** *Ann Neurol* **83**:197–204

69. Holth J. K., et al. (2019) **The sleep-wake cycle regulates brain interstitial fluid tau in mice and CSF tau in humans** *Science* **363**:880–884

70. Kang J.-E., et al. (2009) **Amyloid-beta dynamics are regulated by orexin and the sleep-wake cycle** *Science* **326**:1005–1007

71. Zhao B., et al. (2019) **Chronic Sleep Restriction Induces Aβ Accumulation by Disrupting the Balance of Aβ Production and Clearance in Rats** *Neurochem Res* **44**:859–873

72. Jagirdar R., et al. (2021) **Restoring activity in the thalamic reticular nucleus improves sleep architecture and reduces Aβ accumulation in mice** *Sci Transl Med* **13**

73. Herring W. J., et al. (2020) **Polysomnographic assessment of suvorexant in patients with probable Alzheimer's disease dementia and insomnia: a randomized trial** *Alzheimers Dement* **16**:541–551

74. Ednick M., et al. (2009) **A review of the effects of sleep during the first year of life on cognitive, psychomotor, and temperament development** *Sleep* **32**:1449–1458

75. Dean D. C., et al. (2014) **Brain Differences in Infants at Differential Genetic Risk for Late-Onset Alzheimer Disease A Cross-sectional Imaging Study** *JAMA Neurol* **71**:11–22

76. Quiroz Y. T., et al. (2015) **Brain Imaging and Blood Biomarker Abnormalities in Children With Autosomal Dominant Alzheimer Disease: A Cross-Sectional Study** *JAMA Neurol* **72**:912–919

77. Chen D., Wang X., Huang T., Jia J (2022) **Sleep and Late-Onset Alzheimer's Disease: Shared Genetic Risk Factors, Drug Targets, Molecular Mechanisms, and Causal Effects** *Front. Genet* **13**

78. Leng Y., Ackley S. F., Glymour M. M., Yaffe K., Brenowitz W. D (2021) **Genetic Risk of Alzheimer's Disease and Sleep Duration in Non-Demented Elders** *Ann Neurol* **89**:177–181

79. Muto V., et al. (2021) **Alzheimer's disease genetic risk and sleep phenotypes in healthy young men: association with more slow waves and daytime sleepiness** *Sleep* **44**

80. Jensen A. M. G., et al. (2023) **Dimerization of the Alzheimer's disease pathogenic receptor SORLA regulates its association with retromer** *Proceedings of the National Academy of Sciences* **120**

81. Mishra S., et al. (2022) **The Alzheimer's gene SORL1 is a regulator of endosomal traffic and recycling in human neurons** *Cell. Mol. Life Sci* **79**

82. Burd C., Cullen P. J (2014) **Retromer: a master conductor of endosome sorting** *Cold Spring Harb Perspect Biol* **6**

83. Mishra S., et al. (2023) **Pharmacologic Stabilization of Retromer Rescues Endosomal Pathology Induced by Defects in the Alzheimer's gene SORL1** *bioRxiv* https://doi.org/10.1101/2022.07.31.502217

84. Small S. A., Petsko G. A (2015) **Retromer in Alzheimer disease, Parkinson disease and other neurological disorders** *Nat Rev Neurosci* **16**:126–132

85. Joubert L., et al. (2004) **New sorting nexin (SNX27) and NHERF specifically interact with the 5-HT4a receptor splice variant: roles in receptor targeting** *J Cell Sci* **117**:5367–5379

86. Huang T. Y., et al. (2016) **SNX27 and SORLA Interact to Reduce Amyloidogenic Subcellular Distribution and Processing of Amyloid Precursor Protein** *J Neurosci* **36**:7996–8011

87. Cirrito J. R., et al. (2011) **Serotonin signaling is associated with lower amyloid-β levels and plaques in transgenic mice and humans** *Proc Natl Acad Sci U S A* **108**:14968–14973

88. Terzioglu N., van Rijn R. M., Bakker R. A., De Esch I. J. P., Leurs R (2004) **Synthesis and structure– activity relationships of indole and benzimidazole piperazines as histamine H4 receptor antagonists** *Bioorganic & Medicinal Chemistry Letters* **14**:5251–5256

89. Pereira T. D., et al. (2022) **SLEAP: A deep learning system for multi-animal pose tracking** *Nat Methods* **19**:486–495

90. Mathis A., et al. (2018) **DeepLabCut: markerless pose estimation of user-defined body parts with deep learning** *Nat Neurosci* **21**:1281–1289

91. Myers-Turnbull D., et al. (2022) **Simultaneous analysis of neuroactive compounds in zebrafish** *bioRxiv* https://doi.org/10.1101/2020.01.01.891432

92. Marques J. C., Lackner S., Félix R., Orger M. B. (2018) **Structure of the Zebrafish Locomotor Repertoire Revealed with Unsupervised Behavioral Clustering** *Current Biology* **28**:181–195

93. Wiltschko A. B., et al. (2020) **Revealing the structure of pharmacobehavioral space through motion sequencing** *Nat Neurosci* **23**:1433–1443

94. Aleström P., et al. (2020) **Zebrafish: Housing and husbandry recommendations** *Lab Anim* **54**:213–224

95. Uribe-Salazar J. M., et al. (2022) **Evaluation of CRISPR gene-editing tools in zebrafish** *BMC Genomics* **23**

96. Labun K., et al. (2019) **CHOPCHOP v3: expanding the CRISPR web toolbox beyond genome editing** *Nucleic Acids Research* **47**:W171–W174

97. Moreno-Mateos M. A., et al. (2015) **CRISPRscan: designing highly efficient sgRNAs for CRISPR-Cas9 targeting in vivo** *Nat Methods* **12**:982–988

98. Shen M. W., et al. (2018) **Predictable and precise template-free CRISPR editing of pathogenic variants** *Nature* **563**:646–651

99. Naert T., et al. (2020) **Maximizing CRISPR/Cas9 phenotype penetrance applying predictive modeling of editing outcomes in Xenopus and zebrafish embryos** *Sci Rep* **10**

100. Höijer I., et al. (2022) **CRISPR-Cas9 induces large structural variants at on-target and off-target sites in vivo that segregate across generations** *Nat Commun* **13**

101. Butler M. G., et al. (2015) **SNPfisher: tools for probing genetic variation in laboratory-reared zebrafish** *Development* **142**:1542–1552

102. Terzioglu M., Saralahti A., Piippo H., Rämet M., Andressoo J.-O. (2020) **Improving CRISPR/Cas9 mutagenesis efficiency by delaying the early development of zebrafish embryos** *Sci Rep* **10**

103. Meeker N. D., Hutchinson S. A., Ho L., Trede N. S. (2007) **Method for isolation of PCR-ready genomic DNA from zebrafish tissues** *Biotechniques* **43**

104. Li H., et al. (2009) **The Sequence Alignment/Map format and SAMtools** *Bioinformatics* **25**:2078–2079

105. Quinlan A. R., Hall I. M (2010) **BEDTools: a flexible suite of utilities for comparing genomic features** *Bioinformatics* **26**:841–842

106. Labun K., et al. (2019) **Accurate analysis of genuine CRISPR editing events with ampliCan** *Genome Res* **29**:843–847

107. Joo W., Vivian M. D., Graham B. J., Soucy E. R., Thyme S. B (2021) **A Customizable Low-Cost System for Massively Parallel Zebrafish Behavioral Phenotyping** *Frontiers in Behavioral Neuroscience* **14**

108. Bachour R.-L., Golovko O., Kellner M., Pohl J (2020) **Behavioral effects of citalopram, tramadol, and binary mixture in zebrafish (Danio rerio) larvae** *Chemosphere* **238**

109. Bates D., Mächler M., Bolker B., Walker S (2015) **Fitting Linear Mixed-Effects Models Using lme4** *Journal of Statistical Software* **67**:1–48

110. Winter B. (2013) **Linear models and linear mixed effects models in R with linguistic applications** *arXiv* https://doi.org/10.48550/arXiv.1308.5499

111. Stuart T., et al. (2019) **Comprehensive Integration of Single-Cell Data** *Cell* **177**:1888–1902

112. Choi H. M. T., et al. (2018) **Third-generation in situ hybridization chain reaction: multiplexed, quantitative, sensitive, versatile, robust** *Development* **145**

113. Lister J. A., Robertson C. P., Lepage T., Johnson S. L., Raible D (1999) **W. nacre encodes a zebrafish microphthalmia-related protein that regulates neural-crest-derived pigment cell fate** *Development* **126**:3757–3767

114. Vladimirov N., et al. (2014) **Light-sheet functional imaging in fictively behaving zebrafish** *Nat Methods* **11**:883–884

115. Marquart G. D., et al. (2015) **A 3D Searchable Database of Transgenic Zebrafish Gal4 and Cre Lines for Functional Neuroanatomy Studies** *Frontiers in Neural Circuits* **9**

116. Marquart G. D., et al. (2017) **High-precision registration between zebrafish brain atlases using symmetric diffeomorphic normalization** *GigaScience* **6**

117. Avants B. B., et al. (2011) **A reproducible evaluation of ANTs similarity metric performance in brain image registration** *NeuroImage* **54**:2033–2044

118. Antinucci P., Folgueira M., Bianco I. H (2019) **Pretectal neurons control hunting behaviour** *eLife* **8**

119. Schindelin J., et al. (2012) **Fiji: an open-source platform for biological-image analysis** *Nat Methods* **9**:676–682

120. Walt S. van der, et al. (2014) **scikit-image: image processing in Python** *PeerJ* **2**

121. Szöcs E., Stirling T., Scott E. R., Scharmüller A., Schäfer R (2020) **B. webchem: An R Package to Retrieve Chemical Information from the Web** *Journal of Statistical Software* **93**:1–17

122. Chatterjee A., et al. (2023) **Improving the generalizability of protein-ligand binding predictions with AI-Bind** *Nat Commun* **14**

123. Durinck S., Spellman P. T., Birney E., Huber W (2009) **Mapping identifiers for the integration of genomic datasets with the R/Bioconductor package biomaRt** *Nat Protoc* **4**:1184–1191

Author information

François Kroll
Department of Cell and Developmental Biology, University College London, London, United Kingdom, Institut de la Vision, Sorbonne Université, Paris, France
ORCID iD: 0000-0001-9908-2648

Joshua Donnelly
Department of Cell and Developmental Biology, University College London, London, United Kingdom
ORCID iD: 0009-0009-6167-0239

Güliz Gürel Özcan
Department of Cell and Developmental Biology, University College London, London, United Kingdom
ORCID iD: 0000-0003-0519-8733

Eirinn Mackay
Department of Cell and Developmental Biology, University College London, London, United Kingdom
ORCID iD: 0000-0003-1436-2259

Jason Rihel
Department of Cell and Developmental Biology, University College London, London, United Kingdom
ORCID iD: 0000-0003-4067-2066

For correspondence: j.rihel@ucl.ac.uk

Editors

Reviewing Editor
Jessica Nelson
University of Colorado Anschutz Medical Campus, Aurora, United States of America

Senior Editor
Didier Stainier
Max Planck Institute for Heart and Lung Research, Bad Nauheim, Germany

Reviewer #1 (Public review):

Summary:

In this study, Kroll et al. conduct an in-depth behavioral analysis of F0 knockouts of 4 genes associated with late-onset Alzheimer's Disease (AD), together with 3 genes associated with early-onset AD. Kroll and colleagues developed a web application (ZOLTAR) to compare sleep-associated traits between genetic mutants with those obtained from a panel of small molecules to promote identification of affected pathways and potential therapeutic interventions. The authors make a set of potentially important findings vis-à-vis the relationship between AD-associated genes and sleep. First, they find that loss-of-function in late-onset AD genes universally result in nighttime sleep loss, consistent with the well-supported hypothesis that sleep disruption contributes to Alzheimer's-related pathologies. psen-1, an early-onset associated AD gene, which the authors find is principally responsible for the generation of AB40 and AB42 in zebrafish, also shows a slight increase in activity at night and slight decreases in nighttime sleep. Conversely, psen-2 mutations increase daytime sleep, while appa/appb mutations have no impact on sleep. Finally, using ZOLTAR, the authors identify serotonin receptor activity as potentially disrupted in sorl1 mutants, while betamethasone is identified as a potential therapeutic to promote reversal of psen2 knockout-associated phenotypes.

This is a highly innovative and thorough study, yet a handful of key questions remain. First, are the nighttime sleep loss phenotypes observed in all knockouts for late-onset AD genes in the larval zebrafish a valid proxy for AD risk? Can 5-HT reuptake inhibitors reverse other AD-related pathologies in zebrafish? Can compounds be identified which have a common behavioral fingerprint across all or multiple AD risk genes? Do these modify sleep phenotypes? Finally, the authors propose but do not test the hypothesis that sorl1 might regulate localization/surface expression of 5-HT2 receptors. This could provide exciting / more convincing mechanistic support for the assertion that serotonin signaling is disrupted upon loss of AD-associated genes. Despite these important considerations, this study provides a valuable platform for high-throughput analysis of sleep phenotypes and correlation with small-molecule induced sleep phenotypes. The platform could also be expanded to facilitate comparison of other behavioral phenotypes, including stimulus-evoked behaviors. Moreover, the new analyses looking for pathways that might be co-regulated by AD risk genes and discussion of cholinergic signaling as a potentially meaningful target downstream of 5/7 knockouts are valuable.

Strengths:
- Provides a useful platform for comparison of sleep phenotypes across genotypes/drug manipulations.
- Presents convincing evidence that nighttime sleep is disrupted in mutants for multiple late-onset AD-related genes.
- Provides potential mechanistic insights for how AD-related genes might impact sleep and identifies a few drugs that modify their identified phenotypes.

Weaknesses:
- Exploration of potential mechanisms for serotonin disruption in sorl1 mutants is limited
- The pipeline developed is only used to examine sleep-related / spontaneous movement phenotypes. Stimulus-evoked behaviors are not examined.

https://doi.org/10.7554/eLife.96839.2.sa2

Reviewer #2 (Public review):

Summary:

This work delineates the larval zebrafish behavioral phenotypes caused by F0 knockout of several important genes that increase risk for Alzheimer's disease. Using behavioral pharmacology, comparing the behavioral fingerprint of previously assayed molecules to the newly generated knockout data, compounds were discovered that impacted larval movement in ways that suggest interaction with or recovery of disrupted mechanisms.

Strengths:

This is a well-written manuscript that uses newly developed analysis methods to present the findings in a clear, high-quality way. The addition of an extensive behavioral analysis pipeline is of value to the field of zebrafish neuroscience and will be particularly helpful for researchers who prefer the R programming language. Even the behavioral profiling of these AD risk genes, regardless of the pharmacology aspect, is an important contribution. The recovery of most behavioral parameters in the psen2 knockout with betamethasone, predicted by comparing fingerprints, is an exciting demonstration of the approach. The hypotheses generated by this work are important stepping stones to future studies uncovering the molecular basis of the proposed gene-drug interactions and discovering novel therapeutics to treat AD or co-occurring conditions such as sleep disturbance. Most concerns are sufficiently addressed in the revised manuscript or response to reviewers.

Weaknesses:

- The overarching concept of the work is that comparing behavioral fingerprints can align genes and molecules with similarly disrupted molecular pathways. While the recovery of the psen2 phenotypes by one molecule with the opposite phenotype is interesting, as are previous studies that show similar behaviorally-based recoveries, the underlying assumption that normalizing the larval movement normalizes the mechanism still lacks substantial support. While I agree with the authors detailed response that rescuing most behavioral parameters is a good indication that the underlying mechanism is normalized, I disagree that high-throughput larval behavior kinematics is a sufficient enough representation of most behavioral parameters to be indicative of molecular mechanism normalization. There are many instances of mutants with completely normal kinetics at baseline, but a behavioral difference that emerges during stimulation or in a new paradigm such as hunting. Without testing far more behavioral paradigms than are possible in the multi-well plate format, as well as possibly multiple life stages, I remain unconvinced that this approach will yield valuable therapeutic insights. I do agree that it can yield insight for future investigation, such

as in the case of cntnap2a/cntnap2b and GABA receptor agonists, but even in that instance is it not clear that such an agonist would rescue abnormalities in a meaningful way. In the case of a disorder such as autism, the early locomotor phenotypes may be disconnected from the molecular mechanisms underlying later social deficits, and it is far more challenging to screen on juvenile behaviors that would be a more appropriate target for a behavior-first approach. The added experiment of testing fluvoxamine, a second SSRI, yielded very different behavioral responses to the SSRI citalopram, supporting my assertion that this approach and the disrupted underlying mechanisms are more complicated than suggested by the authors. I disagree that the connection between sorl1 and serotonin is strengthened by this experiment. The authors suggest that since the knockout larvae react differently than control siblings to both SSRIs, it indicates that serotonin is disrupted. There is no negative control included, where a pathway that is clearly not indicated to be important is pharmacologically manipulated. It is possible that the mutants would also behave differently compared to siblings when other pathways are perturbed. The authors acknowledge in the reviewers that they may not have identified the underlying molecular disruption in this mutant, but they did not substantially alter the Discussion section on this point. I agree with the authors that using a different wild-type strain in a different lab could lead to discrepancies, but these issues could have been experimentally mitigated or more clearly highlighted in the manuscript itself.

https://doi.org/10.7554/eLife.96839.2.sa1

Author response:

The following is the authors' response to the original reviews.

> ***Public Reviews:***
>
> ***Reviewer #1 (Public Review):***
>
> *Summary:*
>
> *In this study, Kroll et al. conduct an in-depth behavioral analysis of F0 knockouts of 4 genes associated with late-onset Alzheimer's Disease (AD), together with 3 genes associated with early- onset AD. Kroll and colleagues developed a web application (ZOLTAR) to compare sleep-associated traits between genetic mutants with those obtained from a panel of small molecules to promote the identification of affected pathways and potential therapeutic interventions. The authors make a set of potentially important findings vis-à-vis the relationship between AD-associated genes and sleep. First, they find that loss-of-function in late-onset AD genes universally results in night-time sleep loss, consistent with the well supported hypothesis that sleep disruption contributes to Alzheimer's-related pathologies. psen-1, an early-onset associated AD gene, which the authors find is principally responsible for the generation of AB40 and AB42 in zebrafish, also shows a slight increase in activity at night and slight decreases in night-time sleep. Conversely, psen-2 mutations increase daytime sleep, while appa/appb mutations have no impact on sleep. Finally, using ZOLTAR, the authors identify serotonin receptor activity as potentially disrupted in sorl1 mutants, while betamethasone is identified as a potential therapeutic to promote reversal of psen2 knockout-associated phenotypes.*
>
> *This is a highly innovative and thorough study, yet a handful of key questions remain. First, are night-time sleep loss phenotypes observed in all knockouts for late-onset AD genes in the larval zebrafish a valid proxy for AD risk?*

We cannot say, but it is an interesting question. We selected the four late-onset Alzheimer's risk genes (*APOE*, *CD2AP*, *CLU*, *SORL1*) based on human genetics data and brain expression in zebrafish larvae, not based on their likelihood to modify sleep behaviour, which we could have tried by searching for overlaps with GWAS of sleep phenotypes, for example. Consequently, we find it remarkable that all four of these genes caused a night-time sleep phenotype when mutated. We also find it reassuring that knockout of *appa/appb* and *psen2* did not cause a night-time sleep phenotype, which largely excludes the possibility that the phenotype is a technical artefact (e.g. caused by the F0 knockout method) or a property of every gene expressed in the larval brain.

Having said that, it could still be a coincidence, rather than a special property of genes associated with late-onset AD. In addition to testing additional late-onset Alzheimer's risk genes, the ideal way to answer this question would be to test in parallel a random set of genes expressed in the brain at this stage of development. From this random set, one could estimate the proportion of genes that cause a night-time sleep phenotype when mutated. One could then use that information to test whether late-onset Alzheimer's risk genes are indeed enriched for genes that cause a night-time sleep phenotype when mutated.

> *For those mutants that cause night-time sleep disturbances, do these phenotypes share a common underlying pathway? e.g. Do 5-HT reuptake inhibitors promote sleep across all 4 late-onset genes in addition to psen1? Can 5-HT reuptake inhibitors reverse other AD-related pathologies in zebrafish? Can compounds be identified that have a common behavioral fingerprint across all or multiple AD risk genes? Do these modify sleep phenotypes?*

To attempt to answer these questions, we used ZOLTAR to generate predictions for all the knockout behavioural fingerprints presented in the study, in the same way as for *sorl1* in Fig. 5 and Fig. 5–supplement 1. Here are the indications, targets, and KEGG pathways which are shared by the largest number of knockouts (Author response image 1):

– One indication is shared by 4/7 knockouts: "opioid dependence" (significant for *appa/appb*, *psen1*, *apoea/apoeb*, *cd2ap*).

– Four targets are shared by 4/7 knockouts: "strychnine-binding glycine receptor" (*psen1*, *apoea/apoeb*, *clu*, *sorl1*); "neuronal acetylcholine receptor beta-2" (*psen1*, *apoea/apoeb*, *cd2ap*, *clu*); thyroid peroxidase (*psen1*, *apoea/apoeb*, *cd2ap*, *clu*); carbonic anhydrase IV (*appa/appb*, *psen1*, *psen2*, *cd2ap*).

– Three KEGG pathways are shared by 5/7 knockouts: "cholinergic synapse" (*psen1*, *apoea/apoeb*, *cd2ap*, *clu*, *sorl1*); tyrosine metabolism (*psen2*, *apoea/apoeb*, *cd2ap*, *clu*, *sorl1*); and "nitrogen metabolism" (*appa/appb*, *psen1*, *psen2*, *apoea/apoeb*, *cd2ap*).

As reminder, we hypothesised that loss of Sorl1 affected serotonin signalling based on the following annotations being significant: indication "depression", target "serotonin transporter", and KEGG pathway "serotonergic synapse". Indication "depression" is only significant for *sorl1* knockouts; target "serotonin transporter" is also significant for *appa/appb* and *psen2* knockouts; and KEGG pathway "serotonergic synapse" is also significant for *psen2* knockouts. ZOLTAR therefore does not predict serotonin signalling to be a major theme common to all mutants with a night-time sleep loss phenotype.

Particularly interesting is cholinergic signalling appearing in the most common targets and KEGG pathways. Acetylcholine signalling is a major theme in research on AD. For example, the first four drugs ever approved by the FDA to treat AD were acetylcholinesterase inhibitors, which increase acetylcholine signalling by preventing its breakdown by acetylcholinesterase. These drugs are generally considered only to treat symptoms and not

modify disease course, but this view has been called into question (Munoz-Torrero, 2008; Relkin, 2007). If, as ZOLTAR suggests, mutations in several Alzheimer's risk genes affect cholinergic signalling early in development, this would point to a potential causal role of cholinergic disruption in AD.

Author response image 1.

Common predictions from ZOLTAR for the seven Alzheimer's risk genes tested. Predictions from ZOLTAR which are shared by multiple knockout behavioural fingerprints presented in the study. Only indications, targets, and KEGG pathways which are significant for at least three of the seven knockouts tested are shown, ranked from the annotations which are significant for the largest number of knockouts.

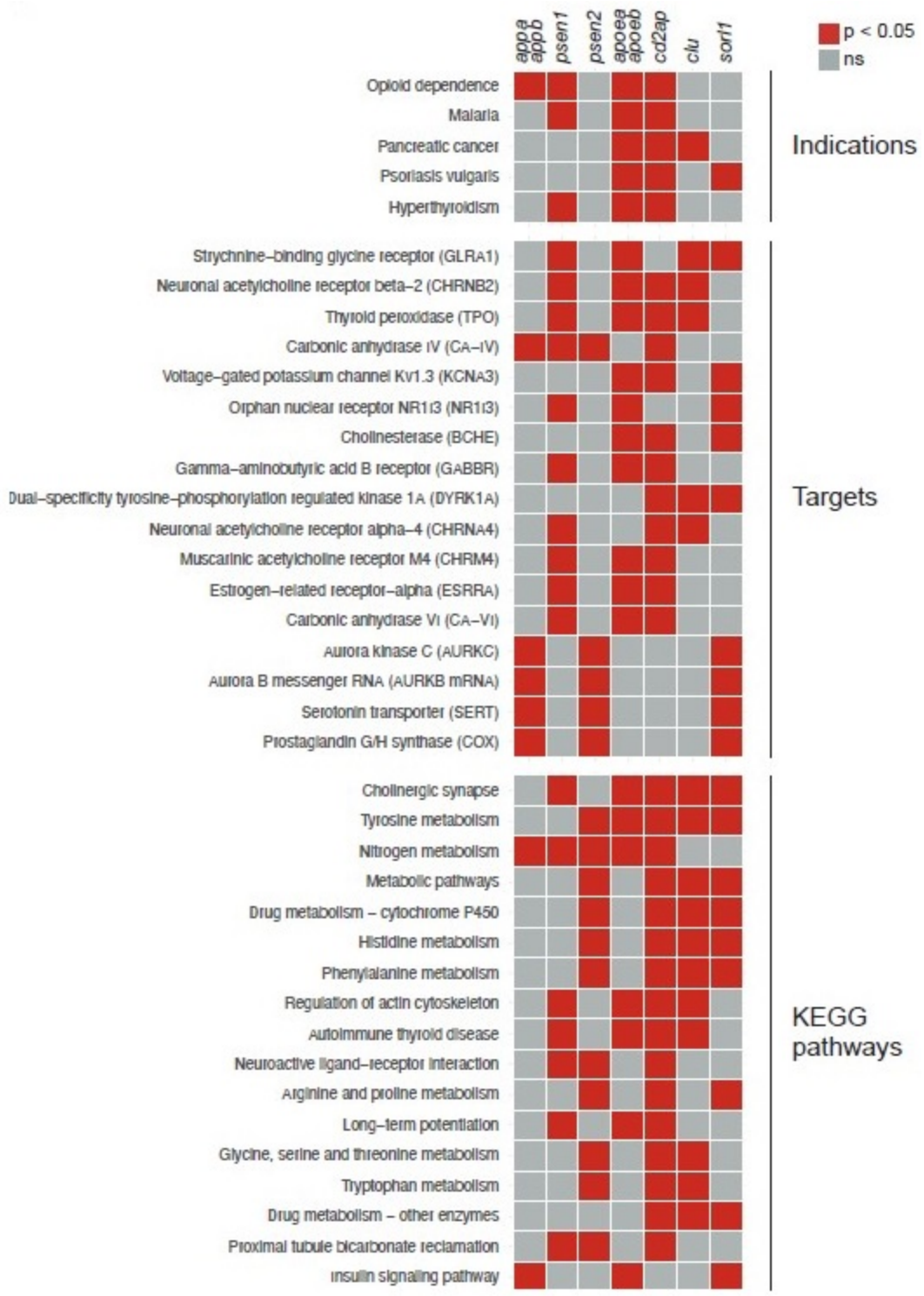

> *Finally, the web- based plasorm presented could be expanded to facilitate comparison of other behavioral phenotypes, including stimulus-evoked behaviors.*

Yes, absolutely. The behavioural dataset we used (Rihel et al., 2010) did not measure other stimuli than day/night light transitions, but the “SauronX” plasorm and dataset (MyersTurnbull et al., 2022) seems particularly well suited for this. To provide some context, we and collaborators have occasionally used the dataset by Rihel et al. (2010) to generate

hypotheses or find candidate drugs that reverse a behavioural phenotype measured in the sleep/wake assay (Ashlin et al., 2018; Hoffman et al., 2016). The present work was the occasion to enable a wider and more intuitive use of this dataset through the ZOLTAR app, which has already proven successful. Future versions of ZOLTAR may seek to incorporate larger drug datasets using more types of measurements.

> *Finally, the authors propose but do not test the hypothesis that sorl1 might regulate localization/surface expression of 5-HT2 receptors. This could provide exciting / more convincing mechanistic support for the assertion that serotonin signaling is disrupted upon loss of AD-associated genes.*

While working on the Author Response, we made some changes to the analysis ran by ZOLTAR to calculate enrichments (see Methods and github.com/francoiskroll/ZOLTAR, notes on v2). With the new version, 5-HT receptor type 2 is not a significantly enriched target for the *sorl1* knockout fingerprint but type 4 is. 5-HT receptor type 4 was also shown to interact with sorting nexin 27, a subunit of retromer, so is a promising candidate (Joubert et al., 2004). Antibodies against human 5-HT receptor type 2 and 4a exist; whether they would work in zebrafish remains to be tested. In our experience, the availability of antibodies suitable for immunohistochemistry in the zebrafish is a serious experimental roadblock.

Note, all the results presented in the “Version of Records” are from ZOLTAR v2.

> *Despite these important considerations, this study provides a valuable plasorm for highthroughput analysis of sleep phenotypes and correlation with small-molecule-induced sleep phenotypes.*
>
> *Strengths:*
>
> *- Provides a useful plasorm for comparison of sleep phenotypes across genotypes/drug manipulations.*
>
> *- Presents convincing evidence that night-time sleep is disrupted in mutants for multiple late onset AD-related genes.*
>
> *- Provides potential mechanistic insights for how AD-related genes might impact sleep and identifies a few drugs that modify their identified phenotypes*
>
> *Weaknesses:*
>
> *- Exploration of potential mechanisms for serotonin disruption in sorl1 mutants is limited. - The pipeline developed can only be used to examine sleep-related / spontaneous movement phenotypes and stimulus-evoked behaviors are not examined.*
>
> *- Comparisons between mutants/exploration of commonly affected pathways are limited.*

Thank you for these excellent suggestions, please see our answers above.

> ***Reviewer #2 (Public Review):***
>
> *Summary:*
>
> *This work delineates the larval zebrafish behavioral phenotypes caused by the F0 knockout of several important genes that increase the risk for Alzheimer's disease. Using behavioral pharmacology, comparing the behavioral fingerprint of previously assayed molecules to the newly generated knockout data, compounds were discovered that impacted larval movement in ways that suggest interaction with or recovery of disrupted mechanisms.*

> *Strengths:*
>
> *This is a well-written manuscript that uses newly developed analysis methods to present the findings in a clear, high-quality way. The addition of an extensive behavioral analysis pipeline is of value to the field of zebrafish neuroscience and will be particularly helpful for researchers who prefer the R programming language. Even the behavioral profiling of these AD risk genes, regardless of the pharmacology aspect, is an important contribution. The recovery of most behavioral parameters in the psen2 knockout with betamethasone, predicted by comparing fingerprints, is an exciting demonstration of the approach. The hypotheses generated by this work are important stepping stones to future studies uncovering the molecular basis of the proposed gene-drug interactions and discovering novel therapeutics to treat AD or co-occurring conditions such as sleep disturbance.*
>
> *Weaknesses:*
>
> *- The overarching concept of the work is that comparing behavioral fingerprints can align genes and molecules with similarly disrupted molecular pathways. While the recovery of the psen2 phenotypes by one molecule with the opposite phenotype is interesting, as are previous studies that show similar behaviorally-based recoveries, the underlying assumption that normalizing the larval movement normalizes the mechanism still lacks substantial support. There are many ways that a reduction in movement bouts could be returned to baseline that are unrelated to the root cause of the genetically driven phenotype. An ideal experiment would be to thoroughly characterize a mutant, such as by identifying a missing population of neurons, and use this approach to find a small molecule that rescues both behavior and the cellular phenotype. If the connection to serotonin in the sorl1 was more complete, for example, the overarching idea would be more compelling.*

Thank you for this cogent criticism.

On the first point, we were careful not to claim that betamethasone normalises the molecular/cellular mechanism that causes the *psen2* behavioural phenotype. Having said that, yes, to a certain extent that would be the hope of the approach. As you say, every compound which normalises the behavioural fingerprint will not normalise the underlying mechanism, but the opposite seems true: every compound that normalises the underlying mechanism should also normalise the behavioural fingerprint. We think this logic makes the "behaviour-first" approach innovative and interesting. The logic is to discover compounds that normalise the behavioural phenotype first, only subsequently test whether they also normalise the molecular mechanism, akin to testing first whether a drug resolves the symptoms before testing whether it actually modifies disease course. While in practice testing thousands of drugs in sufficient sample sizes and replicates on a mutant line is challenging, the dataset queried through ZOLTAR provides a potential shortcut by shortlisting *in silico* compounds that have the opposite effect on behaviour.

You mention a "reduction in movement bouts" but note here that the number of behavioural parameters tested is key to our argument. To take the two extremes, say the only behavioural parameter we measured in *psen2* knockout larvae was time active during the day, then, yes, any stimulant used at the right concentration could probably normalise the phenotype. In this situation, claiming that the stimulant is likely to also normalise the underlying mechanism, or even that it is a genuine "phenotypic rescue", would not be convincing. Conversely, say we were measuring thousands of behavioural parameters under various stimuli, such as swimming speed, position in the well, bout usage, tail movements, and eye angles, it seems almost impossible for a compound to rescue most parameters without also normalising the underlying mechanism. The present approach is somewhere inbetween:

ZOLTAR uses six behavioural parameters for prediction (e.g. Fig 6a), but all 17 parameters calculated by FramebyFrame can be used to assess rescue during a subsequent experiment (Fig. 6c). For both, splitting each parameter in day and night increases the resolution of the approach, which partly answers your criticism. For example, betamethasone rescued the day-time hypoactivity without causing night-time hyperactivity, so we are not making the "straw man argument" explained above of using any broad stimulant to rescue the hypoactivity phenotype.

Furthermore, for diseases where the behavioural defect is the primary concern, such as auFsm or bipolar disorder, perhaps this behaviour-first approach is all that is needed, and whether or not the compound precisely rescues the underlying mechanism is somewhat secondary. The use of lithium to prevent manic episodes in bipolar disorder is a good example. It was initially tested because mania was thought to be caused by excess uric acid and lithium can dissolve uric acid (Mitchell and Hadzi-Pavlovic, 2000). The theory is now discredited, but lithium conFnues to be used without a precise understanding of its mode of action. In this example, behavioural rescue alone, assuming the secondary effects are tolerable, is sufficient to be beneficial to patients, and whether it modulates the correct causal pathway is secondary.

On the second point, we agree that testing first ZOLTAR on a mutant for which we have a fairly good understanding of the mechanism causing the behavioural phenotype could have been a productive approach. Note, however, that examples already exist in the literature (Ashlin et al., 2018; Hoffman et al., 2016). The example from Hoffman et al. (2016) is especially convincing. Drugs generating behavioural fingerprints that positively correlate with the *cntnap2a/cntnap2b* double knockout fingerprint were enriched with NMDA and GABA receptor antagonists. In experiments analogous to our citalopram and fluvoxamine treatments (Fig. 5c,d and Fig. 5–supplement 1c,d), *cntnap2a/cntnap2b* knockout larvae were overly sensitive to the NMDA receptor antagonist MK-801 and the GABAA receptor antagonist pentylenetetrazol (PTZ). Among other drugs tested, zolpidem, a GABAA receptor agonist, caused opposite effects on wild-type and *cntnap2a/cntnap2b* knockout larvae. Knockout larvae were found to have fewer GABAergic neurons in the forebrain. While these studies did not use precisely the same analysis that ZOLTAR runs, they used the same rationale and behavioural dataset to make these predictions (Rihel et al., 2010), which shows that approaches like ZOLTAR can point to causal processes.

On your last point, we hope our experiment testing fluvoxamine, another selective serotonin reuptake inhibitor (SSRI), makes the connection between Sorl1 and serotonin signalling more convincing.

> *- The behavioral difference between the sorl1 KO and scrambled at the higher dose of the citalopram is based on a small number of animals. The KO Euclidean distance measure is also more spread out than for the other datasets, and it looks like only five or so fish are driving the group difference. It also appears as though the numbers were also from two injection series. While there is nothing obviously wrong with the data, I would feel more comfortable if such a strong statement of a result from a relatively subtle phenotype were backed up by a higher N or a stable line. It is not impossible that the observed difference is an experimental fluke. If something obvious had emerged through the HCR, that would have also supported the conclusions. As it stands, if no more experiments are done to bolster the claim, the confidence in the strength of the link to serotonin should be reduced (possibly putting the entire section in the supplement and modifying the discussion). The discussion section about serotonin and AD is interesting, but I think that it is excessive without additional evidence.*

We mostly agree with this criticism. One could interpret the larger spread of the data for *sorl1* KO larvae treated with 10 µM citalopram as evidence that the knockout larvae do

indeed react differently to the drug at this dose, regardless of being driven by a subset of the animals. The result indeed does not survive removing the top 5 (p = 0.87) or top 3 (p = 0.18) *sorl1* KO + 10 μM larvae, but this amounts to excluding 20 (3/14) or 35 (5/14) % of the datapoints as potential outliers, which is unreasonable. In fact, excluding the top 5 *sorl1* KO + 10 μM is equivalent to calling any datapoint with z-score > 0.2 an outlier (z-scores of the top 5 datapoints are 0.2–1.8). Applying consistently the same criterion to the scrambled + 10 μM group would remove the top 6 datapoints (z-scores = 0.5–3.9). Comparing the resulting two distributions again gives the *sorl1* KO + 10 μM distribution as significantly higher (p = 0.0015). We would also mention that Euclidean distance, as a summary metric for distance between behavioural fingerprints, has limitations. For example, the measure will be more sensitive to changes in some parameters but not others, depending on how much room there is for a given parameter to change. We included this metric to lend support to the observation one can draw from the fingerprint plot (Fig. 5c) that *sorl1* mutants respond in an exaggerated way to citalopram across many parameters, while being agnosFc to which parameter might majer most.

Given that the HCR did not reveal anything striking, we agree with you that too much of our argument relied on this result being robust. As you and Reviewer #3 suggested, we repeated this experiment with a different SSRI, fluvoxamine (Fig. 5–supplement 1). We cannot readily explain why the result was opposite to what we found with citalopram, but in both cases *sorl1* knockout larvae reacted differently than their control siblings, which adds an argument to our claim that ZOLTAR correctly predicted serotonin signalling as a disrupted pathway from the behavioural fingerprint. Accordingly, we mostly kept the Discussion on Sorl1 the same, although we concede that we may not have identified the molecular mechanism.

> *- The authors suggest two hypotheses for the behavioral difference between the sorl1 KO and scrambled at the higher dose of the citalopram. While the first is tested, and found to not be supported, the second is not tested at all ("Ruling out the first hypothesis, sorl1 knockouts may react excessively to a given spike in serotonin." and "Second, sorl1 knockouts may be overly sensitive to serotonin itself because post-synaptic neurons have higher levels of serotonin receptors."). Assuming that the finding is robust, there are probably other reasons why the mutants could have a different sensiFvity to this molecule. However, if this particular one is going to be mentioned, it is surprising that it was not tested alongside the first hypothesis. This work could proceed without a complete explanation, but additional discussion of the possibiliFes would be helpful or why the second hypothesis was not tested.*

There are no strong scientific reasons why this hypothesis was not tested. The lead author (F Kroll) moved to a different lab and country so the project was finalised at that time. We do not plan on testing this hypothesis at this stage. However, we adapted the wording to make it clear this is one possible alternative hypothesis which could be tested in the future. The small differences found by HCR are actually more in line with the new results from the fluvoxamine experiment, so it may also be that both hypotheses (pre-synaptic neurons releasing less serotonin when reuptake is blocked; or post-synaptic neurons being less sensitive) contribute. The fluvoxamine experiment was performed in a different lab (ICM, Paris; all other experiments were done in UCL, London) in a different wild-type strain (TL in ICM, AB x Tup LF in UCL), which complicates how one interprets this discrepancy.

> *- The authors claim that "all four genes produced a fairly consistent phenotype at night". While it is interesting that this result arose in the different lines, the second clutch for some genes did not replicate as well as others. I think the findings are compelling, regardless, but the sometimes missing replicability should be discussed. I wonder if the F0 strategy adds noise to the results and if clean null lines would yield stronger*

> *phenotypes. Please discuss this possibility, or others, in regard to the variability in some phenotypes.*

For the first part of this point, please see below our answer to Reviewer #3, point (2) c.

Regarding the F0 strategy potentially adding variability, it is an interesting question which we tested in a larger dataset of behavioural recordings from F0 and stable knockouts for the same genes (unpublished). In summary, the F0 knockout method does not increase clutchto-clutch or larva-to-larva variability in the assay. F0 knockout experiments found many more significant parameters and larger effect sizes than stable knockout experiments, but this difference could largely be explained by the larger sample sizes of F0 knockout experiments. In fact, larger sample sizes within individual clutches appears to be a major advantage of the F0 knockout approach over in-cross of heterozygous knockout animals as it increases sensiFvity of the assay without causing substantial variability. We plan to report in more detail on this analysis in a separate paper as we think it would dilute the focus of the present work.

> *- In this work, the knockout of appa/appb is included. While APP is a well-known risk gene, there is no clear justification for making a knockout model. It is well known that the upregulation of app is the driver of Alzheimer's, not downregulation. The authors even indicate an expectation that it could be similar to the other knockouts ("Moreover, the behavioural phenotypes of appa/appb and psen1 knockout larvae had lijle overlap while they presumably both resulted in the loss of Aβ." and "Comparing with early-onset genes, psen1 knockouts had similar night-time phenotypes, but loss of psen2 or appa/appb had no effect on night-time sleep."). There is no reason to expect similarity between appa/appb and psen1/2. I understand that the app knockouts could unveil interesting early neurodevelopmental roles, but the manuscript needs to be clarified that any findings could be the opposite of expectation in AD.*

On “there is no reason to expect similarity […]”, we disagree. Knockout of *appa/appb* and knockout of *psen1* will both result in loss of Aβ (*appa/appb* encode Aβ and *psen1* cleaves Appa/Appb to release Aβ, cf. Fig. 3e). Consequently, a phenotype caused by the loss of Aβ, or possibly other Appa/Appb cleavage products, should logically be found in both *appa/appb* and *psen1* knockouts.

On “it is well known that the upregulation of *APP* is the driver of Alzheimer’s, not downregulation”; we of course agree. Among others, the examples of Down syndrome, APP duplication (Sleegers et al., 2006), or mouse models overexpressing human *APP* show definitely that overexpression of *APP* is sufficient to cause AD. Having said that, we would not be so quick in dismissing *APP* knockout as potentially relevant to understanding of AD.

Loss of soluble Aβ due to aggregation could contribute to pathology (Espay et al., 2023). Without getting too much into this intricate debate, links between levels of Aβ and risk of disease are often counter-intuitive too. For example, out of 138 PSEN1 mutations screened *in vitro*, 104 reduced total Aβ production and 11 even seemingly abolished the production of both Aβ40 and Aβ42 (Sun et al., 2017). In short, loss of soluble Aβ occurs in both AD and in our *appa/appb* knockout larvae.

We added a sentence in Results (section *psen2 knockouts […]*) to briefly justify our *appa/appb* knockout approach. To be clear, we do not want to imply, for example, that the absence of a night-time sleep phenotype for *appa/appb* is contradictory to the body of literature showing links between Aβ and sleep, including in zebrafish (Özcan et al., 2020). As you say, our experiment tested loss of App, including Aβ, while the literature typically reports on overexpression of APP, as in *APP/PSEN1*-overexpressing mice (Jagirdar et al., 2021).

> ***Reviewer #3 (Public Review):***
>
> *In this manuscript by Kroll and colleagues, the authors describe combining behavioral pharmacology with sleep profiling to predict disease and potential treatment pathways at play in AD. AD is used here as a case study, but the approaches detailed can be used for other genetic screens related to normal or pathological states for which sleep/arousal is relevant. The data are for the most part convincing, although generally the phenotypes are relatively small and there are no major new mechanistic insights. Nonetheless, the approaches are certainly of broad interest and the data are comprehensive and detailed. A notable weakness is the introduction, which overly generalizes numerous concepts and fails to provide the necessary background to set the stage for the data.*
>
> *Major points*
>
> *(1) The authors should spend more time explaining what they see as the meaning of the large number of behavioral parameters assayed and specifically what they tell readers about the biology of the animal. Many are hard to understand--e.g. a "slope" parameter.*

We agree that some parameters do not tell something intuitive about the biology of the animal. It would be easy to speculate. For example, the “activity slope” parameter may indicate how quickly the animal becomes Fred over the course of the day. On the other hand, fractal dimension describes the “roughness/smoothness” of the larva’s activity trace (Fig. 2–supplement 1a); but it is not obvious how to translate this into information about the physiology of the animal. We do not see this as an issue though. While some parameters do provide intuitive information about the animal’s behaviour (e.g. sleep duration or sunset startle as a measure of startle response), the benefit of having a large number of behavioural parameters is to compare behavioural fingerprints and assess rescue of the behavioural phenotype by small molecules (Fig. 6c). For this purpose, the more parameters the better. The “MoSeq” approach from Wiltschko et al., 2020 is a good example from literature that inspired our own Fig. 6c. While some of the “behavioural syllables” may be intuitive (e.g. running or grooming), it is probably pointless to try to explain the ‘meaning’ of the “small left turn in place with head motion” syllable (Wiltschko et al., 2020). Nonetheless, this syllable was useful to assess whether a drug specifically treats the behavioural phenotype under study without causing too many side effects. Unfortunately, ZOLTAR has to reduce the FramebyFrame fingerprint (17 parameters) to just six parameters to compare it to the behavioural dataset from Rihel et al., 2010, but here, more parameters would almost certainly translate into better predictions too, regardless of their intuitiveness.

It is true however that we did not give much information on how some of the less intuitive parameters, such as activity slope or fractal dimension, are calculated or what they describe about the dataset (e.g. roughness/smoothness for fractal dimension). We added a few sentences in the legend of Fig. 2–supplement 1.

> *(2) Because in the end the authors did not screen that many lines, it would increase confidence in the phenotypes to provide more validation of KO specificity. Some suggestions include:*
>
> *a. The authors cite a psen1 and psen2 germline mutant lines. Can these be tested in the FramebyFrame R analysis? Do they phenocopy F0 KO larvae?*

We unfortunately do not have those lines. We invesFgated the availability of importing a *psen2* knockout line from abroad, but the process of shipping live animals is becoming more and more cost and time prohibitive. However, we observed the same pigmentation phenotype for *psen2* knockouts as reported by Jiang et al., 2018, which is at least a partial confirmation of phenocopying a loss of function stable mutant.

> *b. psen2KO is one of the larger centerpieces of the paper. The authors should present more compelling evidence that animals are truly functionally null. Without this, how do we interpret their phenotypes?*

We disagree that there should be significant doubt about these mutants being truly functionally null, given the high mutation rate and presence of the expected pigmentation phenotype (Jiang et al., 2018, Fig. 3f and Fig. 3–supplement 3a). The *psen2* F0 knockouts were virtually 100% mutated at three exons across the gene (mutation rates were locus 1: 100 ± 0%; locus 2: 99.99 ± 0.06%; locus 3: 99.85 ± 0.24%). Additionally, two of the three mutated exons had particularly high rates of frameshift mutations (locus 1: 97 ± 5%; locus 2: 88 ± 17% frameshift mutation rate). It is virtually impossible that a functional protein is translated given this burden of frameshift mutations. Phenotypically, in addition to the pigmentation defect, double *psen1/psen2* F0 knockout larvae had curved tails, the same phenotype as caused by a high dose of the γ-secretase inhibitor DAPT (Yang et al., 2008). These double F0 knockouts were lethal, while knockout of *psen1* or *psen2* alone did not cause obvious morphological defects. Evidently, most larvae must have been *psen2* null mutants in this experiment, otherwise functional Psen2 would have prevented early lethality.

Translation of zebrafish *psen2* can start at downstream start codons if the first exon has a frameshift mutation, generating a seemingly functional Psen2 missing the N-terminus (Jiang et al., 2020). Zebrafish homozygous for this early frameshift mutation had normal pigmentation, showing it is a reliable marker of Psen2 function even when it is mutated. This mechanism is not a concern here as the alternative start codons are still upstream of two of the three mutated exons (the alternative start codons discovered by Jiang et al., 2020 are in exon 2 and 3, but we targeted exon 3, exon 4, and exon 6).

We understand that the zebrafish community may be cauFous about F0 phenotyping compared to stably generated mutants. As mentioned to Reviewer #2, we are planning to assemble a paper that expressly compares behavioural phenotypes measured in F0 vs. stable mutants to allay some of these concerns. Our current manuscript, which combines CRISPR-Cas9 rapid F0 screening with *in silico* pharmacological predictions, inevitability represents a first step in characterizing the functions of these genes.

> *c. Related to the above, for cd2AP and sorl1 KO, some of the effect sizes seem to be driven by one clutch and not the other. In other words, great clutch-to-clutch variability. Should the authors increase the number of clutches assayed?*

Correct, there is substantial clutch-to-clutch variability in this behavioural assay. This is not specific to our experiments. Even within the same strain, wild-type larvae from different clutches (i.e. non-siblings) behave differently (Joo et al., 2021). This is why it is essenFal to compare behavioural phenotypes within individual clutches (i.e. from a single pair of parents, one male and one female), as we explain in Methods (section Behavioural videotracking) and in the documentation of the FramebyFrame package. We o en see two different experimental designs in literature: comparing non-sibling wild-type and mutant larvae, or pooling different clutches which include all genotypes (e.g. pooling multiple clutches from heterozygous in-crosses or pooling wild-type clutches before injecting them). The first experimental design causes false positive findings (Joo et al., 2021), as the clutchto-clutch variability we and others observe gets interpreted as a behavioural phenotype. The second experimental design should not cause false positives but likely decreases the sensiFvity of the assay by increasing the spread within genotypes. In both cases, the clutch-to-clutch variability is hidden, either by interpreting it as a phenotype (first case) or by adding it to animal-to-animal variability (second case). Our experimental design is technically more challenging as it requires obtaining large clutches from unique pairs of parents. However, this approach is better as it clearly separates the different sources of variability (clutch-to-

clutch or animal-to-animal). As for every experiment, yes, a larger number of replicates would be better, but we do not plan to assay additional clutches at this time. Our work heavily focuses on the *sorl1* and *psen2* knockout behavioural phenotypes. The key aspects of these phenotypes were effectively tested in four experiments (five to six clutches) as *sorl1* knockout larvae were also tracked in the citalopram and fluvoxamine experiments (Fig. 5 and Fig. 5–supplement 1), and *psen2* knockout larvae were also tracked in the small molecule rescue experiment (Fig. 6 and Fig. 6–supplement 1).

The *psen2* behavioural phenotype replicated well across the six clutches tested (pairwise cosine similariFes: 0.62 ± 0.15; Author response image 2a). 5/6 clutches were less active and initiating more sleep bouts during the day, as we claimed in Fig. 3.

In the citalopram experiment, the H_2O-treated *sorl1* knockout fingerprint replicated fairly well the baseline recordings in Fig. 4, despite the smaller sample size (cos = 0.30 and 0.78; Author response image 2b, see "KO Fig. 5"). 5/6 of the significant parameters presented in Fig. 4–supplement 4 moved in the same direction, and knockout larvae were also hypoactive during the day but hyperactive at night. Note that two clutches were tracked on the same 96-well plate in this experiment. We calculated each larva's z-score using the average of its control siblings, then we averaged all the z-scores to generate the fingerprint. The H_2O treated *sorl1* knockout clutch from the fluvoxamine experiment did not replicate well the baseline recordings (cos = 0.08 and 0.11; Author response image 2b, see "KO Fig. 5–suppl. 1"). Knockout larvae were hypoactive during the day as expected, but behaviour at night was not as robustly affected. As mentioned above, knockouts were made in a different genetic background (TL, instead of AB x Tup LF used for all other experiments), which could explain the discrepancy.

We also took the opportunity to check whether our SSRI treatments replicated well the data from Rihel et al., 2010. For both citalopram (n = 3 fingerprints in the database) and fluvoxamine (n = 4 fingerprints in the database), replication was excellent (cos ≥ 0.67 for all comparisons of a fingerprint from this study vs. a fingerprint from Rihel et al. 2010; Author response image 2c,d). Note that the scrambled + 10 µM citalopram and + 10 µM fluvoxamine fingerprints correlate extremely well (cos = 0.92; can be seen in Author response image 2c,d), which was predicted by the small molecule screen dataset.

Author response image 2.

Replication of *psen2* and *sorl1* F0 knockout fingerprints and SSRI treatments from Rihel et al., 2010. a, (left) Every *psen2* F0 knockout behavioural fingerprint generated in this study. Each dot represents the mean deviation from the same-clutch scrambled-injected mean for that parameter (z-score, mean ± SEM). From the experiments in Fig. 6, presented is the *psen2* F0 knockout + H_2O fingerprints. The fingerprints in grey ("not shown") are from a preliminary drug treatment experiment we did not include in the final study. These fingerprints are from *psen2* F0 knockout larvae treated with 0.2% DMSO, normalised to scrambled-injected siblings also treated with 0.2% DMSO. (right) Pairwise cosine similarities (−1.0–1.0) for the fingerprints presented. b, Every *sorl1* F0 knockout behavioural fingerprint, as in a). c, The scrambled-injected + citalopram (10 µM) fingerprints (grey) in comparison to the citalopram (10–15 µM) fingerprints from the Rihel et al., 2010 database (green). d, The scrambled-injected + fluvoxamine (10 µM) fingerprint (grey) in comparison to the fluvoxamine fingerprints from the Rihel et al., 2010 database (pink). In c) and d), the scrambled-injected fingerprints are from the experiments in Fig. 5 and Fig. 5–suppl. 1, but were converted here into the behavioural parameters used by Rihel et al., 2010 for comparison. Parameters: 1, average activity (sec active/min); 2, average waking activity (sec active/min, excluding inactive minutes); 3, total sleep (hr); 4, number of sleep bouts; 5, sleep bout length (min); 6, sleep latency (min until first sleep bout).

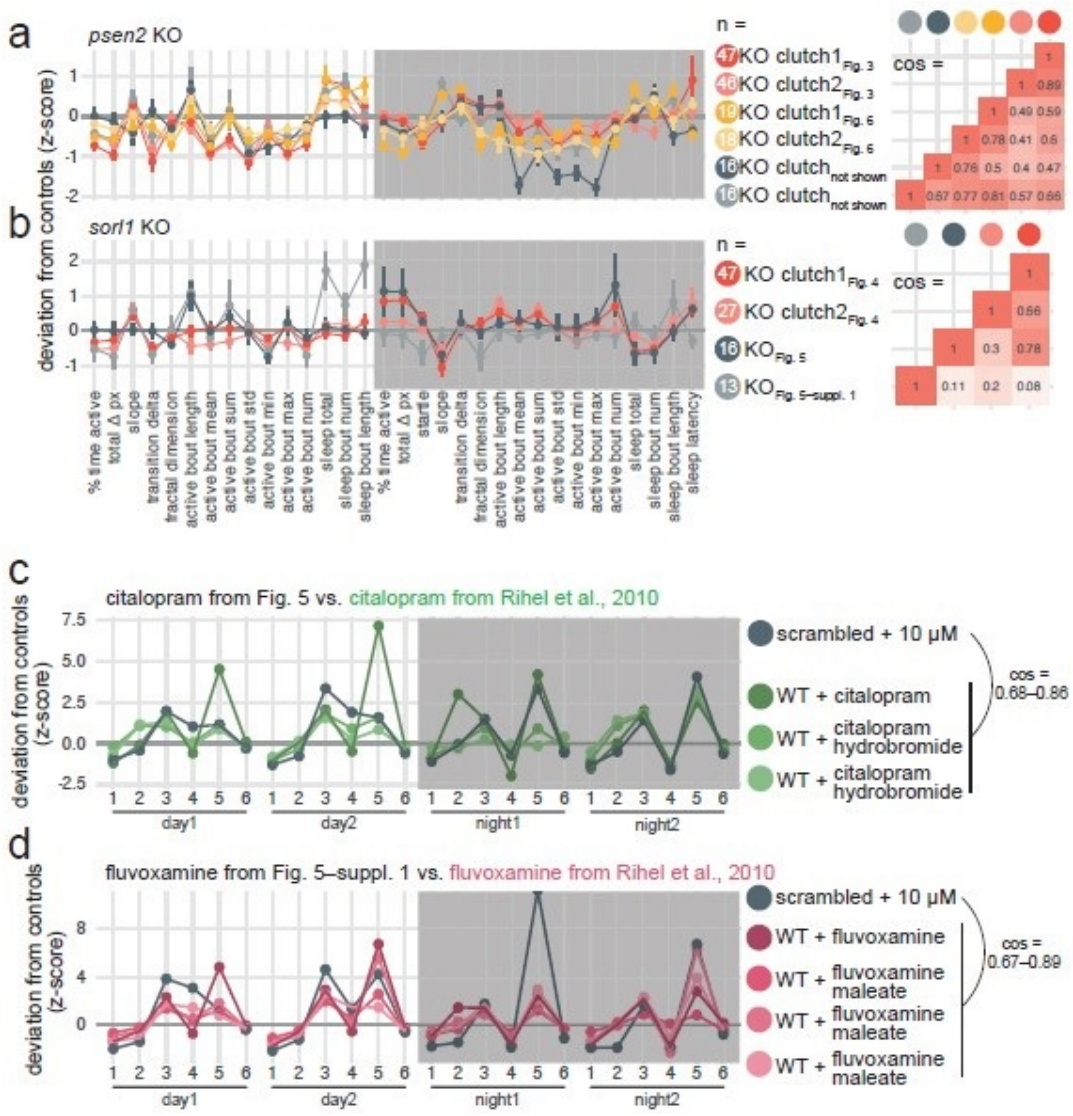

> *(3) The authors make the point that most of the AD risk genes are expressed in fish during development. Is there public data to comment on whether the genes of interest are expressed in mature/old fish as well? Just because the genes are expressed early does not at all mean that early- life dysfunction is related to future AD (though this could be the case, of course). Genes with exclusive developmental expression would be strong candidates for such an early-life role, however. I presume the case is made because sleep studies are mainly done in juvenile fish, but I think it is really a prejy minor point and such a strong claim does not even need to be made.*

This is a fair criticism but we do not make this claim ("early-life dysfunction is related to future AD") from expression alone. The reviewer is probably referring to the following quote:

"[…] most of these were expressed in the brain of 5–6-dpf zebrafish larvae, suggesRng they play a role in early brain development or function," which does not mention future risk of AD. We do *suggest* that these genes have a function in development. After all, every gene that plays a role in brain development must be expressed during development, so this wording seemed reasonable. Nevertheless, we adapted the wording to address this point and Reviewer #2's complaint below. As noted, the primary goal was to check that the genes we selected were indeed expressed in zebrafish larvae before performing knockout experiments. Our

discussion does raise the hypothesis that mutations in Alzheimer's risk genes impact brain development and sleep early in life, but this argument primarily relies on our observation that knockout of late-onset Alzheimer's risk genes causes sleep phenotypes in 7-day old zebrafish larvae and from previous work showing brain structural differences in children at high genetic risk of AD (Dean et al., 2014; Quiroz et al., 2015), not solely on gene expression early in life.

Please also see our answer to a similar point raised by Reviewer #2 below (cf. Author response image 7).

> *(4) A common quandary with defining sleep behaviorally is how to rectify sleep and activity changes that influence one another. With psen2 KOs, the authors describe reduced activity and increased sleep during the day. But how do we know if the reduced activity drives increased behavioral quiescence that is incorrectly defined as sleep? In instances where sleep is increased but activity during periods during wake are normal or elevated, this is not an issue. But here, the animals might very well be unhealthy, and less active, so naturally they stop moving more for prolonged periods, but the main conclusion is not sleep per se. This is an area where more experiments should be added if the authors do not wish to change/temper the conclusions they draw. Are psen2 KOs responsive to startling stimuli like controls when awake? Do they respond normally when quiescent? Great care must be taken in all models using inactivity as a proxy for sleep, and it can harm the field when there is no acknowledgment that overall health/activity changes could be a confound. Particularly worrisome is the betamethasone data in Figure 6, where activity and sleep are once again coordinately modified by the drug.*

This is a fair criticism. We agree it is a concern, especially in the case of *psen2* as we claim that *day-time* sleep is increased while zebrafish are diurnal. We do not rely heavily on the day-time inactivity being sleep (the ZOLTAR predictions or the small molecule rescue do not change whether the parameter is called sleep or inactivity), but our choice of labelling can fairly be challenged.

To address "are *psen2* KO responsive to startling stimuli like controls when awake/when quiescent", we looked at the larvae's behaviour immediately a er lights abruptly switched on in the mornings. Almost every larva, regardless of genotype, responded strongly to every lights-*off* transition during the experiment. Instead, we chose the lights-*on* transition for this analysis because it is a weaker startling stimulus for the larvae than the lights-off transition (Fig. 3–supplement 3), potentially exposing differences between genotypes or behavioural states (quiescent or awake). We defined a larva as having reacted to the lights switching on if it made a swimming bout during the second (25 frames) a er the lights-on transition. Across two clutches and two lights-on transitions, an average of 65% (range 52–73%) of all larvae reacted to the stimulus. *psen2* knockout larvae were similarly likely, if not *more* likely, to respond (in average 69% responded, range 60–76%) than controls (60% average, range 44–75%). When the lights switched on, about half of the larvae (39–51%) would have been classified as asleep according to the one-minute inactivity definition (i.e. the larva did not move in the minute preceding the lights transition). This allowed us to also compare behavioural states, as suggested by the reviewer. For three of the four light transitions, larvae which were awake when lights switched on were more likely to react than asleep larvae, but this difference was not striking (overall, awake larvae were only 1.1× more likely to react; Author response image 3). Awake *psen2* knockout larvae were 1.1× (range 1.04–1.11×) more likely to react than awake control larvae, so, yes, *psen2* knockout larvae respond normally when awake. Asleep *psen2* knockout larvae were 1.4× (range 0.63–2.19×) more likely to react than asleep control larvae, so *psen2* knockouts are also more or equally likely to react than control larvae when asleep. In summary, the overall health of *psen2* knockouts did not seem to be a significant confound in the experiment. As the reviewer suggested, if *psen2* knockout

larvae were seriously unhealthy, they would not be as responsive as control larvae to a startling stimulus.

Author response image 3.

psen2 F0 knockouts react normally to lights switching on, indicating they are largely healthy. At each lights-on transition (9 AM), each larva was categorised as awake if it had moved in the preceding one minute or asleep if it had been inactive for at least one minute. Darker tiles represent larvae which performed a swimming bout during the second following lights-on; lighter tiles represent larvae which did not move during that second. The total count of each waffle plot was normalised to 25 so plots can be compared to each other. The real count is indicated in the corner of each plot. Data is from the baseline *psen2* knockout trackings presented in Fig. 3 and Fig. 3–suppl. 2.

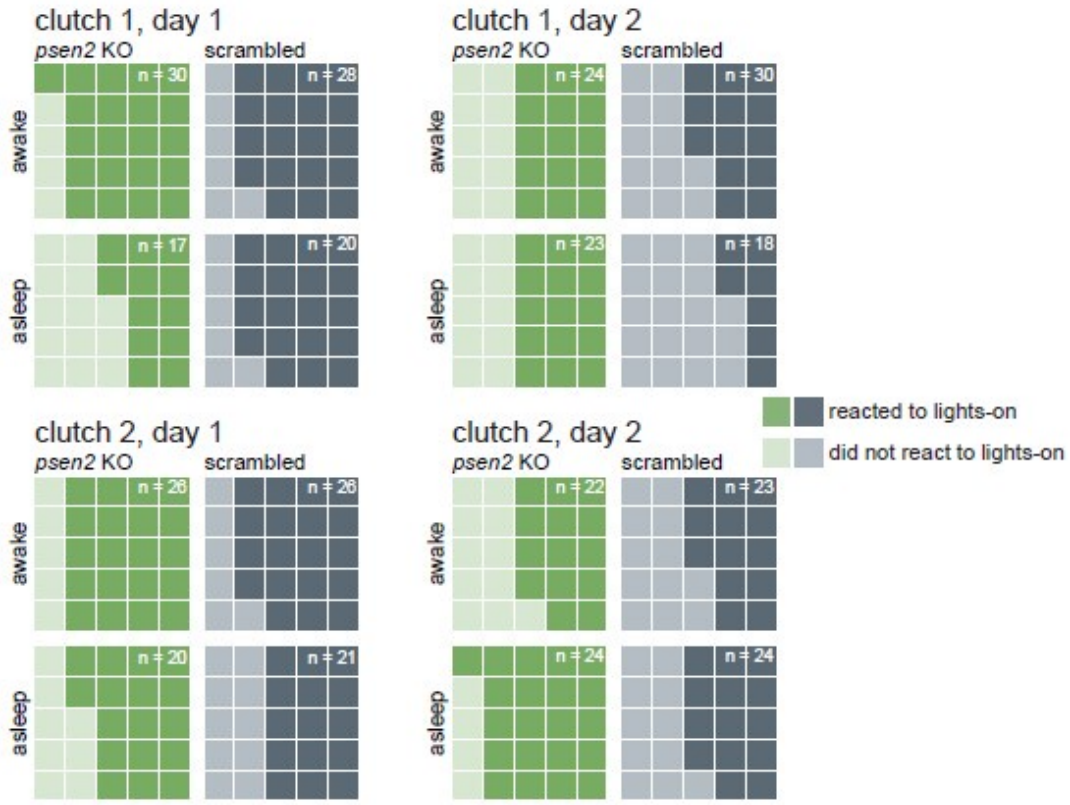

Next, we compared inactive period durations during the day between *psen2* and control larvae. If *psen2* knockout larvae indeed sleep more during the day compared to controls, we may predict inactive periods longer than one minute to increase disproportionately compared to the increase in shorter inactive periods. This broadly appeared to be the case, especially for one of the two clutches (Author response image 4). In clutch 1, inactive periods lasting 1–60 sec were equally frequent in both *psen2* and control larvae (fold change 1.0× during both days), while inactive periods lasting 1–2 min were 1.5× (day 1) and 2.5× (day 2) more frequent in *psen2* larvae compared to control larvae. In clutch 2, 1–60 sec inactive periods were also equally frequent in both *psen2* and control larvae, while inactive periods lasting 1–2 min were 3.4× (day 1) and 1.5× (day 2) more frequent in *psen2* larvae compared to control larvae. Therefore, *psen2* knockouts disproportionately increased the frequency of inactive periods longer than one minute, suggesting they genuinely slept more during the day.

Author response image 4.

psen2 F0 knockouts increased preferentially the frequency of longer inactive bouts. For each day and clutch, we calculated the mean distribution of inactive bout lengths across larvae of same genotype (*psen2* F0 knockout or scrambled-injected), then compared the frequency of inactive bouts of different lengths between the two genotypes. For example, in clutch 1 during day 2, 0.01% of the average scrambled-injected larva's inactive bouts lasted 111–120 seconds (X axis 120 sec) while 0.05% of the average *psen2* F0 knockout larva lasted this long, so the fold change was 5×. Inactive bouts lasting < 1 sec were excluded from the analysis. In clutch 2, day 1 plot, two datapoints fall outside the Y axis limit: 140 sec, Y = 32×; 170 sec, Y = 16×. Data is from the baseline *psen2* knockout trackings presented in Fig. 3 and Fig. 3–suppl. 2.

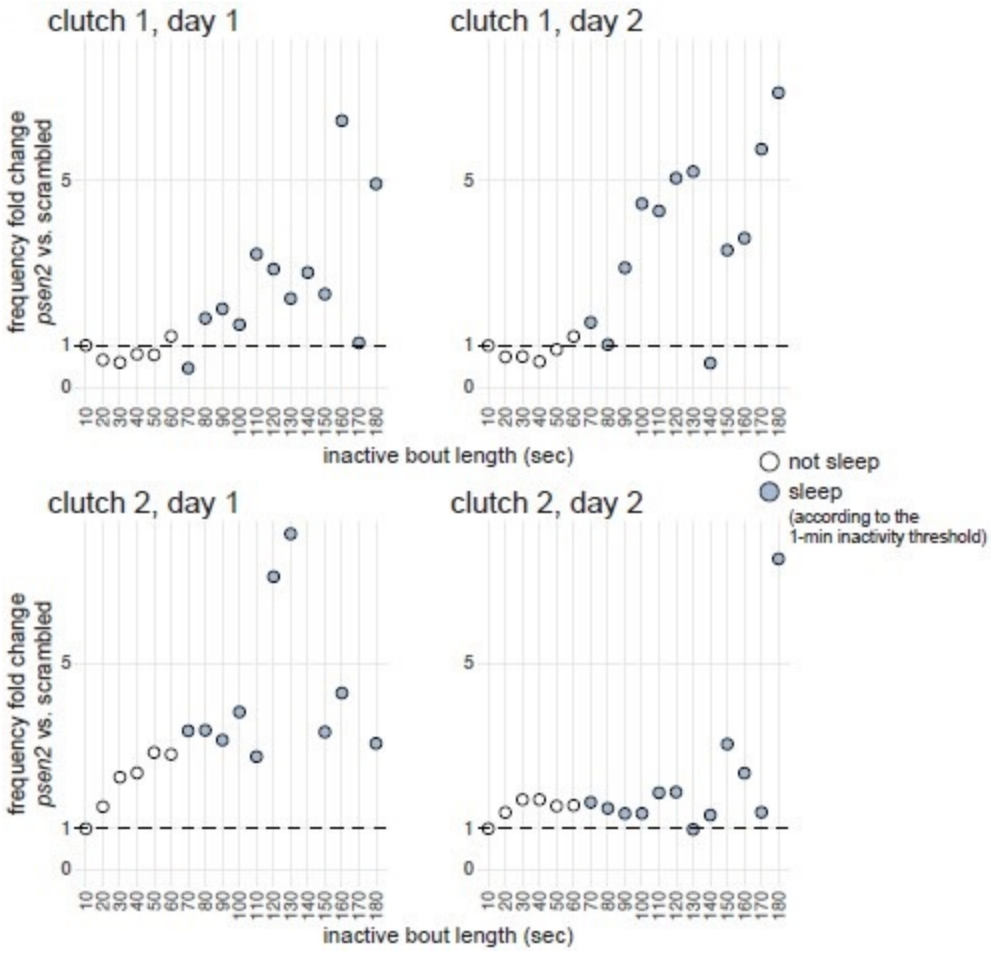

Ultimately, this criticism seems challenging to definitely address experimentally. A possible approach could be to use a closed-loop system which, after one minute of inactivity, triggers a stimulus that is sufficient to startle an awake larva but not an asleep larva. If *psen2* knockout larvae indeed sleep more during the day, the stimulus should usually not be sufficient to startle them. Nevertheless, we believe the two analyses presented here are consistent with *psen2* knockout larvae genuinely sleeping more during the day, so we decided to keep this label. We agree with the reviewer that the one-minute inactivity definition has limitations, especially for day-time inactivity.

> *(5) The conclusions for the serotonin section are overstated. Behavioural pharmacology purports to predict a signaling pathway disrupted with sorl1 KO. But is it not just possible*

> *that the drug acts in parallel to the true disrupted pathway in these fish? There is no direct evidence for serotonin dysfunction - that conclusion is based on response to the drug. Moreover, it is just 1 drug - is the same phenotype present with another SSRI? Likewise, language should be toned down in the discussion, as this hypothesis is not "confirmed" by the results (consider "supported"). The lack of measured serotonin differences further raises concern that this is not the true pathway. This is another major point that deserves further experimental evidence, because without it, the entire approach (behavioral pharm screen) seems more shaky as a way to identify mechanisms. There are any number of testable hypotheses to pursue such as a) Using transient transgenesis to visualize 5HT neuron morphology (is development perturbed: cell number, neurite morphology, synapse formation); b) Using transgenic Ca reporters to assay 5HT neuron activity.*

Regarding the comment, “is it not just possible that the drug acts in parallel to the true disrupted pathway”, we think no, assuming we understand correctly the question. Key to our argument is the fact that *sorl1* knockout larvae react differently to the drug(s) than control larvae. As an example, take night-time sleep bout length, which was not affected by knockout of *sorl1* (Fig. 4–supplement 4). For the sake of the argument, say only dopamine signalling (the “true disrupted pathway”) was affected in *sorl1* knockouts and that serotonin signalling was intact. Assuming that citalopram specifically alters serotonin signalling, then treatment should cause the same increase in sleep bout length in both knockouts and controls as serotonin signalling is intact in both. This is not what we see, however. Citalopram caused a *greater* increase in sleep bout length in *sorl1* knockouts than in scrambled-injected larvae. In other words, the effect is non-additive, in the sense that citalopram did not add the same number of z-scores to *sorl1* knockouts or controls. We think this shows that serotonin signalling is somehow different in *sorl1* knockouts. Nonetheless, we concede that the experiment does not necessarily say much about the importance of the serotonin disruption caused by loss of Sorl1. It could be, for example, that the most salient consequence of loss of Sorl1 is cholinergic disruption (see reply to Reviewer #1 above) and that serotonin signalling is a minor theme.

Furthermore, we agree with the reviewer and Reviewer #2 that the conclusions were overly confident. As suggested, we decided to repeat this experiment with another SSRI, fluvoxamine. Please find the results of this experiment in Fig. 5–supplement 1. The suggestions to further test the serotonin system in the *sorl1* knockouts are excellent as well, however we do not plan to pursue them at this stage.

> ***Recommendations for the authors:***
>
> ***Reviewer #1 (Recommendations For The Authors):***
>
> *Major Comments:*
>
> *- Data are presented in a variety of different ways, occasionally making comparisons across figures difficult. Perhaps at a minimum, behavioral fingerprints as in Figure 3 - Supplementary Figure 1 should be presented for all mutants in the main figures.*

We like this suggestion! Thank you. We brought the behavioural fingerprints figure (previously Fig. 4–supplement 5) as main Fig. 4, and put the figure focused on the *sorl1* knockout behavioural phenotype in supplementary, with the other gene-by-gene figures.

> *- It is not clear why some data were selected for supplemental rather than main figures. In many cases, detailed phenotypic data is provided for one example mutant in the main figures, and then additional mutants are described in detail in the supplement. Again, to*

> *facilitate comparisons between mutants, fingerprints could be provided for all mutants in a main figure, with detailed analyses moved to the supplements.*

The logic was to dedicate one main figure to *psen2* (Fig. 3) as an example of an early-onset Alzheimer's risk gene, and one to *sorl1* (previously Fig. 4) as an example of a late-onset Alzheimer's risk gene. We focused on them in main figures as they are both tested again later (Fig. 5 and Fig. 6). Having said that, we agree that the fingerprints may be a better use of main figure space than the parameters plots. In addition to the above (fingerprints of lateonset Alzheimer's risk genes in main figure), we rearranged the figures in the early-onset AD section to have the *psen2* F0 knockout fingerprint in main.

> *- The explication of the utility of behavioral fingerprinting on page 35 is somewhat confusing. The authors describe drugs used to treat depression as enriched among small molecules anti-correlating with the sorl1 fingerprint. However, in Figure 5 - Supplementary Figure 1, drugs used to treat depression are biased toward positive cosines, which are indicated as having a more similar fingerprint to sorl1. These drugs should be described as more present among compounds positively correlating with the sorl1 fingerprint.*

Sorry, the confusion is about "(anti-)correlating". Precisely, we meant "correlating and/or anti-correlating", not just anti-correlating. We changed to that wording. In short, the analysis is by design agnosFc to whether compounds with a given annotation are found more on the positive cosines side (le side in Fig. 5–supplement 1a) or the negative cosines side (right side). This is because the dataset o en includes both agonists and antagonists to a given pathway but these are difficult to annotate. For example, say 10 compounds in the dataset target the dopamine D4 receptor, but these are an unknown mix of agonists and antagonists. In this case, we want ZOLTAR to generate a low p-value when all 10 compounds are found at extreme ends of the list, regardless of which end(s) that is (e.g. top 8 and bojom 2 should give an extremely low p-value). Initially, we were splitting the list, for each annotation, into positive-cosine fingerprints and negative-cosine fingerprints and testing enrichment on both separately, but we think the current approach is better as it reflects better the cases we want to detect and considers all available examples for a given annotation in one test. In sum, yes, in this case drugs used to treat depression were mostly in the positive-cosine side, but the other drugs on the negative-cosine side also contributed to what the p-value is, so it reflects better the analysis to say "correlating and/or anticorrelating". You can read more about our logic for the analysis in Methods (section Behavioural pharmacology from *sorl1* F0 knockout's fingerprint).

> *- The authors conclude the above-described section by stating: "sorl1 knockout larvae behaved similarly to larvae treated with small molecules targeting serotonin signaling, suggesting that the loss of Sorl1 disrupted serotonin signaling." Directionality here may be important. Are all of the drugs targeting the serotonin transporter SSRIs or similar? If so, then a correct statement would be that loss of Sorl1 causes similar phenotypes to drugs enhancing serotonin signaling. Finally, based on the correlation between serotonin transporter inhibitor trazodone and the sorl1 crispant phenotype, it is potentially surprising that the SSRI citalopram caused the opposite phenotype from sorl1, that is, increased sleep during the day and night. It is potentially interesting that this result was enhanced in mutants, and suggests dysfunction of serotonin signaling, but the statement that "our behavioral pharmacology approach correctly predicted from behaviour alone that serotonin signaling was disrupted" is too strong a conclusion.*

We understand "disrupt" as potentially going either way, but this may not be the common usage. We changed to "altered".

The point regarding directionality is excellent, however. We tested the proportion of serotonin transporter agonists and antagonists (SSRIs) on each side of the ranked list of small molecule fingerprints. We used the STITCH database for this analysis as it has more drug–target interactions, but likely less curated, than the TherapeuFc Target Database (Szklarczyk et al., 2016). As with the TherapeuFc Target Database, most fingerprints of compounds interacting with the serotonin transporter SLC6A4 were found on the side of positive cosines (p ~ 0.005 using the custom permutation test), which replicates Fig. 5a with a different source for the drug–target annotations (Author response image 5). On the side of positive cosines (small molecules which generate behavioural fingerprints correlating with the *sorl1* fingerprint), there were 2 agonists and 26 antagonists. On the side of negative cosines (small molecules which generate behavioural fingerprints anti-correlating with the *sorl1* fingerprint), there were 3 agonists and 2 antagonists. Using a Chi-squared test, this suggests a significant (p = 0.002) over-representation of antagonists (SSRIs) on the positive side (expected count = 24, vs. 26 observed) and agonists on the negative side (expected count = 1, vs. 3 observed). If SLC6A4 antagonists, i.e. SSRIs, indeed tend to cause a similar behavioural phenotype than knockout of *sorl1*, this would point in the direction of our original interpretation of the citalopram experiment; which was that excessive serotonin signalling is what causes the *sorl1* behavioural phenotype.

Author response image 5.

Using the STITCH database as source of annotations also predicts SLC6A4 as an enriched target for the *sorl1* behavioural fingerprint. Same figures as Fig. 5a,b but using the STITCH database (Szklarczyk et al., 2016) as source for the drug targets. a, Compounds annotated by STITCH as interacting with the serotonin transporter SLC6A4 tend to generate behavioural phenotypes similar to the *sorl1* F0 knockout fingerprint. 40,522 compound–target protein pairs (vertical bars; 1,592 unique compounds) are ranked from the fingerprint with the most positive cosine to the fingerprint with the most negative cosine in comparison with the mean *sorl1* F0 knockout fingerprint. Fingerprints of drugs that interact with SLC6A4 are coloured in yellow. Simulated p-value = 0.005 for enrichment of drugs interacting with SLC6A4 at the top (positive cosine) and/or bottom (negative cosine) of the ranked list by a custom permutation test. b, Result of the permutation test for top and/or bottom enrichment of drugs interacting with SLC6A4 in the ranked list. The absolute cosines of the fingerprints of drugs interacting with SLC6A4 (n = 52, one fingerprint per compound) were summed, giving sum of cosines = 15.9. To simulate a null distribution, 52 fingerprints were randomly drawn 100,000 times, generating a distribution of 100,000 random sum of cosines. Here, only 499 random draws gave a larger sum of cosines, so the simulated p-value was p = 499/100,000 = 0.005 **.

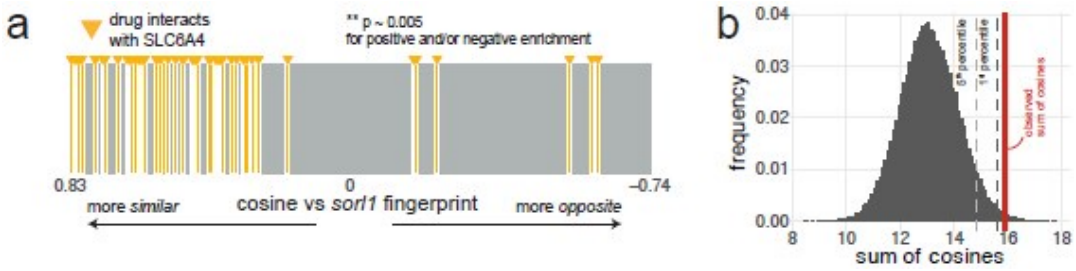

If this were true, we would expect, as the reviewer suggested, SSRI treatment (citalopram or fluvoxamine) on control larvae to give a similar behavioural phenotype as knockout of *sorl1*. However, this generally did not appear to be the case (*sorl1* knockout fingerprint vs. SSRI-treated control fingerprint, cosine = 0.08 ± 0.35; Author response image 6).

Author response image 6.

sorl1 F0 knockouts in comparison to controls treated with SSRIs. a, *sorl1* F0 knockout fingerprints (baseline recordings and *sorl1* + H_2O fingerprint from the citalopram experiment) in comparison with the scrambled-injected + citalopram (1 or 10 µM) fingerprints. Each dot represents the mean deviation from the same-clutch scrambled-injected H_2O-treated mean for that parameter (z-score, mean ± SEM). b, As in a), *sorl1* F0 knockout fingerprints (baseline recordings and *sorl1* + H_2O fingerprint from the fluvoxamine experiment) in comparison with the scrambled-injected + fluvoxamine (10 µM) fingerprint.

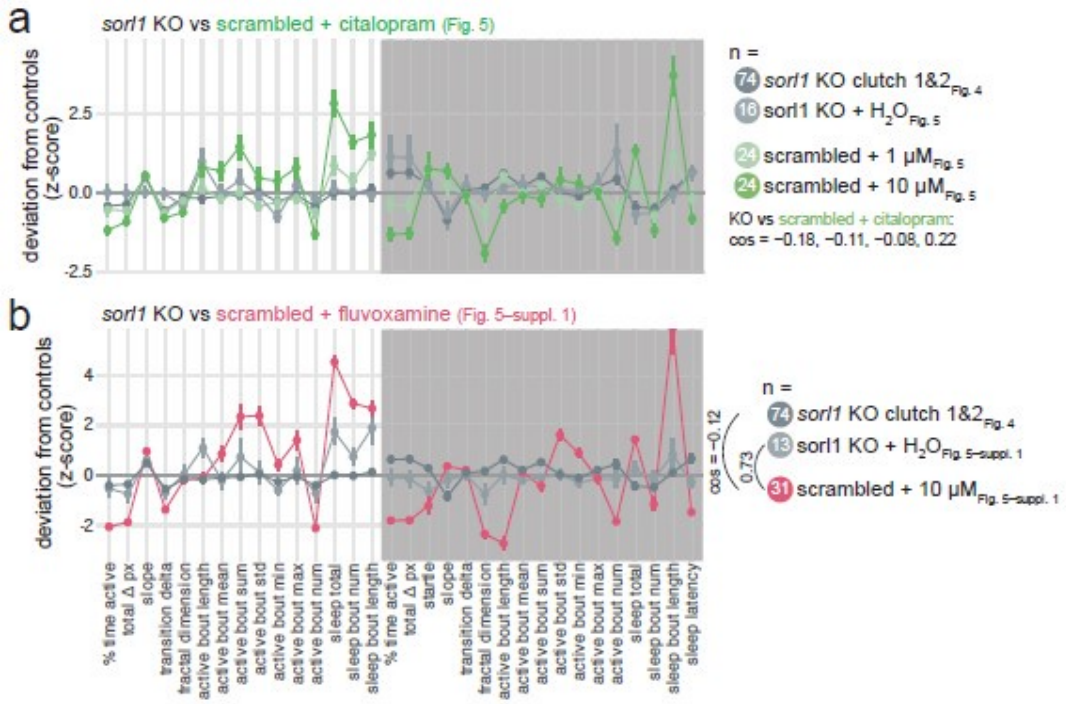

The comparison with trazodone is an interesting observation, but it is only a weak serotonin reuptake inhibitor (Ki for SLC6A4 = 690 nM, vs. 8.9 nM for citalopram; Owens et al., 1997) and it has many other targets, both as agonist or antagonist, including serotonin, adrenergic, and histamine receptors (Mijur, 2011). In any case, the average trazodone fingerprint does not correlate particularly well to the *sorl1* knockout fingerprint (cos = 0.3). Finally, the *sorl1* knockout behavioural phenotype could be primarily caused by altered serotonin signalling in the hypothalamus, where we found both the biggest difference in *tph1a/1b/2* HCR signal intensity (Fig. 5f) and the highest expression of *sorl1* across scRNA-seq clusters (Fig. 1–supplement 2). In this case, it would be correct to expect *sorl1* knockouts to react differently to SSRIs than controls, but it would be incorrect to expect SSRI treatment to cause the same behavioural phenotype, as it concurrently affects every other serotonergic neuron in the brain.

Finally, we agree the quoted conclusion was too strong given the current evidence. We since tested another SSRI, fluvoxamine, on *sorl1* knockouts.

> *- Also in reference to Figure 5: in panel c, data are presented as deviation from vehicle treated. Because of this data presentation choice, it's no longer possible to determine whether, in this experiment, sorl1 crispants sleep less at night relative to their siblings. Does citalopram rescue / reverse sleep deficits in sorl1 mutants?*

On your first point, please see our response to Reviewer #3 (2)c and Author Response 2b above.

On “does citalopram rescue/reverse sleep deficits in *sorl1* mutants”: citalopram (and fluvoxamine) tends to *reverse* the key aspects of the *sorl1* knockout behavioural phenotype by reducing night-time activity (% time active and total Δ pixels), increasing night-time sleep, and shortening sleep latency (Author response image 7). Extrapolating from the hypothesis presented in Discussion, this may be interpreted as a hint that *sorl1* knockouts have reduced levels of 5-HT receptors, as increasing serotonin signalling using an SSRI tends to rescue the phenotype. However, we do not think that focusing on the significant behavioural parameters necessarily make sense here. Rather, one should take all parameters into account to conclude whether knockouts react differently to the drug than wild types (also see answer to Reviewer #3, (7) on this). For example, citalopram increased *more* the night-time sleep bout length of *sorl1* knockouts than the one of controls (Fig. 5), but this parameter was not modified by knockout of *sorl1* (Fig. 4). To explain the rationale more informally, citalopram is only used as a tool here to probe serotonin signalling in *sorl1* knockouts, whether it worsens or rescues the behavioural phenotype is somewhat secondary, the key question is whether knockouts react differently than controls.

Author response image 7.

Comparing untreated *sorl1* F0 knockouts vs. treated with SSRIs. a, *sorl1* F0 knockout fingerprints (baseline recordings and *sorl1* + H_2O fingerprint from the citalopram experiment) in comparison with the *sorl1* knockout + citalopram (1 or 10 µM) fingerprints. Each dot represents the mean deviation from the same-clutch scrambled-injected H_2O-treated mean for that parameter (z-score, mean ± SEM). b, As in a), *sorl1* F0 knockout fingerprints (baseline recordings and *sorl1* + H_2O fingerprint from the fluvoxamine experiment) in comparison with the *sorl1* + fluvoxamine (10 µM) fingerprint.

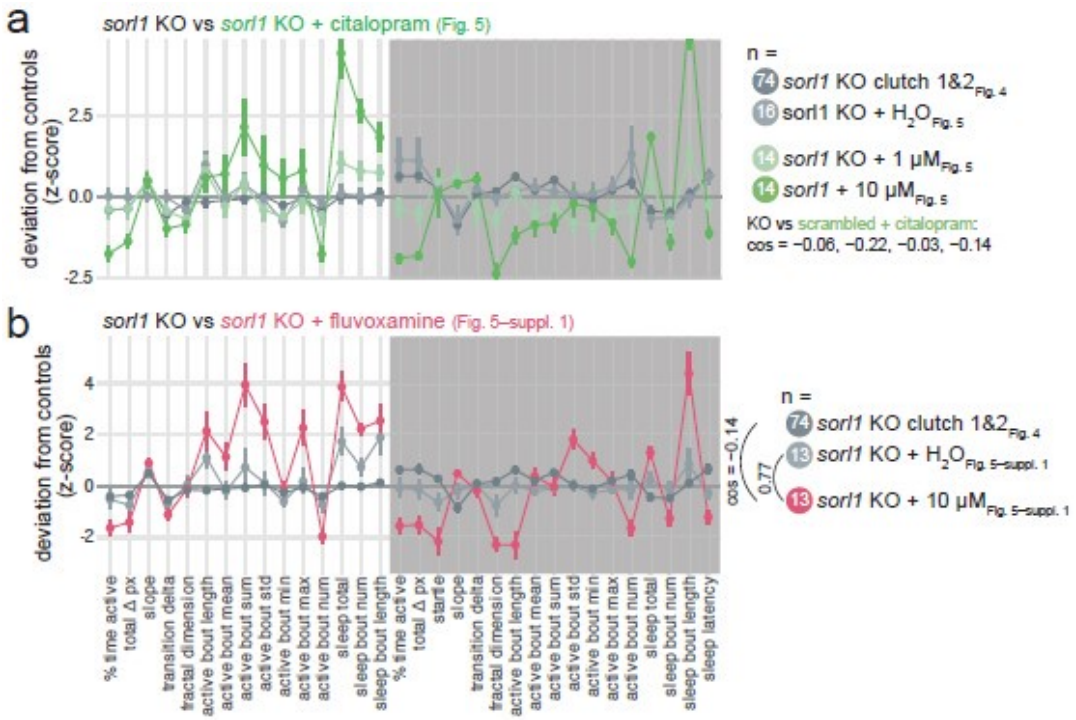

> - *Possible molecular pathways targeted by Fnidazole, fenoprofen, and betamethasone are not described.*

Tinidazole is an antibiotic, fenoprofen is a non-steroidal anti-inflammatory drug (NSAIDs), betamethasone is a steroidal anti-inflammatory drug. Interestingly, long-term use of NSAIDs reduces the risk of AD (in 't Veld Bas A. et al., 2001). Several mechanisms are possible (Weggen et al., 2007), including reduction of Aβ42 production by interacting with γ-secretase (Eriksen et al., 2003). However, we did not explore the mechanism of action of these drugs on *psen2* knockouts so do not feel comfortable speculating. We do not know, for example, whether these findings apply to betamethasone.

> *Minor Comments:*
>
> *- On page 25, panel "g" should be labeled as "f".*

Thank you!

> *- On page 35, a reference should be provided for the statement "From genomic studies of AD, we know that mutations in genes such as SORL1 modify risk by disrupting some biological processes.".*

Thank you, this is now corrected. There were the same studies as mentioned in Introduction.

> *- On page 43, the word "and" should be added - "in wild-type rats and mice, overexpressing mutated human APP and PSEN1, AND restricting sleep for 21 days...".*

Right, this sentence could be misread, we edited it. "overexpressing [...]" only applied to the mice, not the rats (as they are wild-type); and both are sleep-deprived.

> *- On page 45, a reference should be provided for the statement "SSRIs can generally be used conFnuously with no adverse effects" and this statement should potentially be softened.*

The reference is at the end of that sentence (Cirrito et al., 2011). You are correct though; we reformulated this statement to: "SSRIs can generally be used safely for many years". SSRIs indeed have side effects.

> *- On page 54, a 60-minute rolling average is described as 45k rows, but this seems to be a 30-minute rolling average.*

Thank you! We corrected. It should have been 90k rows, as in: 25 frames-per-second × 60 seconds × 60 minutes.

> ***Reviewer #2 (Recommendations For The Authors)**:*
>
> *"As we observed in the scRNA-seq data, most genes tested (appa, appb, psen1, psen2, apoea, cd2ap, sorl1) were broadly expressed throughout the 6-dpf brain (Fig. 1d and Fig. 1supplement 3 and 4)."*
>
> *- apoea and appb are actually not expressed highly in the scRNA-seq data, and the apoea in situ looks odd, as if it has no expression. The appb gene mysteriously does not look as though it has high expression in the Raj data, but it is clearly expressed based on the in situ. I had previously noticed the same discrepancy, and I ajribute it to the transcriptome used to map the Raj data, as the new DanioCell data uses a new*

> *transcriptome and indicates high appb expression in the brain. Please point out the discrepancy and possible explanation, perhaps in the figure legend.*

All excellent points, thank you. We included them directly in Results text.

> *"most of these were expressed in the brain of 5-6-dpf zebrafish larvae, suggesting they play a role in early brain development or function."*
>
> *- Evidence of expression does not suggest function, particularly not a function in brain development. As one example, almost half of the genome is expressed prior to the maternal-zygotic transition but does not have a function in those earliest stages of development. There are numerous other instances where expression does not equal function. Please change the sentence even as simply as "it is possible that they".*

We mostly agree and edited to “[…], so they could play a role […]”.

Out of curiosity, we plojed, for each zebrafish developmental stage, the proportion of Alzheimer’s risk gene orthologues expressed in comparison to the proportion of all genes expressed (Author response image 8). We defined “all genes” as every gene that is expressed in at least one of the developmental stages (n = 24,856), not the complete transcriptome, to avoid including genes that are never expressed in the brain or whose expression is always below detection limit. We counted a gene as “expressed” if at least three cells had detectable transcripts. Using these definitions, 82 ± 7% of genes are expressed during development. For every developmental stage except 5 dpf (so 11/12), a larger proportion of Alzheimer’s risk genes than all genes are expressed (+5 ± 4%).

Author response image 8.

Proportion of Alzheimer’s risk genes orthologues expressed throughout zebrafish development. Proportion of Alzheimer’s risk genes orthologues (n = 42) and all genes (n = 24,856) expressed in the zebrafish brain at each developmental stage, from 12 hours post-fertilisation (hpf) to 15 days post-fertilisation (dpf). “All genes” corresponds to every gene expressed in the brain at any of the developmental stages, not the complete transcriptome. A gene is considered “expressed” (green) if at least three cells had detectable transcripts. Single-cell RNA-seq dataset from Raj et al., 2020.

> *"This frame-by-frame analysis has several advantages over previous methods that analysed activity data at the one-minute resolution."*
>
> *- Which methods are these? There are no citations. There are certainly existing methods in the zebrafish field that can produce similar data to the method developed for this project. This new package is useful, as most existing so ware is not written in R, so it would help scienFsts who prefer this programming language. However, I would be*

> *careful not to oversell it's novelty, since many methods do exist that produce similar results.*

We added the references. There were referenced above after “we combined previous sleep/wake analysis methods”, but should have been referenced again here.

We are not convinced by this criticism. We would obviously not claim that the FramebyFrame package is as sophisticated and versatile as video-tracking tools like SLEAP or DeepLabCut, but we do think it answers a genuine need that was not addressed by other methods. Specifically, we know of many labs recording pixel count data across multiple days using the Zebrabox or DanioVision (we added support for DanioVision data a er submission), but there were no packages to extract behavioural parameters from these data. Other methods involved standalone scripts with no documentation or version tracking. We would concede the FramebyFrame package is mostly targeted at these labs, but we already know of six labs rouFnely using it and were recently contacted by a researcher tracking Daphnia in the Zebrabox.

> *"F0 knockouts of both cutches" - "clutches"*

Thank you!

> ***Reviewer #3 (Recommendations For The Authors):***
>
> *I would suggest totally revamping the Introduction section, and being sure to provide readers with the context and background they need for the data that comes therea er. Key areas to touch on, in no particular order, include:*
>
> *• Far more detail on the behavioral pharm screen upon which this paper builds, as a brief overview of that approach and the data generated are needed.*

Thank you for the suggestion, we added a sentence hinting at this work in the last Introduction paragraph.

> *• Limitations of current zebrafish sleep/arousal assays that moFvated the authors to develop a new, temporally high-resolution system.*

We think this is better explained in Results, as is currently. For example, we need to point to Fig. 2–supplement 2a,b,c to explain that one-minute methods were missing sleep bouts and how FramebyFrame resolves this issue.

> *• A paragraph about sleep and AD, that does a better job of citing work in humans, mammalian, and invertebrate models that moFvate the interest in the connection pursued here.*

Sorry, we think this would place too much focus on sleep and AD. We want the main topic of the paper to be the behavioural pharmacology approach, not AD or sleep *per se*. As the Introduction states, we see Alzheimer’s risk genes as a case study for the behavioural pharmacology approach, rather than the reason why the approach was developed. Additionally, presenting sleep and AD in Introduction risks sounding like ZOLTAR is specifically designed for this context, while we conceived of it as much more generalisable and explicitly encourage its use to study genes associated to other diseases. Note that the paragraph you suggest is, we think, mostly present in Discussion (section Disrupted sleep and serotonin signalling […]).

> *• I modestly suggest eliminating making such a strong case for a gene-first approach being the best way to understand disease. It is not a zero-sum game, and there is plenty to learn from proteomics, metabolomics, etc. I suspect nobody will argue with the authors saying they leveraged the strength of their system and focused on key AD genes of interest.*

From your point below, we understand the following quote is the source of the issue: “For finding causal processes, studying the genome, rather than the transcriptome or epigenome, is advantageous because the chronology from genomic variant to disease is unambiguous […]”. We did not want to suggest it is a zero-sum game, but we now understand how it can be read this way. We adapted slightly the wording. What we want to do is highlight the causality argument as the advantage of the genomics approach. We feel we do not read this argument o en enough, while it remains a ‘magic power’ of genomics. One essentially does not have to worry about causality when studying a pathogenic germline variant, while it is a constant concern when studying the transcriptome or epigenome (i.e. did the change in this transcript’s level cause disease, or vice-versa?). To take an example in the context of AD, arguments based on genomics (e.g. Down syndrome or APP duplication) are often the definite arbiters when debating the amyloid hypothesis, exactly because their causality cannot be doubted.

> *Minor comments*
>
> *(1) The opening of the introduction is perhaps overly broad, spending an entire paragraph on genome vs transcriptome, etc and making the claim that a gene-first approach is the best path. It isn't zero-sum, and the authors could just get right into AD and study genes of interest. Similar issues occur throughout the manuscript, with sentences/paragraphs that are not necessarily needed.*

Please see our answer to your previous point. On the introduction being overly broad, we perfectly agree it is broad, but related to your point about presenting sleep and AD in the Introduction, we wish to talk about finding causal processes from genomics findings using behavioural pharmacology. We purposefully present research on AD as one instance of this broader goal, not the primary topic of the paper.

> *Another example are these sentences, which could be totally removed as the following paragraph starts off making the same point much more succinctly. "From genomic studies of AD, we know that mutations in genes such as SORL1 modify risk by disrupting some biological processes. Presumably, the same processes are disrupted in zebrafish sorl1 knockouts, and some caused the behavioural alterations we observed. Can we now follow the thread backwards and predict some of the biological processes in which Sorl1 is involved based on the behavioural profile of sorl1 knockouts?"*

Thanks for the suggestion, but we think these sentences are useful to place back this Results section in the context of the Introduction. Think of the paper as mainly about the behavioural pharmacology approach, not on Alzheimer’s risk genes. The function of the paragraph here is not simply to explain the method by which we decided to study *sorl1*; it is to reiterate the rationale behind the behavioural pharmacology approach so that the reader understands where this Results section fits in the overall structure.

> *(2) Related to the above, the authors use lecanemab as an example to support their approach, but there has been a great deal of controversy regarding this drug. I don't think such extensive justification is needed. This study uses AD risk genes as a case study in a newly developed behavioral pharm pipeline. A great deal of the rest of the intro*

> *seems to just fill space and could be more focused on the study at hand. Interestingly, a er gene selection, the next step in their pipeline is sleep/wake analysis yet nothing is covered about AD and sleep in the intro. Some justification of that approach (why focus on sleep/wake as a starting point for behavioral pharm rather than learning and memory?) would be a better use of intro space.*

There has indeed been controversy about lecanemab, but even the harshest criFques of the amyloid hypothesis concede that it slows down cognitive decline (Espay et al., 2023). That is all that is needed to support our argument, which is that research on AD started primarily from genomics and thereby yielded a disease-modifying drug. The controversy seems mostly focused on whether this effect size is clinically significant, and we think we correctly represent this uncertainty (e.g. _“_antibodies against Aβ such as lecanemab show promise in slowing down disease progression” and “the beneficial effects from targeRng Aβ aggregaRon currently remain modest”).

Your next point is entirely fair. We mostly answered it above. To explain further, the primary reason why we measured sleep/wake behaviour is to match the behavioural dataset from Rihel et al., 2010 so we can use it to make predictions, not to study sleep in the context of AD *per se*. Sure, perhaps learning and memory would have been interesting, but we do not know of any study testing thousands of small molecules on zebrafish larvae during a memory task. We understand it can be slightly confusing though, as we then spend a paragraph of Discussion on sleep as a causal process in AD, but we obviously need to discuss this topic given the findings. However, to reiterate, we purposefully designed FramebyFrame and ZOLTAR to be useful beyond studying sleep/wake behaviour. For example, FramebyFrame would not calculate 17 behavioural parameters if the only goal was to measure sleep. We now mention the Rihel et al., 2010 study in the Introduction as you suggested above (“Far more detail on the behavioral pharm screen […]”), as that is the real reason why sleep/wake behaviour was measured in the first place.

> *(3) Also related to the above, another more relevant point that could be talked about in the intro is the need for more refined approaches to analyze sleep in zebrafish, given the effort that went into the new analysis system described here. Again, I think the context for why the authors developed this system would be more meaningful than the current content.*

Thank you, we think we answered this point above (especially below Limitations of current zebrafish sleep/arousal assays […]).

> *(4) GWAS can stand for Genome-wide associate studies (plural) so I do not think the extra "s" is needed (GWASs) .*

Indeed, that seems to be the common usage. Thank you.

> *(5) AD candidate risk genes were determined from loci using "mainly statistic colocalization". Can the authors add a few more details about what was done and what the "mainly" caveat refers to?*

“Mainly” simply refers to the fact that other methods were used by Schwartzentruber et al. (2021) to annotate the GWAS loci with likely causal genes, but that most calls were ultimately made from statistic colocalisation. Readers can refer to this work to learn more about the methods used.

> *(6) The authors write "The loss of psen1 only had mild effects on behaviour" but I think they mean "sleep behaviors" as there could be many other behaviors that are disrupted*

> *but were not assessed. The same issue a few sentences later with "Behaviour during the day was not affected" and at the end of the following paragraph.*

Yes, that would be more precise, thank you.

> *(7) For the Sorl1 pharmacology data, it is very hard to understand what is being measured behaviorally. Are the authors measuring sleep +/- citalopram, or something else, and why the change to Euclidean distance rather than all the measures we were just introduced to earlier in the manuscript?*

We understand these plots (Fig. 5c,d) are less intuitive, but it is important that we show the difference in behaviour compared to H_2O-treated larvae of same genotype. The claim is that citalopram has a larger effect on knockouts than on controls, so the reader needs to focus on the effect of the drug on each genotype, not on the effect of *sorl1* knockout. We added the standard fingerprints (i.e. setting controls to z-score = 0) here in Author response figures.

Euclidean distance takes as input all the measures we introduced. The point is precisely not to select a single measure. For example, say we were only plotting active bout number during the day, we would conclude that 10 µM citalopram has the same effect on knockouts and controls. Conversely, if we had taken sleep bout length at night, we would conclude 10 µM has a stronger effect on knockouts. What is the correct parameter to select? Using Euclidean distance resolves this by taking all parameters into account, rather than arbitrarily choosing one.

> *And what exactly is a "given spike in serotonin"? and how is this hypothesis the conclusion based on the lack of evidence for the second hypothesis? As the authors say, there could be other ways sorl1 knockouts are more sensitive to citalopram, so the absence of evidence for one hypothesis certainly does not support the other hypothesis.*

We mean a given release of serotonin in the synaptic cleft. We have fixed this wording.

We tend to disagree on the second point. We can think of two ways that *sorl1* knockouts are more sensitive to citalopram: 1) they produce more serotonin, so blocking reuptake causes a larger spike in knockouts; or 2) blocking reuptake causes the same increase in both knockouts and wild-types but knockouts react more strongly to serotonin. We cannot in fact think of another way to explain the citalopram results. Not finding overwhelming evidence for 1) surely supports 2) somewhat, even if we do not have direct evidence for it. As an analogy, if two diagnoses are possible for a patient, testing negative for the first one supports the other one, even before it is directly tested.

> *(8) Again some language is used without enough care. Fish are referred to as "drowsier" under some drug conditions. How do the authors know the animal is drowsy? The phenotype is more specific - more sleep, less activity.*

Thank you, we switched to “Furthermore, fenoprofen worsened the day-time hypoactivity of *psen2* knockout larvae [...]”.

> *(9) This sentence is misleading as it gives the impression that results in this manuscript suggest the conclusion: "Our observation that disruption of genes associated with AD diagnosis a er 65 years reduces sleep in 7-day zebrafish larvae suggest that disrupted sleep may be a common mechanism through which these genes exert an effect on risk." That idea is widely held in the field, and numerous other previous manuscripts/reviews should be cited for clarity of where this hypothesis came from.*

This idea is not widely held in the field. You likely read this point as “disrupted sleep is a risk factor for AD”, which, yes, is widely discussed in the field, but is not precisely what we are saying. We hypothesise that mutations in some of the Alzheimer’s risk genes *cause* disrupted sleep, possibly from a very early age, which then causes AD decades later. Studies and reviews on sleep and AD rarely make this hypothesis, at least not explicitly. The closest we know of are a few recent human genetics studies, typically using Mendelian Randomisation, finding that higher genetic risk of AD correlates with some sleep phenotypes, such as sleep duration (Chen et al., 2022; Leng et al., 2021). The work of Muto et al. (2021) is particularly interesting as it found correlations between higher genetic risk of AD and some sleep phenotypes in men in their early twenFes, which seems unlikely to be a consequence of early pathology (Muto et al., 2021). Note, however, that even these studies do not mention sleep possibly being disrupted early in development, which is what our findings in zebrafish larvae support. As we mention, we think a team should test whether sleep is different in infants at higher genetic risk of AD, essentially performing an analogous, but obviously much more difficult, experiment as we did in zebrafish larvae. We do not know of any study testing this or even raising this idea, so evidently it is not widely held. Having said that, the studies we mention here were not referenced in the Discussion paragraph. We have now corrected this.

Ashlin TG, Blunsom NJ, Ghosh M, Cockcro6 S, Rihel J. 2018. Pitpnc1a Regulates Zebrafish Sleep and Wake Behavior through Modulation of Insulin like Growth Factor Signaling. *Cell Rep* 24:1389–1396. doi:10.1016/j.celrep.2018.07.012

Chen D, Wang X, Huang T, Jia J. 2022. Sleep and LateOnset Alzheimer’s Disease: Shared Genetic Risk Factors, Drug Targets, Molecular Mechanisms, and Causal Effects. *Front Genet* 13. doi:10.3389/fgene.2022.794202

Cirrito JR, Disabato BM, Restivo JL, Verges DK, Goebel WD, Sathyan A, Hayreh D, D’Angelo G, Benzinger T, Yoon H, Kim J, Morris JC, Mintun MA, Sheline YI. 2011. Serotonin signaling is associated with lower amyloid-β levels and plaques in transgenic mice and humans. *Proc Natl Acad Sci U S A* 108:14968–14973. doi:10.1073/pnas.1107411108

Dean DC, Jerskey BA, Chen K, Protas H, Thiyyagura P, RoonJva A, O’Muircheartaigh J, Dirks H, Waskiewicz N, Lehman K, Siniard AL, Turk MN, Hua X, Madsen SK, Thompson PM, Fleisher AS, Huentelman MJ, Deoni SCL, Reiman EM. 2014. Brain Differences in Infants at Differential Genetic Risk for Late-Onset Alzheimer Disease A Cross-sectional Imaging Study. *JAMA Neurol* 71:11–22. doi:10.1001/jamaneurol.2013.4544

Eriksen JL, Sagi SA, Smith TE, Weggen S, Das P, McLendon DC, Ozols VV, Jessing KW, Zavitz KH, Koo EH, Golde TE. 2003. NSAIDs and enanJomers of flurbiprofen target γ-secretase and lower Aβ42 in vivo. *J Clin Invest* 112:440–449. doi:10.1172/JCI18162

Espay AJ, Herrup K, Kepp KP, Daly T. 2023. The proteinopenia hypothesis: Loss of Aβ42 and the onset of Alzheimer’s Disease. *Ageing Res Rev* 92:102112. doi:10.1016/j.arr.2023.102112

Hoffman EJ, Turner KJ, Fernandez JM, Cifuentes D, Ghosh M, Ijaz S, Jain RA, Kubo F, Bill BR, Baier H, Granato M, Barresi MJF, Wilson SW, Rihel J, State MW, Giraldez AJ. 2016. Estrogens Suppress a Behavioral Phenotype in Zebrafish Mutants of the AuJsm Risk Gene, CNTNAP2. *Neuron* 89:725–733. doi:10.1016/j.neuron.2015.12.039

in ’t Veld Bas A., Ruitenberg Annemieke, Hofman Albert, Launer Lenore J., van Duijn Cornelia M., Stijnen Theo, Breteler Monique M.B., Stricker Bruno H.C. 2001. Nonsteroidal Anti inflammatory Drugs and the Risk of Alzheimer’s Disease. *N Engl J Med* 345:1515–1521. doi:10.1056/NEJMoa010178

Jagirdar R, Fu C-H, Park J, Corbek BF, Seibt FM, Beierlein M, Chin J. 2021. Restoring acJvity in the thalamic reJcular nucleus improves sleep architecture and reduces Aβ accumulaJon in

mice. *Sci Transl Med* 13:eabh4284. doi:10.1126/scitranslmed.abh4284

Jiang H, Newman M, Lardelli M. 2018. The zebrafish orthologue of familial Alzheimer's disease gene PRESENILIN 2 is required for normal adult melanoJc skin pigmentaJon. *PLOS ONE* 13:e0206155. doi:10.1371/journal.pone.0206155

Jiang H, Pederson SM, Newman M, Dong Y, Barthelson K, Lardelli M. 2020. Transcriptome analysis indicates dominant effects on ribosome and mitochondrial funcJon of a premature terminaJon codon mutaJon in the zebrafish gene psen2. *PloS One* 15:e0232559. doi:10.1371/journal.pone.0232559

Joo W, Vivian MD, Graham BJ, Soucy ER, Thyme SB. 2021. A Customizable Low-Cost System for Massively Parallel Zebrafish Behavioral Phenotyping. *Front Behav Neurosci* 14.

Joubert L, Hanson B, Barthet G, Sebben M, Claeysen S, Hong W, Marin P, Dumuis A, Bockaert J. 2004. New sorJng nexin (SNX27) and NHERF specifically interact with the 5-HT4a receptor splice variant: roles in receptor targeJng. *J Cell Sci* 117:5367–5379. doi:10.1242/jcs.01379 Leng Y, Ackley SF, Glymour MM, Yaffe K, Brenowitz WD. 2021. GeneJc Risk of Alzheimer's Disease and Sleep Duration in Non-Demented Elders. *Ann Neurol* 89:177–181. doi:10.1002/ana.25910

Mitchell PB, Hadzi-Pavlovic D. 2000. Lithium treatment for bipolar disorder. *Bull World Health Organ* 78:515–517.

Mikur A. 2011. Trazodone: properJes and uJlity in mulJple disorders. *Expert Rev Clin Pharmacol* 4:181–196. doi:10.1586/ecp.10.138

Munoz-Torrero D. 2008. Acetylcholinesterase Inhibitors as Disease-Modifying Therapies for Alzheimer's Disease. *Curr Med Chem* 15:2433–2455. doi:10.2174/092986708785909067

Muto V, Koshmanova E, Ghaemmaghami P, Jaspar M, Meyer C, Elansary M, Van Egroo M, Chylinski D, Berthomier C, Brandewinder M, Mouraux C, Schmidt C, Hammad G, Coppieters W, Ahariz N, Degueldre C, Luxen A, Salmon E, Phillips C, Archer SN, Yengo L, Byrne E, Collette F, Georges M, Dijk D-J, Maquet P, Visscher PM, Vandewalle G. 2021. Alzheimer's disease geneJc risk and sleep phenotypes in healthy young men: associaJon with more slow waves and dayJme sleepiness. *Sleep* 44. doi:10.1093/sleep/zsaa137

Myers-Turnbull D, Taylor JC, Helsell C, McCarroll MN, Ki CS, Tummino TA, Ravikumar S, Kinser R, Gendelev L, Alexander R, Keiser MJ, Kokel D. 2022. Simultaneous analysis of neuroacJve compounds in zebrafish. doi:10.1101/2020.01.01.891432

Owens MJ, Morgan WN, Plok SJ, Nemeroff CB. 1997. Neurotransmiker receptor and transporter binding profile of anJdepressants and their metabolites. *J Pharmacol Exp Ther* 283:1305– 1322.

Özcan GG, Lim S, Leighton PL, Allison WT, Rihel J. 2020. Sleep is bi-direcJonally modified by amyloid beta oligomers. *eLife* 9:e53995. doi:10.7554/eLife.53995

Quiroz YT, Schultz AP, Chen K, Protas HD, Brickhouse M, Fleisher AS, Langbaum JB, Thiyyagura P, Fagan AM, Shah AR, Muniz M, Arboleda-Velasquez JF, Munoz C, Garcia G, Acosta-Baena N, Giraldo M, Tirado V, Ramírez DL, Tariot PN, Dickerson BC, Sperling RA, Lopera F, Reiman EM. 2015. Brain Imaging and Blood Biomarker Abnormalities in Children With Autosomal Dominant Alzheimer Disease: A CrossSecJonal Study. *JAMA Neurol* 72:912–919. doi:10.1001/jamaneurol.2015.1099

Relkin NR. 2007. Beyond symptomaJc therapy: a reexaminaJon of acetylcholinesterase inhibitors in Alzheimer's disease. *Expert Rev Neurother* 7:735–748. doi:10.1586/14737175.7.6.735

Rihel J, Prober DA, Arvanites A, Lam K, Zimmerman S, Jang S, Haggarty SJ, Kokel D, Rubin LL, Peterson RT, Schier AF. 2010. Zebrafish Behavioral Profiling Links Drugs to Biological Targets and Rest/Wake RegulaJon. *Science* 327:348–351. doi:10.1126/science.1183090

Sleegers K, Brouwers N, Gijselinck I, Theuns J, Goossens D, Wauters J, Del-Favero J, Cruts M, van Duijn CM, Van Broeckhoven C. 2006. APP duplicaJon is sufficient to cause early onset Alzheimer's demenJa with cerebral amyloid angiopathy. *Brain J Neurol* 129:2977–2983. doi:10.1093/brain/awl203

Sun L, Zhou R, Yang G, Shi Y. 2017. Analysis of 138 pathogenic mutaJons in presenilin-1 on the in vitro producJon of Aβ42 and Aβ40 pepJdes by γ-secretase. *Proc Natl Acad Sci* 114:E476–E485. doi:10.1073/pnas.1618657114

Szklarczyk D, Santos A, von Mering C, Jensen LJ, Bork P, Kuhn M. 2016. STITCH 5: augmenJng protein– chemical interacJon networks with Jssue and affinity data. *Nucleic Acids Res* 44:D380–D384. doi:10.1093/nar/gkv1277

Weggen S, Rogers M, Eriksen J. 2007. NSAIDs: small molecules for prevenJon of Alzheimer's disease or precursors for future drug development? *Trends Pharmacol Sci* 28:536–543. doi:10.1016/j.Jps.2007.09.004

Wiltschko AB, Tsukahara T, Zeine A, Anyoha R, Gillis WF, Markowitz JE, Peterson RE, Katon J, Johnson MJ, Daka SR. 2020. Revealing the structure of pharmacobehavioral space through moJon sequencing. *Nat Neurosci* 23:1433–1443. doi:10.1038/s41593-020-00706-3

Yang T, Arslanova D, Gu Y, Augelli-Szafran C, Xia W. 2008. QuanJficaJon of gamma-secretase modulaJon differenJates inhibitor compound selecJvity between two substrates Notch and amyloid precursor protein. *Mol Brain* 1:15. doi:10.1186/1756-6606-1-15

https://doi.org/10.7554/eLife.96839.2.sa0